GENERATION OF A GENETICALLY MODIFIED ONCOLYTIC PLATFORM FOR CANCER IMMUNOTHERAPY

Madeleine Sjöberg
University of Helsinki
Faculty of Pharmacy
Division of Pharmaceutical Biosciences

April 2018

Tiedekunta/Osasto Fakultet/Sektion – Faculty	Osasto/Sektion– Department	
Faculty of Pharmacy	Division of Pharmaceutical Biosciences	
Tekijä/Författare – Author		
Madeleine Sjöberg		
Työn nimi / Arbetets titel – Title		
Generation of a genetically modified oncolytic platform for cancer immunotherapy		
Oppiaine /Läroämne – Subject		
Biopharmacy		
Työn laji/Arbetets art – Level	Aika/Datum – Month and year	Sivumäärä/ Sidoantal – Number of pages
Master's thesis	April 2018	93 (+appendicies)

Tiivistelmä/Referat – Abstract

Cancer afflicts an ever-growing number of people globally each year. In part due to a complex pathophysiology where much is still unknown, the need for new cancer treatments has been persistent, fuelled further by the issue of treatment resistance. An emerging field holding much promise in oncology is immunotherapy, a subgroup of which is oncolytic virus treatments. These treatments utilize the inherent or acquired ability of certain viruses to selectively replicate in tumor cells to fight cancer. One of these viruses is the adenovirus. With these viruses it is possible to modulate the immune response e.g. through the expression of certain genes.

The thesis focuses on genetically arming an oncolytic adenovirus in an effort to enhance treatment efficacy. The transgene of choice is the CD40 ligand (CD40L), a costimulatory molecule capable of aiding in the development of systemic antitumor immunity. Adenoviruses have previously been designed expressing the CD40L, however, a novel aspect was introduced with the design and incorporation of a soluble a form of the protein. The main aim of the study was the construction of four functional oncolytic adenoviruses, encoded with either the human or mouse variants of the two CD40L proteins (full-length and soluble). Successful completion required protocols for the cloning, bacterial colony screening, and primary virus production to be established.

Insertion of the CD40L transgenes into the E3-gp19k region of the chosen Ad5Δ24 backbone was first attempted with the traditional approach of homologous recombination. The method that ultimately proved successful was a one-step Gibson Assembly® reaction. Screening the bacterial colonies with colony polymerase chain reaction, the potential CD40L positive clones underwent restriction analysis to affirm the presence of the transgene in the viral genome, as well as the retainment of critical elements. Two out of three recombined plasmids carrying the full-length CD40L proceeded to transfection and virus propagation in A549 cells, after which the presence of the adenovirus and CD40L expression was confirmed with immunostaining.

Finally, a protocol was successfully established by the construction of one of the intended four viruses. The protocol entails all the main steps from cloning until primary virus production, additionally offering the option of applying it to the genetic arming of the Ad5Δ24 with other transgenes of interest. In terms of future perspectives for the project, following construction of the remaining viruses, the intentions are to validate transgene expression and functionality for all constructs, as well as compare the immunogenicity between the full-length and soluble CD40L. In the event of promising results, the project will hopefully proceed to *in vivo* studies.

Avainsanat – Nyckelord – Keywords

Oncolytic adenovirus, CD40 ligand, genetic arming, homologous recombination, Gibson Assembly®

Säilytyspaikka – Förvaringställe – Where deposited

Division of Pharmaceutical Biosciences

Muita tietoja – Övriga uppgifter – Additional information

Supervisors: Karita Peltonen, Vincenzo Cerullo

Tiedekunta/Osasto Fakultet/Sektion – Faculty	Osasto/Sektion– Department	
Farmasian tiedekunta	Farmaseuttisten biotieteiden osasto	
Tekijä/Författare – Autho		
Madeleine Sjöberg		
Työn nimi / Arbetets titel – Title		
Geneettisesti muunnellun onkolyyttisen viruksen kehittäminen syövän immunoterapiaan		
Oppiaine /Läroämne – Subject		
Biofarmasia		
Työn laji/Arbetets art – Level	Aika/Datum – Month and year	Sivumäärä/ Sidoantal – Number of pages
Pro Gradu	Huhtikuu 2018	93 (+liitteet)

Tiivistelmä/Referat – Abstract

Maailmalla sairastuu vuosittain yhä enemmän ihmisiä syöpään. Uusien syöpähoitojen tarve on ollut jatkuva johtuen mm. syövän monimutkaisesta ja vielä osittain tuntemattomasta patofysiologiasta ja hoitoresistenssistä. Immunoterapia on lupaava kasvava ala onkologiassa, josta yksi osa-alue on onkolyyttiset virushoidot. Nämä virushoidot hyödyntävät joidenkin virusten luontaista tai muunneltua kykyä selektiiviselle monistumiselle syöpäsoluissa. Yksi näistä viruksista on adenovirus. Näillä viruksilla on mahdollista muunnella immuunivastetta, esim. saamalla ne ekspressoimaan tietyt geenit.

Tämä työ keskittyy onkolyyttisen adenoviruksen geneettiseen aseistamiseen hoidon tehokkuuden parantamiseksi. Kostimulatorinen molekyyli CD40 ligandi (CD40L) valittiin transgeeniksi sen immuunijärjestelmää stimuloivan kyvyn vuoksi. CD40L ekspressoivia adenoviruksia on suunniteltu aikaisemminkin, mutta uutuusarvoa toi liukenevan CD40L suunnittelu ja sisällytys projektiin. Tutkimuksen päätavoite oli neljän toiminallisen onkolyyttisen adenoviruksen tuotanto, jossa kukin kantaa joko ihmis- tai hiirivarianttia kokopitkästä tai liukenevasta CD40L:sta. Tavoitteen onnistunut toteutus vaati protokollien perustamisen kloonaukseen, bakteeripesäkkeiden seulontaan ja primaarivirustuotantoon.

CD40L transgeenien sijoittaminen valittuun Ad5Δ24 plasmidin E3-gp19k alueeseen yritettiin ensin perinteisellä homologisella rekombinaatiolla. Kloonaus onnistui lopulta soveltamalla yksivaiheinen Gibson Assembly® reaktio. Bakteeripesäkkeet seulottiin ensin polymeraasiketjureaktiolla, jonka jälkeen mahdolliset CD40L positiiviset kloonit jatkoivat restriktioanalyysin vahvistaakseen transgeenin integraatio viruksen perimään. Myös kriittisten elementtien säilyminen varmistettiin. Kaksi kolmesta kokopitkää ihmisperäistä CD40L kantavaa rekombinoitua plasmidia transfektoitiin A549 soluihin tuottamaan primaarivirusta, jonka jälkeen adenoviruksen läsnäolo ja CD40L ekspressio vahvistettiin immunovärjäyksellä.

Lopulta protokollaa perustettiin onnistuneesti konstruoimalla yksi neljästä suunnitelluista viruksista. Protokolla kattaa kaikki geneettisen aseistamisen päävaiheet kloonauksesta primaarivirustuotantoon, tarjoten myös mahdollisuuden sovittaa sitä Ad5Δ24 aseistamiseen muilla kiinnostavilla transgeeneillä. Projektin seuraavassa vaiheessa, jäljellä olevien kolmen viruksien tuotannon jälkeen, validoidaan transgeenien ekspressio ja toiminnallisuutta kaikilla konstruktioilla. Tämän jälkeen verrataan liukenevan ja kokopitkän CD40L immuunijärjestelmää stimuloivaa kykyä ja tuloksien olleen lupaavia, siirrytään toivottavasti *in vivo*-kokeisiin.

Avainsanat – Nyckelord – Keywords

Onkolyyttinen adenovirus, CD40 ligandi, geneettinen aseistaminen, homologinen rekombinaatio, Gibson Assembly®

Säilytyspaikka – Förvaringställe – Where deposited

Farmaseuttisten biotieteiden osasto

Muita tietoja – Övriga uppgifter – Additional information

Ohjaajat: Karita Peltonen, Vincenzo Cerullo

TABLE OF CONTENTS

APPENDICIES

ABBREVIATIONS

Ad	adenovirus
Ad3	adenovirus serotype 3
Ad5	adenovirus serotype 5
APC	antigen-presenting cell
bp	base-pairs
ca	circa
CD40L	CD40 ligand
CMV	cytomegalovirus
CPE	cytopathic effect
CRAd	Conditionally Replicating Adenovirus
CTL	cytotoxic T cell
DC	dendritic cell
DMEM	Dulbeccos Modified Eagle's Medium
EMA	European Medicines Agency
E. coli	*Escherichia coli*
FDA	Food and Drug Administration
GFP	green fluorescent protein
HEK	human embryonic kidney cells
ITR	inverted terminal repeat
kb	kilo base-pairs
LB	Luria-Bertani
MHC	major histocompatibility complex
OAd	oncolytic adenovirus
OV	oncolytic virus
PeptiCRAd	Peptide-coated Conditionally Replicating Adenovirus
PBS	phosphate buffered saline
PCR	polymerase chain reaction
Rb	retinoblastoma
RGD	arginyl glycyl aspartic acid

SC	supercoiled
TAA	tumor-associated antigen
TAE	Tris-acetate-EDTA
Th	T helper cell
TERT	telomerase reverse transcriptase
TME	tumor microenvironment
UV	ultraviolet
WHO	World Health Organization

1 INTRODUCTION

Cancer is a global problem, claiming the lives of over 8 million people in the year 2012 alone (Ferlay *et al.* 2015). Furthermore, as the global population continues to grow and age, the number of new diagnoses is estimated to rise from approximately 14 million in 2012 to 20 million by the year 2025 (Bray 2014; Ferlay *et al.* 2015). Translating these statistics to Finland, the National Institute for Health and Welfare assessed in 2013 that around a third of the population will develop cancer at some point during their lifetime (Vartiainen *et al*. 2013). The same year, the Finnish Cancer Registry (2017) reported over 32,000 new diagnosed cancer cases, a number which is estimated to exceed 40,000 by the year 2025. Aside from the devastation cancer afflicts on the life of the people affected, whether patient or family member, the global economic impact of cancer is estimated to have amounted to US$ 1.16 trillion in the year 2010 alone (Knaul *et al*. 2014).

Despite diligent cancer research and development of new treatments, much is still unknown about these maladies. Many cancers can be cured if diagnosed early and treated properly, and 30-50% of cancers are preventable with the help of prevention strategies and the avoidance of risk factors (World Health Organization 2017). There are even vaccines that can be utilized that protect people from carcinogenic infections. Over 2 million of the 14 million newly diagnosed cancer patients in 2012 were due to infectious agents such as human papilloma virus, hepatitis B virus, and *Helicobacter pylori* bacteria (Plummer *et al.* 2016).

Currently, cancer treatments are designed individually for each patient by a multidisciplinary team that plan the best treatment based on relevant factors, including the type of cancer, stage of progression, molecular markers, and other preexisting conditions. A fundamental aspect in the treatment strategy is to consider whether the aim is to cure the patient, manage the disease, prevent relapse, or alleviate the symptoms. Surgery, chemotherapeutics, and radiation therapy have long been pillars in cancer treatment with immunotherapy potentially emerging as a fourth (Farkona *et al*. 2016). Immunotherapy relies on immune system activation in the patient to treat the disease, a

few of the strategies employed including cytokines, immune checkpoint inhibition, cell-based therapies such as vaccines, and different combination therapies.

An interesting field in immunotherapy is oncolytic viruses (OVs) which are viruses with a natural or genetically modified propensity to selectively proliferate in tumor cells (Kaufman *et al*. 2015). There are several viruses that can be harnessed for this purpose, one being the adenovirus (Ad). The first reported observations of natural virus infection coinciding with tumor regression date back to the mid-1800s (Kelly & Russell 2007). Based on the many case reports that have accumulated since then, one of the conclusions that have been drawn is that there are circumstances in which certain viruses can destroy tumors without excessive harm to the patient. Aside from lysing tumor cells, the OVs can also be utilized as gene vectors of immunostimulatory compounds, thereby further promoting the elicitation of an immune system response and, ideally, systemic antitumor immunity.

The first OV treatment was approved by the China's State Food and Drug Administration in the year 2005 (Garber 2006). Since then, the oncolytic adenovirus (OAd) H101 has been used for the treatment of head and neck cancer, albeit only in China. In late 2015, the herpesvirus talimogene laherparepvec (T-Vec) became the first oncolytic virus treatment approved by the Food and Drug Administration and the European Medicines Agency (EMA press release 2015; FDA press announcement 2015). With several other treatments at various stages of the development pipeline, the H101 and T-Vec are hopefully only the beginning for OVs.

This work aims to delve into OV based therapies in oncology and the potential they provide in finding a cure for cancer. After briefly examining cancer on a global scale as well as addressing characteristics and challenges related to the diseases, the field of oncolytic immunotherapy is explored regarding the adenovirus (Ad) and the advantages and disadvantages it brings. Finally, a protocol is conceived for the generation of a genetically armed OAd, from cloning until primary virus production.

2 CANCER

Cancer is a hypernym used to describe the more than 100 diseases that can develop in almost any part of the human body (Stratton *et al.* 2009). These diseases have varying risk factors and epidemiology but share one characteristic which is the uncontrolled growth of abnormal cells. The evolution of different cancers is the product of repetitive clonal expansion, positive selection, and genetic diversification in the tissue the cancer develops (Greaves & Maley 2012). This process of tumor development is referred to as oncogenesis.

Two central terms in oncology are tumor and cancer. The meaning of these words lacks certain consistency as they are at times used interchangeably to describe all forms of abnormal tissue growths (neoplasms). The term tumor usually encompasses both benign and malignant neoplasms, whereas cancer is generally reserved for malignant neoplasms. The morphological differentiation can at times be difficult, but generally benign tumor cells proliferate into one discernable tumor mass contained to one area. In contrast, malignant tumor cells invade surrounding tissues with the potential of spreading to other parts of the body by dislodging clusters of cells. These clusters are capable of forming new tumors referred to as metastases. If unhindered, malignant tumors will expand aggressively and continue to spawn metastases, thereby increasing the tumor burden. In 90% of cancer cases, metastases are the main cause for morbidity and mortality (Monteiro & Fodde 2010).

2.1 The Cancer Genome

Cancer is a genetic disease that develops progressively through genetic alterations to the cell genome (Hanahan & Weinberg 2000). The encompassing notion is that cancer is the product of Darwinian evolution between cell populations in a microenvironment (Stratton *et al.* 2009). This evolutionary process is based upon the acquisition of heritable genetic variation among individual cells by essentially random mutation and the natural selection among the different phenotypes that develop as a result.

The alterations found in a cancer genome have accumulated over the lifetime of the patient (Stratton *et al.* 2009). DNA damage can arise spontaneously or as the result of endogenous or exogenous agents known as mutagens (Stratton *et al*. 2009; Helleday *et al*. 2014). Endogenous mutagens can originate from normal metabolic processes, whereas exogenous mutagens stem from either physical or chemical environmental sources (Helleday *et al*. 2014). Examples of exogenous mutagens include non-ionizing ultraviolet (UV) radiation, asbestos, and tobacco smoke. DNA damage and replication errors are generally dealt with by repair mechanisms in the cell. However, should the damage go undetected or be repaired erroneously, the mutations will become permanent (Stratton *et al.* 2009). Mutagenic or non-mutagenic agents that increase the risk of developing cancer by damaging cells are referred to as carcinogens.

The mutations observed in the cancer genome can be divided into germ line and somatic mutations. Germ line mutations are inherited from the parent cell whereas somatic mutations are acquired independently over the lifespan of the cell (Stratton *et al.* 2009). Depending on their significance in oncogenesis, somatic mutations can be further classified as either driver or passenger mutations. Of these two, the driver mutations actively contribute to disease development whereas passenger mutations fail to confer any growth advantage. Driver mutations reside in cancer genes, bestowing a growth advantage for the cell that causes their positive selection during cancer development.

The metamorphosis undergone by a cancer cell reflects the dynamic alterations whereby the regulatory circuits that normally control cell proliferation and homeostasis become defective (Hanahan & Weinberg 2000). On average, common solid tumors of colon, breast, brain, and pancreas origin have 33-66 genes with slight somatic mutations that cause changes in the produced proteins (Vogelstein *et al.* 2013). The number of mutations does, however, vary between different cancer types, with melanomas and lung tumors having circa (ca) 200 mutations that alter the nucleotide encoded amino acid sequences. The high frequency is a testament to the potency of the mutagens involved, i.e. ultraviolet light in melanoma and tobacco smoke in lung cancer.

There are certain common mutagenic targets for several cancer types that increase cancer promoting gene (oncogene) expression and reduce tumor inhibiting gene (tumor suppressor gene) expression. An estimated 90% of somatically mutated cancer genes behave dominantly and thus aid in cancer development even when present in only one allele (Stratton *et al.* 2009). The remaining 10% of the genes that act recessively generally cancel protein production upon expression and are alternatively referred to as tumor suppressor genes. Two intensely studied tumor suppressors that are common mutagenic targets in cancer are the retinoblastoma (Rb) gene family and the p53 gene.

The Rb receives its name from the cancer retinoblastoma from which the first tumor suppressor gene Rb1 was identified (Lapenna & Giordano 2009). Nonetheless, the loss of Rb protein occurs in several other cancers as well (Sherr & McCormick 2002). The encoded proteins of the Rb family are important regulators of cell proliferation, for example participating in the inhibition of transition from the G1 phase to the S phase of the cell cycle where DNA replication occurs (Lapenna & Giordano 2009). Consequently, the deregulation of the Rb pathway by gene inactivation promotes proliferation of cancer cells.

The p53 gene encodes for a transcription factor of the same name, which is activated in the event of DNA damage, hypoxia, and oncogene activation (Sherr & McCormick 2002). The p53 transcription factor can regulate gene expression that either blocks the cell cycle from continuing or induces apoptosis. Mutations of p53 can be found in over 50% of human cancers (Kaufman *et al.* 2015). In the remaining cancers with normal p53 gene activity the genes affecting its function are generally mutated

In contrast to the aforementioned tumor suppressor genes, the Ras gene family has been found to be subject to mutagenic activation in cancer. The family consists of N-, H-, and K-Ras which are small guanosine triphosphatases (Ancrile *et al.* 2008). The Ras proteins are important regulators of many crucial signaling pathways that control normal cellular proliferation (Downward 2003). Mutations in certain tumors target the Ras genes, thereby rendering the encoded Ras protein perpetually activated, stimulating growth and differentiation autonomously (Bos 1989). Even if the genes themselves are unaffected,

alterations in the components of the signaling pathways preceding or succeeding them cause aberrant Ras function to be found in the most human tumors (Downward 2003).

The incidence of the highlighted mutations varies between different tumors and can present independently of each other. The impact these mutations have on oncogenesis and tumor growth make them attractive targets for certain cancer treatments. The approaches range from utilizing the aberrant function of the subsequent signaling pathways, or attempts to restore or replace the normal gene functions.

2.2 The tumor microenvironment

Normal tissue physiology is achieved and upheld by a strictly regulated balance between cell death and proliferation (Joyce & Pollard 2009). Different components of the microenvironment contribute to achieving and maintaining this homeostasis in various ways. In tumors, however, the microenvironment can become corrupt, promoting the survival and growth of tumor cells in favor of upholding normal tissue physiology. The subsequent milieu that develops is referred to as the tumor microenvironment (TME). The TME and the tumor cells share a symbiotic and dynamic relationship that develops early in malignancies and continues to evolve with the tumor (Turley *et al.* 2015). The TME affects tumor cell growth in many ways, such as metastatic dissemination and tumor cell survival and is therefore a target for some anticancer therapies.

Despite the numerous differences between cancer types, certain shared characteristics have been identified. Hanahan and Weinberg compiled a list in the year 2000 that based on extensive literature review, presented six hallmarks for cancer; see Figure 1. These characteristics were introduced as: sustained growth signals, evasion of growth inhibitors, eluding apoptosis, infinite proliferation, continued angiogenesis, and tissue invasion as well as metastasis. Later in 2011, Hanahan and Weinberg expanded on the list to involve altered energy metabolism and immune evasion as emerging hallmarks, as well as presenting two enabling characteristics, namely genetic instability and tumor-promoting inflammation. The TME is an important aspect in the development of these traits, the different components often participating in several hallmarks.

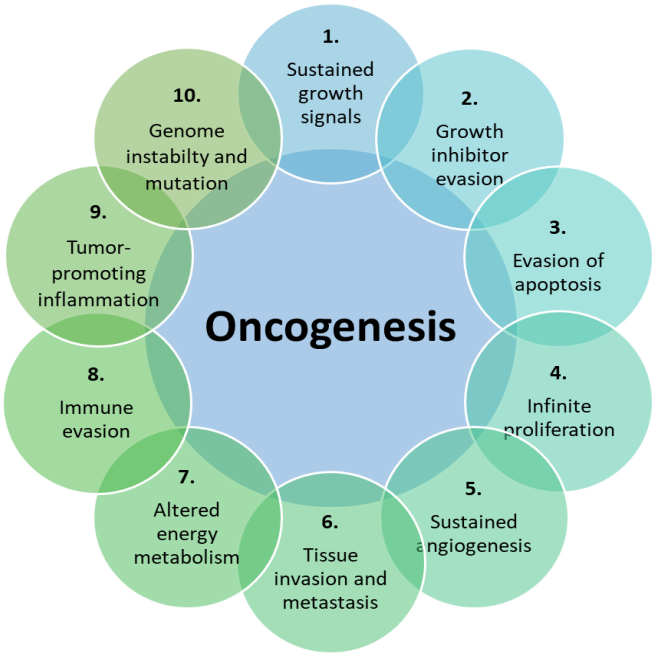

Figure 1: The hallmarks of cancers. The image depicts the hallmarks (1-6), emerging hallmarks (7 and 8), and enabling characteristic (9 and 10) generally associated with cancer. Modified Figure 6 from Hanahan and Weinberg (2011).

2.3 Components of the Tumor Microenvironment

The TME is a heterogenous entity comprised of several components that provide a complex microenvironment that rivals and may even supersede the one found in normal tissues (Hanahan & Weinberg 2011; Pattabiraman & Weinberg 2014). The components vary in proportion between tumors of different origins and development, but can often be divided into non-cellular and cellular groups (Pattabiraman & Weinberg 2014).

The major non-cellular component in the TME is the extracellular matrix (ECM) that in normal tissues is an important regulator of tissue homeostasis (Joyce & Pollard 2009; Pattabiraman & Weinberg 2014). The ECM fulfils several functions by, for example, providing architectural support and different signals for survival and differentiation (Joyce & Pollard 2009). The basic components of the ECM are water, proteins, and polysaccharides; however, the composition and topology of the ECM is unique for every tissue (Frantz *et al.* 2010). The singular structures are the result of a dynamic and reciprocal exchange between several cellular components, such as epithelial, fibroblast,

and endothelial elements, and is continuously remodeled enzymatically and non-enzymatically.

Because of age or disease, the activity of the remodeling enzyme can become deregulated and manifests as abnormal ECM dynamics (Lu *et al.* 2012). This aberrant remodeling can be divided into either the excessive degeneration or formation of ECM. In tumors, there is commonly a notable stiffening of the ECM compared to normal tissue, a characteristic that can be traced to ECM deposition and remodeling by fibroblasts as well as increased contractility of the epithelium (Frantz *et al.* 2010). The release of growth factors through ECM remodeling, enhances vascular permeability and fosters angiogenesis. The positive-feedback loop that is generated by the subsequent interstitial tissue pressure, potentiates tumor growth and survival which ultimately promotes metastasis. Several of the hallmarks of cancer are influenced by the surrounding ECM (Pickup *et al.* 2014).

The major cellular components of the TME can be divided into cells of bone marrow cell (mesenchymal) or blood cell (hematopoietic) lineages. The mesenchymal cell lineage originates from the mesenchymal stem cells that differentiate into many cell types that include adipocytes, fibroblasts, myocytes, pericytes, and osteoblasts (Turley *et al.* 2015). Normally, these cells contribute to maintaining tissue homeostasis and wound healing, functions that upon corruption by the tumor can evolve to become pro-tumorigenic.

In tumors, the cells of the mesenchymal cell lineage have varying ways of contributing to the oncogenesis and continued survival of the tumor. The mesenchymal stem cells themselves possess immune regulating abilities that may contribute to the development of a tolerance promoting environment in the tumor, though this contribution still lacks unequivocal evidence (Turley *et al.* 2015). For the differentiated progenies of these stem cells, however, there are more studies implicating a stronger evidence-based connection between them and protumor activity. One of these cell types are the pericytes, which are stromal cells involved in angiogenesis and immune regulation.

The cells of hematopoietic origin are further divided into two lineages: lymphoid and myeloid (Pattabiraman & Weinberg 2014). Cells types belonging to the lymphoid lineage include T and B lymphocytes and natural killer cells whereas cell types of the myeloid

lineage include macrophages and neutrophils. An additional cell type developing from both cell lines are the dendritic cells (DC). The different innate and adaptive immune cells can have dual roles in the tumor environment (Table 1). When anti- and protumor functions are a possibility, the action that prevails is largely dependent on the molecules being expressed as well as the abundance and activation state of various cell types (Grivennikov *et al.* 2010).

Table 1: The role of different immune and inflammatory cells regarding antitumor immunity and protumor inflammation. Modified from Table 1 Grivennikov *et al.* 2010.

CELL TYPE	ANTITUMOR	PROTUMOR
Macrophages Dendritic cells Myeloid-derived suppressor cells	Antigen presentation Cytokine production	Immunosuppression Production of: Cytokines, chemokines, proteases, growth factors, and angiogenic factors
Mast cells	-	Cytokine production
B cells	Possibly tumor-specific antibody production	Immunosuppression Producton of cytokines and antibodies Activation of mast cells.
Cytotoxic T cells	Direct lysis Cytotoxic cytokine production	Cytokine production?
T helper 1 cells	Aid cytotoxic T cells in tumor rejection Cytokine production	Cytokine production
T helper 2 cells	-	Cytokine production B cell activation Education of macrophages
T helper 17 cells	Activation of cytotoxic T cells	Cytokine production
T regulator cells	Suppression of inflammation	Immunosuppression Cytokine production
Natural killer Cells Natural killer T cells	Direct cytotoxicity Cytokine production	-
Neutrophils	Direct cytotoxicity Regulation of cytotoxic T cell responses	Production of: cytokines, proteases, and ROS

There are two main groups of mature T cells, the division of which is based on whether they express γδ or αβ receptors (Grivennikov *et al.* 2010). The T cells in the αβ group are either cytotoxic (CTLs) or helper cells (Th cells) depending on their effector functions, with the Th cells being further divided into the subsets Th1, Th2, Th17, T regulatory, and natural killer T cells. Depending on which T cells are activated, their effect can either be tumor promoting or suppressive. Studies have implicated many T cell subsets in solid tumors to participate in tumor promotion, progression, or metastasis, such as CTLs, Th1

cells, and Th2 cells. It is difficult to evaluate the importance of immunity and inflammation in early oncogenesis but the most abundant immune cells in the TME are T cells and the tumor-associated macrophages. Macrophages and different subsets of T cells can function as tumor promoters and either by themselves or together contribute to tumor progression and metastasis (Pollard 2004; DeNardo *et al.* 2009; Pattabiraman & Weinberg 2014).

2.4 Therapeutic Targets in in the Tumor Microenvironment

The TME is able to influence treatment responses by modifying cancer cell sensitivity to e.g. chemotherapy as well as targeted agents (Chen *et al.* 2015; Sun 2015). The recognition of the impact of TME components on disease progression and successful treatment outcome have generated an interest in developing new treatments targeting the TME. The TME impacts tumor development by shaping tumor cell phenotypes through induction of stress responses and genomic instability (Marusyk *et al*. 2012).

The stromal cells of the TME are as opposed to cancer cells generally genetically and epigenetically stable, thereby having a reduced risk for developing resistance (Chen *et al.* 2015). Conventional therapies are known to contribute to acquired resistance and compromise treatment outcome by inducing alterations to the TME. As of such, it is necessary to consider the overall TME response in clinical interventions. Therapeutics targeting specific stromal compartments have been successfully implemented and include e.g. bevacizumab (angiogenesis inhibitor), letrozole (aromatase inhibitor), and nivolumab (immune checkpoint inhibitor) (Kenny *et al.* 2007; Chen *et al.* 2015).

Aside from the stromal cells, there are several immunological targets in the TME. By targeting immunoregulatory pathways or by introducing immunostimulatory compounds, the balance can be shifted in favor of immune activation over tolerance. Should antitumor immunity successfully develop, this approach provides the benefit of systemic tumor eradication as well as lifelong protection against that particular tumor. Hence, immunotherapy currently holds some of the greatest expectations and potential in oncology.

3 ADENOVIRUSES

Ads belong to the genus *Mastadenovirus*, one of the major lineages of the *Adenoviridae* family (Davison *et al.* 2003). To date, 57 serotypes are known to affect humans and these are further classified into seven species (A-G) as is depicted in Table 2 (Buckwalter *et al.* 2012; Kaufman *et al*. 2015). The classification of the different serotypes depends on their characteristics regarding: serology, hemagglutination, oncogenic potential in rodents, genome sequence, and transformation of primary cells (Berk 2013).

Table 2: The major sites of infection for different serotypes. Derived from Table 56.1 by Wold and Ison (2013).

Species	Serotype	Respiratory	Urinary	Gastro-intestinal	Ocular
A	12, 18, 31	X	X	X	
B	3, 7, 11, 14, 16, 21, 34, 35, 50, 55	X	X	X	X
C	1, 2, 5, 6, 57	X	X	X	
D	8, 9, 10, 13, 15, 17, 19, 20, 22, 21, 23, 24, 25, 26, 27, 28, 29, 30, 32, 33, 36, 37, 38, 39, 42, 43, 44, 45, 46, 47, 48, 49, 51, 53, 54, 55, 56			X	X
E	4	X			X
F	40, 41			X	
G	52			X	

The Ad is a vertebrate virus that derives its name from adenoid from which it was first isolated (Rowe *et al.* 1953; Hilleman & Werner 1954). The virus is transmitted via aerosols and direct contact, generally causing mild self-limiting symptoms in immunocompetent individuals, e.g. keratoconjunctivitis and respiratory infections *(*Zhang & Bergelson 2005*;* Echavarría 2008; Kaufman *et al.* 2015). In children and immunocompromised individuals, adenoviral infections can cause severe conditions such as meningoencephalitis and pneumonia (Krilov 2005; Echavarría 2008).

The Ad structure consists of a non-enveloped icosahedral capsid comprised mainly of the of proteins hexon, fiber, and penton (Law & Davidson 2005). The viral capsid measures around 90 nm in diameter, excluding the protrusions from the surface of the capsid that

can be seen in Figure 2. These protrusions consist of fiber protein that are anchored to the hexon capsid by a pentameric penton base at the proximal end, while forming a globular domain at the distal end known as a knob (Zhang & Bergelson 2005). The capsid of the Ad encases a linear double-stranded DNA that is 26,000-45,000 bp in size (Davison *et al.* 2003).

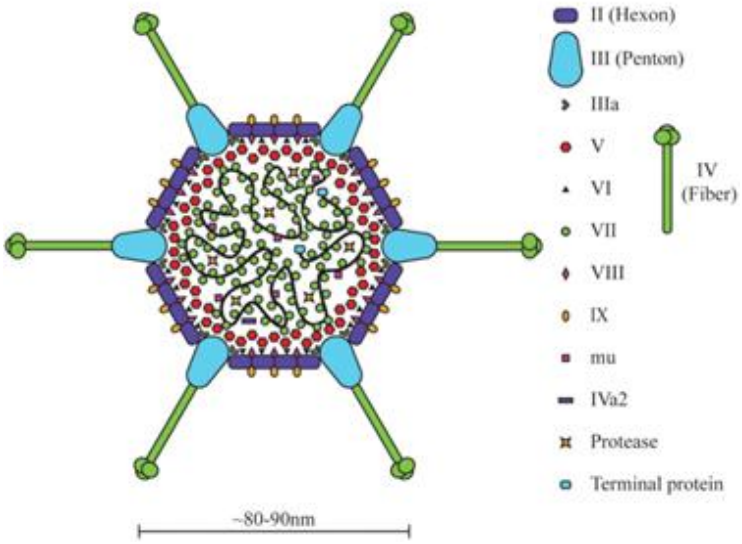

Figure 2: The adenovirus ranges from ca 80 to 90 nm in diameter and is structurally comprised of a capsid enveloping a linear double-stranded DNA genome. The main capsid components are hexon, fiber, and penton (Giberson *et al.* 2012).

The Ad5 consist of a ca 36,000 bp genome that encodes around 39 genes (Giberson *et al.* 2012). The genome is sectioned into several transcription units that are expressed during the replication cycle that is generally divided into an early phase and a late phase (Berk 2013). The early transcription units are identified as E1A, E1B, E2, E3, and E4 and the late transcription unit as one major late transcription unit further processed into late mRNAs L1-L5 through post-translational processing (Giacca & Zacchigna 2012). Additionally, four intermediate transcription units (IX, IVa2, L4 intermediate, and E2 late) are transcribed at the beginning of viral DNA replication that marks the transition from early to late phase (Berk 2013). The transcription units of the Ad genome will be explored in further detail later in the chapter. The viral genome and the location of the different units are gathered in a simplified rendition (Figure 4) on the following page.

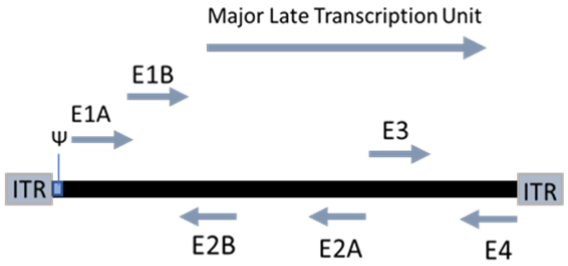

Figure 4: The Ad5 genome. Comprised of early (E1, E2, E3, and E4) and late transcription units (L1-L5) part of the major late transcription unit, the linear genome is flanked by inverted terminal repeats (ITRs) with a packaging signal (Ψ) on the left-hand side. Modified from Giberson *et al.* (2012) and Wold and Ison (2013).

3.1 Infection of a host cell

The Ad have a wide tissue tropism in the human body, as can be attested by Table 2 (page 11). The species A, C, D, E, and F recognize and utilize the coxsackievirus and adenovirus receptor (CAR) for cell binding as part of cell entry (Roelvink *et al.* 1998). The CAR is a 46,000 Dalton transmembrane protein belonging to the immunoglobulin gene superfamily with two immunoglobulin-like extracellular domains expressed beneath tight junctions on the basolateral surface of polarized epithelial cells (Bergelson *et al.* 1997; Smith *et al.* 2010). Alternative ways for Ads to attach to cells include interactions with e.g. CD46, sialic acid, and integrins such as α3β1 (Salone *et al.* 2003; Smith *et al.* 2010)

The host cell infection pathway may vary between different serotypes. However, Ad2 and Ad5 infections are generally two-part processes, beginning with primary receptor attachment followed by interaction with a secondary receptor that allows for the virus-receptor complex to be internalized (Zhang & Bergelson 2005). For example, the Ad5 binds to the primary receptor CAR with its fiber knobs which are a major means of attachment. Following receptor binding, the arginyl glycyl aspartic acid (RGD) contained in the penton base acts as the secondary recognition site for several cellular integrins. The RGD engagement of integrins induces activation signals for various proteins that are important for rearrangements in the actin cytoskeleton and the initiation of Ad internalization (Meier & Greber 2004; Zhang & Bergelson 2005).

The Ad enters the host cell in clathrin-coated vesicles, a process during which, in certain host cell types, the virus loses the fiber proteins during internalization in clathrin-coated pits (Meier & Greber 2004; Kremer & Nemerow 2015). Following vesicle maturation into endosomes, the capsid dissociation proceeds, allowing the release of amongst others the endosomolytic protein VI (Wiethoff *et al.* 2005). The protein is a minor capsid component that is released from its inner surface upon Ad uncoating and aids virus escape into the cytosol by mediating degeneration of the endosomal membrane.

The journey to the nucleus of the partially uncoated virus occurs along microtubules following association with the dynein protein that recognizes either the hexon or protein VI (Kremer & Nemerow 2015). Upon reaching the nucleus, the Ad can deposit the genetic material by docking to a nuclear pore complex receptor (Meier & Greber 2004). Aiding in further uncoating the virus, the complex constitutes an entry point for the exposed viral genome that once inside the nucleus can undergo transcription and replication (Greber *et al*. 1997). The whole infection sequence is summarized in Figure 3.

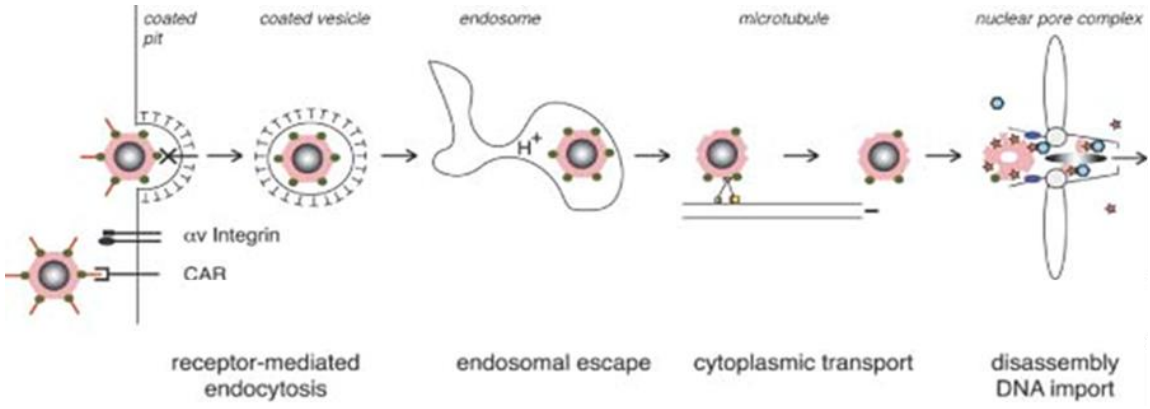

Figure 3: The cascade of Ad cell entry, uncoating, and the ultimate deliery of viral DNA into the nucleus. Modified from Meier and Greber (2004).

3.2 Virus replication

When the viral genome has successfully been delivered to the nucleus, the virus DNA transcription process can commence. During the early stage of the replication cycle, the translation of viral mRNA occurs alongside with host DNA (Berk 2013). However, as the infection progresses to the late phase, virtually all translation apparatuses of the host cell

exclusively process viral mRNA. The very first region to be transcribed is located in the E1A transcription unit (Nevins *et al.* 1979). The E1A region encodes gene products that activate transcription and participate in both entry into the S phase of cell cycle entry, as well as the generation of protective measures to elude antiviral defenses (Berk 2013). One central host cell mechanism affected by the expression of E1A regions are e.g. Rb family proteins.

The E4 encoded proteins support successful virus replication by inducing altered cell signaling and account for disparate functions such as RNA splicing and translational regulation (Berk 2013). Similarly, the E1B transcription unit encodes products that serve to inhibit host cell antiviral response mechanisms. Two prominent proteins contribute to this goal by inhibiting apoptosis induced by the p53 protein, the activity and amount of which are elevated following the abnormal cell cycle entry promoted by the E1A. A generated complex between an E1B and E4 protein affect several proteins having detrimental functions to viral DNA replication by causing their proteasomal degradation; one of the affected proteins is the p53. Additionally, the complex is also necessary for e.g. nuclear export of viral late mRNAs and the inhibition of host mRNA nuclear export.

To ensure the successful completion of the replication cycle of the virus, the antiviral response elements of the host are modulated by proteins encoded by the E3 transcription unit. Their expression aids the virus in avoiding detection by the immune system through regulation of host antiviral response elements (Hawkins *et al*. 2001; Giacca & Zacchigna 2012). One such protein, the E3-gp19K, resides in the endoplasmic reticulum where it binds to the major histocompatibility complex class I (MHC-I) heavy chain, preventing transport of the complex to the cell surface and consequent detection and destruction by CTLs (Wold & Ison 2013).

The transition to the late phase is marked by the onset of viral DNA replication, a stage mediated by the direct participation of E2 encoded proteins (Giberson *et al*. 2012; Berk 2013). Consequently, the E2 region transcription reaches its height as the last region of the early phase, amounting to higher levels than any other early region (Berk 2013). The virus genome is replicated as single-stranded DNA in the presence of only three

replication proteins: terminal protein primer, viral DNA polymerase, and the single-stranded DNA binding protein. The process is biphasic, the synthesis beginning at or near the terminal end of one entire strand, followed by the synthesis of the complete complementary strand (Lechner & Kelly 1977). All Ad genomes have a hallmark inverted terminal repeat (ITR) ranging from 36 to over 200 bp in size (Davison *et al.* 2003). The ITRs act as origins of DNA replication and allow the circularization of single-stranded DNA by base-pairing the terminal sequences (Berk 2013). As opposed to conventional DNA replication which occurs from the 5' to the 3' end, the second complementary strand is synthesized from the 3' to the 5' end and not as Okazaki fragments (Lechner & Kelly 1977).

In the late phase, the major late promotor regulates the one late transcription unit (Giacca & Zacchigna 2012; Berk 2013). The late gene products include the viral capsid protein components as well as proteins that participate in virion assembly (Berk 2013). Produced in the cytoplasm, the structural proteins are transported into the cell nucleus where, upon entry, the virion assembly begins. The construction commences 20 to 24 hours after infection, initiating with the encasing of the viral DNA in capsid proteins in an event requiring the participation of the packaging signal sequence (Ψ) (Berk 2013; Wold & Ison 2013). Two to three days later, ca 100,000 viral progenies are released by host cell lysis, capable of infecting new cells and repeating the infection cycle.

3.3 Areas of application

Ad infect *in vitro* and *in vivo* a variety of dividing and nondividing cells that are primarily epithelial cells (Boyer *et al*. 1959; Wold & Ison 2013). Due to beneficial properties, such as the proficiency with which the Ad can seize control of the cell machinery for virion production and their extensively studied biology, the virus has become an attractive and efficient vector in gene therapy and vaccinations (Shiver *et al.* 2002; Giacca & Zacchigna 2012; Wold & Ison 2013).

The different Ad vectors are summarized in Figure 5, utilizing the Ad5 genome as an example. The genomes are either classified as replication-defective (II and III) or

replication-competent (I) vectors (Wold & Ison 2013). The replication-defective vectors are utilized in transgene delivery and vaccines while replication-competent vectors are applied to cases where Ad replication in a target cell is required. The genome of a replication-defective Ad is often modified by deleting one or several essential genes to increase the cloning capacity, generating first-, second-, and third-generation vectors.

The first-generation vectors typically have their E1 and/or E3 regions substituted with foreign DNA and while the second-generation have additional deletion in the E2 and E4 regions (Giacca & Zacchigna 2012). Lastly, the third-generation vectors have undergone substitution of their whole viral genome aside from regions needed for in cis viral DNA replication and packaging. The removal of E1 in all vectors causes the need for *in trans* provision of the encoded protein by specific cell lines to ensure viral replication (Danthinne & Imperiale 2000). In the case of the third-generation vectors, a helper vector must be supplied in trans, encoding all the necessary proteins (Giacca & Zacchigna 2012).

Figure 5: Summarizing the genetic modifications for different Ad5 vectors: wild-type (I), first- and/or second-generation vector (II), third-generation vector (III), Modified from Figure 56.10. Wold and Ison (2013).

The Ad vector is an extensively studied virus with much of its structure and function elucidated. Due to being a widely utilized vector in gene therapy and vaccination, the Ad has undergone several clinical trials that have indicated it to be very well tolerated (Wold & Ison 2013). With the genome being relatively easy to modify and a broad range of host cells, the Ad has spread to other fields as an attractive vector for different treatments.

4 ONCOLYTIC ADENOVIRUSES

OVs are naturally occurring or genetically modified viruses able to infect, replicate in, and lyse neoplastic cells (Kaufman *et al.* 2015). Viruses utilized in this field include e.g. coxsackievirus, adenovirus, herpes simplex virus, and vaccinia virus. First applied to oncology in the late 1800s when the concept of the nature of a virus was still largely unknown, viruses underwent vigorous research as experimental agents in oncology in the 1950s and 1960s (Kelly & Russell 2007). In the following two decades, interest in viruses as cancer destruction agents dwindled while the field of virology remained an area of vast interest that has yielded extensive knowledge, making viruses one of the most thoroughly understood organisms.

Unique challenges in drug development long prevented the approval of OVs as a new class of anticancer drugs (Kaufman *et al*. 2015). Suboptimal tumor specificity and vulnerability to antiviral host defenses have constituted some of the challenges preventing the development of an efficient OV treatment (Kelly & Russell 2007). However, with the approval of the first treatment for clinical use in the USA and Europe at the end of 2015, an important milestone was reached, constituting what is hopefully the beginning of a series of efficient cancer treatments of this kind.

One of the predominantly used viruses in clinical development of OV therapies is the Ad (Kaufman *et al.* 2015). Its adaption is propagated by e.g. the ease with which the viral pathogenicity can be attenuated, the transgene encoding capacity, as well as the established safety of the virus in clinical use. However, to enable extensive clinical application of Ad-based therapies it requires the consideration of certain concerns regarding the virus. These include the widespread distribution of CAR, strong immunogenicity, and the implied need for numerous modifications to both enhance oncolytic activity and improve clinical safety (Yamamoto *et al.* 2017). Some of these aforementioned challenges have been exploited to improve Ad-based treatments, such as viral immunogenicity. Other issues have attempted to be resolved with the application of genome modifications, the details of a few of them being explored in further detail in this chapter.

4.1 Targeted replication

As opposed to viruses such as the parvovirus and Newcastle disease virus, the Ad possesses no natural preference for cancer cells as hosts (Russell *et al.* 2012). Therefore, the Ad must be engineered or adapted for increased cancer specificity by surface or genome modification. Structural modifications to the surface of the Ad utilize the fact that different serotypes have different tropisms. The Ad applied most extensively in the development of OAd belong to the C species, particularly the Ad5, but other emerging serotypes with the potential to be OVs in terms of efficacy and safety are, e.g. the Ad serotypes 6 and 11 (Shashkova *et al.* 2009).

There are varying approaches to increase tumor cell infection of the OAd, one focusing on the infection pathway. The primary receptor for Ad5 infection of host cells, the CAR, is sparingly expressed on many tumor cells because of reduced expression following tumor progression (Wold & Ison 2013; Yamamoto *et al.* 2017). This issue can be circumvented with the design of an Ad5 based vector with an RGD motif incorporated into the Ad5 fiber knobs (Yamamoto & Curiel 2010; Wold & Ison 2013). This modification enables the virus to infect cells through integrin pathways that are abundant on cancer cells. Another approach to CAR deficiency is fiber switching, a process whereby the part of the Ad5 capsid (the fiber domain) is exchanged for that of another serotype (Yamamoto *et al.* 2017). For one such chimeric vector, the Ad5/3, which is the Ad5 virus with the fiber domains of the Ad3, this modification improved tumor cell delivery due to CAR-independent infection (Yamamoto & Curiel 2010; Pesonen *et al.* 2012).

Another aspect in the selective replication of OAds in cancer cells involves directed deletions to specific areas of the Ad genome. As explored in the previous chapter (page 15), the Ad have the ability of inactivating pathways in host cells to enable the completion of the infection cycle. The pathways often referred to are the p53 and the Rb which are coincidentally common targets for mutational inactivation in tumors. This can be exploited by restricting the OAd proliferation to p53 and/or Rb deficient cells through the removal of the innate ability of the virus to inactivate these pathways. Unable to prevent

the antiviral response in normal cells, non-tumor cells infected by the modified OAd will undergo apoptosis before the infection cycle is completed. Viruses engineered in this manner are referred to as conditionally replicating Ads (CRAds).

Among the first examples of CRAds are the viruses ONYX-015 and H101. In these viruses, restriction of replication to tumor cells is mediated by the loss of late viral RNA export (ONYX-015) or p53 inactivation (H101) by deletions in the E1B-55K gene (Bischoff *et al.* 1996; O'Shea *et al.* 2004; Yamamoto *et al.* 2017); see Figure 6 I. Another common deletion targets the E1A-CR2 region, limiting the virus replication to Rb aberrant tumor cells by disrupting the Rb-binding domain, a deletion also referred to as the delta24 (Δ24) (Fueyo *et al.* 2000; Yamamoto *et al.* 2017); see Figure 6 II.

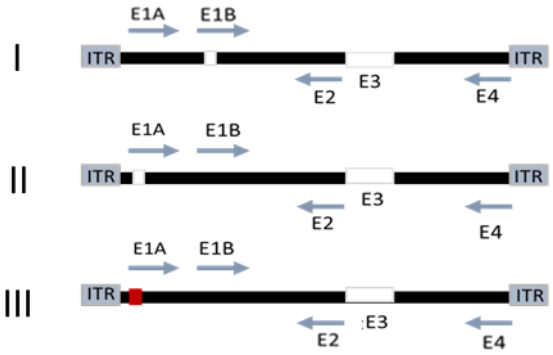

Figure 6: Replication-competent Ad genomes. E1B-55K deleted vector (I), E1A mutated vector (II), and promoter substituted vector where the promotor of E1A is exchanged for a cancer-specific promotor (III). Modified from Figure 56.10. by Wold and Ison (2013).

OAd replication can also be restricted to cancer cells with cancer or tissue specific promoters for early gene expression (Buijs *et al.* 2015). There are several OAds that have been designed where the expression of early genes and/or transgenes of interest have been regulated with this method, e.g. the CN706 (later renamed CV706) where the E1A expression is controlled by a prostate specific antigen promotor for application in prostate cancer (Rodriguez *et al.* 1997; DeWeese *et al.* 2001); see Figure 6 III. Other promotors that have been used with OAds are the cytomegalovirus (CMV), human telomerase reverse transcriptase (hTERT) (CGTG-401), and E2F1 (CG0070) (Huang *et al.* 2016). There are also hybrid promotors that have different response elements such as hypoxia and the presence of specific hormones driving virus replication. The promotors have been applied in viruses used as monotherapies as well as in combination with other treatments.

4.2 Efficacy

OV based treatment have long struggled to gain sufficient efficacy, but as recent successes with e.g. the T-Vec virus prove, it is a hurdle that can be overcome. Immunological treatments such as OVs rely in their mode of action on immune system activation, particularly a strong antitumor response. The details of OV mediated antitumor immunity is still incompletely understood, but seemingly consists of two mechanisms of action: selective replication in tumor cells, culminating in cell lysis, and an induced systemic antitumor immunity (Kaufman *et al*. 2015). Several factors affect the respective contribution of the mechanisms, for example characteristics of the OV as well as interactions between the virus and the immune system. The ability of OVs to lyse tumor cells is influenced by the efficiency of cell receptor targeting, virus proliferation, and host cell antiviral response elements.

In the immune storm often created upon OV infection, both innate and adaptive antitumor immune responses can be stimulated (Melcher *et al*. 2011). In fact, it has proven that these immune responses triggered by the virus infection are pivotal for the clinical benefit of these type of treatments. However, while the virus contributes to an antitumor immune response by enabled tumor antigen presentation during an active viral infection, neutralizing antiviral measures can impede virus replication and infection of tumor cells (Kaufman *et al*. 2015). How this impacts the therapeutic outcome depends on the interplay between these opposing forces. Should the virus cause an antiviral immune response, it can induce viral clearance, which in turn impacts the induction of tumor immunity. The extent of the influence on tumor immunity may be affected by several variables, primarily the characteristics of the virus and the TME.

The immunogenicity of particularly the Ads is an issue that also extends to its administration. The capsid proteins of the Ad vector elicit a rapid innate immune response upon systemic exposure (Appledorn *et al*. 2008). This response limits the available time for successful infection and systemic spread, which is desired in e.g. metastasize cancers. To increase the spreading of the virus to distal tumors, attempts at reducing OV immunogenicity have been made (Loskog 2015). Particularly regarding CRAd based

therapies, pre-existing immunity is often regarded as a significant hurdle for CRAd functionality and has resulted in the immune system being regarded as an impediment to OV delivery and efficacy (Yamamoto & Curiel 2010; Melcher *et al*. 2011). Local administration seems to circumvent the issue of neutralizing antibodies on therapeutic outcome by resulting in lower levels of antibody formation (Bramson *et al*. 1997; Malmström *et al*. 2010; Yamamoto & Curiel 2010).

There are several ways to improve treatment efficacy of OVs. Some strategies utilize conventional treatments (surgery, radiation therapy, and chemotherapy) in combination with OVs. Chemotherapeutic agents that have been used together with OVs include cisplatin, docetaxel, and 5-fluorouracil/leucovorin (Russell *et al.* 2012; Kaufman *et al.* 2015). The reasoning behind these combinations rely on the expectation that while the OV themselves are unaffected by the concomitant treatments, the virus could target residual cancer (Kaufman *et al.* 2015). Another novel approach is the direct adsorption of tumor-specific peptides onto the surface of OAd through electrostatic interactions, generating a virus known as PeptiCRAd (Peptide-coated Conditionally Replicating Adenovirus) (Capasso *et al.* 2016). The PeptiCrad utilizes the immunogenicity of the OAds to direct the immune response towards the attached exogenous tumor epitopes. This approach has shown great promise in animal melanoma models and holds potential for further adaptions.

The presence of immunosuppressive cytokines and cells (e.g. tumor growth factor beta and regulatory T cells) often impedes the mounting of an antitumor response (Russell *et al*. 2012). In order to target and counteract these tolerogenic functions, the OVs can be genetically armed. The armament of the viruses serves to contribute to direct or indirect tumor cell destruction or alternatively provide increased focus towards eliciting an antitumor response. There is a wide array of genes that can be encoded into the viral genomes, ranging from suicide genes to immunostimulatory genes. Immune genes successfully incorporated into OAds include granulocyte macrophage colony stimulating factor, interferons, tumor necrosis factor-α, interleukin-12, and cytotoxic T-lymphocyte–associated antigen-4 antibody (Cerullo *et al.* 2010; Hirvinen *et al.* 2015; Huang *et al.* 2016).

However, in regards to the gene encoding capacity, it is worth noting that the Ad has evolved an optimized genome and capsid for ultimate aptitude (Kennedy & Parks 2009). As such, the substitution of viral genes with therapeutic genes frequently compromises this balance by altering the interplay between the genome and the physical structure of the virion. Study of the Ad5 has proven that increasing the size of the wild-type viral genome over 105% can results in poor vector growth and rapid rearrangement, leading to loss of the insert (Bett *et al.* 1993). Vectors that in turn retain a net genome size below 105% after DNA insertion are relatively stable and grow well.

In Ad5, an ideal site for transgene insertion is the E3 region because of efficient transgene expression (Hawkins *et al*. 2001). Transgene insertions can disrupt virtually all gene coding sequences in the E3, but because the E3 region is comprised of several transcription units, over seven E3 proteins can be expressed at varying times and amounts during the viral infection. Another area for transgene substitution is in the E1B region (Wold & Toth 2013).

4.3 Systemic Immunity

The cancer-immunity cycle is a sequence of steps required for development of effective antitumor immunity (Chen & Mellman 2013). These steps involve the activation of the adaptive immune system, i.e. the CTLs, an event that has evolved to require specific activation signals. These signals involve antigen presentation on MHC-I, the binding of a costimulatory molecule, and the secretion of specific cytokines (Thaiss *et al.* 2011). The DCs are catalyzers of the aforementioned signals, enabling them to induce and regulate the CTL response towards tumors and viruses. Generally, the DCs are immature and weak antigen presenting cells (APC) that possess a high antigen capture activity, low costimulatory molecule expression, and restricted cytokine secretion (Veglia & Gabrilovich 2017). Following stimulation by pathogens or tissue damage, the activation and maturation of the DCs can be initiated which inverts its characteristics to, for example, reduce the antigen capture activity and a heightened ability for cytokine production.

In OV based therapies, following the successful infection and lysis of tumor cells, several immunogenic components are released into the TME. These compounds include the pathogen-associated molecular patterns (viral particles), danger-associated molecular pattern signals (host cell proteins), and tumor-associated antigens (TAAs) (Kaufman *et al.* 2015). The pathogen-associated molecular patterns and danger-associated molecular pattern signals elicit an immune response through the activation of specific receptors, e.g. Toll-like receptors. In the immunogenic environment that develops, the TAAs are picked up, among other antigens, by APCs in the vicinity. The subsequent presentation of the antigens on the MHC-I of the amassing DC constitutes the first activation step towards DC licensing for cross-priming (Thaiss *et al.* 2011). Furthermore, the binding of the tumor protein partially activates the DCs, prompting them to find a Th1 cell that recognizes the captured antigen, now also presented on MHC-II. When found, Th1 cell can provide the second activation signal for full DC maturation.

The Th1 cells have costimulatory molecules mounted on their outer membrane, one being the CD40 ligand (CD40L). These ligands bind to a corresponding receptor (such as CD40) on the surface of the DC which upon stimulation, licenses the DC for CTL activation by TAA presentation on the MHC-I (Thaiss *et al.* 2011). The DC can acquire this second signal, e.g. in regional lymph nodes where the priming of naïve CTLs also occurs (Thaiss *et al.* 2011; Turley *et al.* 2015). This need for a "second opinion" approval before CTL activation functions as a safety measure to avoid misguided cytotoxicity (Thaiss *et al.* 2011).

To stimulate CTL expansion and differentiation the T cells require, aside from TAA presentation on the MHC-I, the presence of immunomodulatory cytokines which are secreted by the licensed DC (Thaiss *et al.* 2011). The interaction between CD40L and the receptor CD40 is known to primarily induce the production of interleukin-12 as the third signal for CTL activation (Schulz *et al.* 2000). Ultimately, the primed CTLs are guided back to the tumor from the blood stream by chemokine gradients and adhesion molecules to begin the eradication of cells expressing their cognate antigen *(*Turley *et al.* 2015*).* See Figure 7 or the cascade of CTL activation.

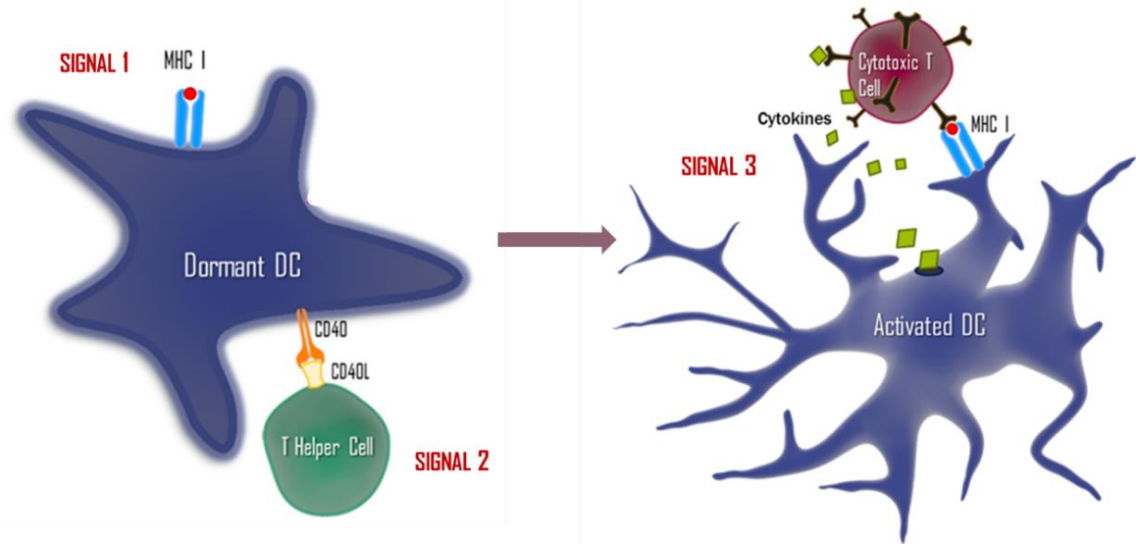

Figure 7: The activation of the cytotoxic T lymphocytes (CTLs) of the adaptive immune system requires three activation signals that are catalyzed by the dendritic cell (DC). The activation signals are the binding of an antigen on the major histocompatibility complex (MHC) (signal 1), the binding of a costimulatory molecule provided by the T helper 1 cell (signal 2), and the secretion of specific cytokines and interleukins by the matured DC (signal 3). The image was constructed using templates provided by somersault18:24.

The tumor cell death has the potential of causing the release of more tumor antigen which upon reaching the draining lymph node can elicit another revolution of the cancer immunity-cycle (Turley *et al*. 2015). Ideally, the cycle culminates in the eradication of malignant cells and development of tumor-specific immunological memory, preventing tumor progression. It is worth noting that the DC and macrophage mediated production of different pro-inflammatory mediators can prove lethal at doses of sufficient magnitude (Wold & Ison 2013). In spite of this, CRAd based treatments are regarded as generally safe and well tolerated in clinical use when administered locally or at low doses (Pesonen *et al*. 2012; Buijs *et al.* 2015).

The DCs are essential for antitumor activity, however, simultaneously they are known to function inefficiently in cancer (Veglia & Gabrilovich 2017). Stromal cells in the TME express molecules, such as interleukins-6 and 10, that can inhibit immune activation by suppressing Th cells and CTLs as well as activating immunosuppressive myeloid cells (Turley *et al.* 2015). Numerous approaches have been considered to counteract the tolerogenic environment propagated by the tumor cells and TME.

4.4. Premise of the Thesis

Immune activation is a key aspect in OV efficacy since it is critical for positive treatment outcome. Regarding the adaptive immune system activation cascade, one area of improvement is found in acquiring the second activation signal. This stage requires the partially activated DC to find the correct Th1 cell while under the tolerogenic pressure of the tumor. Furthermore, as stated in an article by Loskog (2015), in the absence of cytokine production and sufficient costimulation, the T cells are tolerized rather than activated against the antigens presented by the DCs.

The most straightforward solutions to aid in DC maturation is the expression of the costimulatory molecule directly in the tumor, utilizing genetic arming of an OAd. This approach would enable quick successive acquisition of the two first activation signals by the DC, thus shortening the time required to mount an immune response. The transgene chosen for the study was one of the most potent costimulatory molecules, the CD40L, also known as CD154.

The CD40 ligand is a 33 kilodalton type II transmembrane protein of the tumor necrosis factor superfamily, expressed on the surface of both hematopoietic and non-hematopoietic cells (Aloui *et al.* 2014). The protein consists of three domains, intracellular, transcellular, and extracellular, binding mainly to the 48 kilodalton CD40 receptor, constitutively expressed on APCs (Henn *et al*. 2001; Aloui *et al*. 2014). Natively, the CD40L is a membrane bound protein, but a soluble form has been identified. The 18 kilodalton soluble CD40L is shed from membrane bound CD40L on activated T cells and platelets by protease mediated cleaving of the extracellular domain (Aloui *et al*. 2014). Trimeric recombinant soluble CD40L has been found biologically active and able to initiate similar functions as the membrane bound form, one being the activation of DCs (Mazzei *et al*. 1995; Mclellan *et al*. 1999).

Ultimately, the hypothesis of the thesis crystallized into the cascade presented in Figure 8. Following successful infection of the OAd5, the CD40L would be expressed and released alongside TAA upon tumor cell lysis. Binding to the CD40 receptor on partially

activated DC, the matured DC could travel to a regional lymph node and prime naïve CTLs. Once activated, the CTLs, would expand and return to the infected tumor and successfully destroy the remaining tumor cells. Simultaneously, the cytotoxic cells would also scourge the body and eradicate any secondary tumors they may come upon, effectively curing the patient.

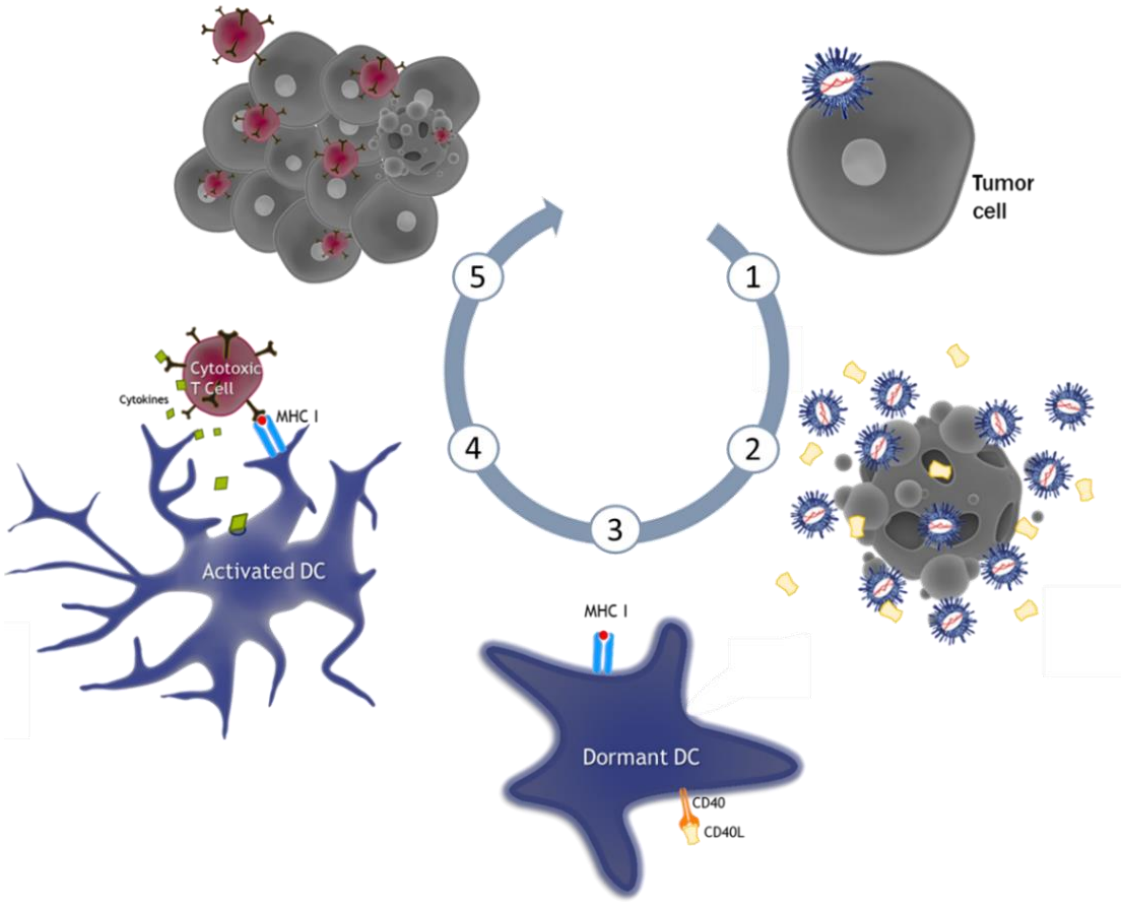

Figure 8: The hypothesis to acquire improve adaptive immune system activation and immunity. Infecting tumor cells with CD40L armed OAd5 (1), viral progenies and the transgene are released upon cell lysis (2). The tumor-associated antigen (TAA) and CD40L binding (3) enable DC maturation that subsequently allows naïve cytotoxic T cells to be primed (4) and return to destroy the remaining tumor cells (5). Additionally, tumors encountered elsewhere in the body are also eradicated. The image was made with the aid of templates from somersault18:24.

5 AIMS

In of the thesis, protocols would be established for the cloning, screening of colonies, and primary virus production. Four different transgene variants would be required for the subsequent *in vitro* and *in vivo* studies. To generate the armed OAd there were three distinct aims that needed to be met.

I. Generate four recombined replication-deficient Ad constructs by homologous recombination that carry the transgenes encoding for human or mouse variants of membrane bound or soluble CD40L.

II. Primary virus and appropriate stock production of all constructs by transfection into a virus producing cell line as well as virus propagation and titer determination.

III. Elucidation of transgene expression and functionality by immunostaining, fluorescence microscopy, Western blotting or ELISA, and Ramos-Blue™ cells and QUANTI-Blue™ assay.

6 MATERIALS AND METHODS

The following chapter is dedicated to the methods and materials in the generation of the Ad5Δ24-CD40L virus. After first recounting the utilized materials, the methods are described for the cloning, screening, transfection, and immunostaining in their respective sections. Supplementary information is provided in the appendices when necessary.

6.1 Transgenes and Plasmids

The transgenes in the study encoded for the CD40L of human and mouse species. There were two forms of the proteins, the native membrane bound form (also referred to as the full-length) and the soluble form. The soluble form was designed based on the CD40L protein information relayed by the UniProt database, with an additional signal peptide incorporated to ensure excretion upon expression. The full-length CD40L amino acid sequence was used without further modification, more details on these sequences are found in APPENDIX 1. The abbreviations for the different transgenes used from here on are relayed in Table 3.

Table 3: The four different constructs design for the study. Human and mouse variants of CD40L full-length and soluble transgenes.

Description	Human	Mouse
Full-length	hCD40L-FL	mCD40L-FL
Soluble	hCD40L-S	mCD40L-S

The transgenes were ordered from GeneArt™ with lengths of 786 bp for human full-length, 783 bp for mouse full-length, and 510 bp for the soluble CD40L of both human and mouse origin. In preparation for the cloning, the transgenes were transferred from the shipping vector to an in-house shuttle plasmid, the pTHSN, possessing the antibiotic resistance gene for ampicillin. The final sizes of the pTHSN carrying the CD40L (pTHSN-CD40L) were ca 6,800 bp (full-length) and 6,500 bp (soluble). A plasmid map of the empty pTHSN is presented in Figure 9.

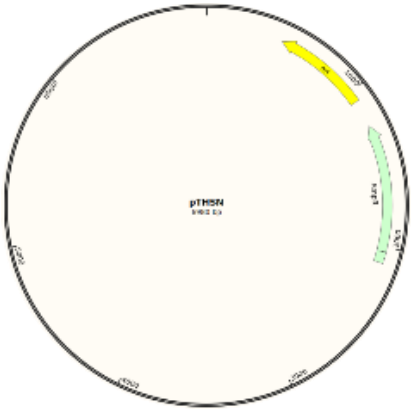

Figure 9: The shuttle plasmid pTHSN without a transgene, visualizing the location of the ampicillin resistance gene (green arrow) and the origin of replication (yellow arrow). The plasmid map was made in SnapGene Viewer.

Aside from the pTHSN, the other plasmid used in the study, also found in-house, was the rescue plasmid pAd5Δ24. Alternatively referred to as the backbone plasmid, it contained the whole Ad5 genome aside from a Δ24 deletion, giving it a size of ca 38,800 bp. The antibiotic resistance gene in the rescue plasmid was kanamycin. A plasmid map of the pAd5Δ24 is presented below in Figure 10. The final plasmids would with the full-length transgenes be ca 38,600 bp and the soluble transgenes ca 38,400 bp.

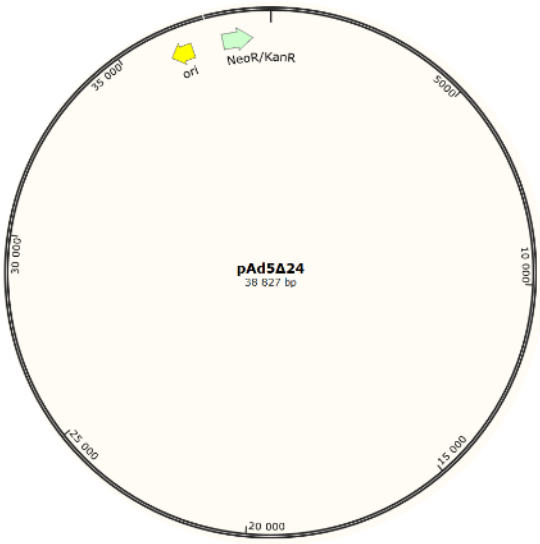

Figure 10: A depiction of the rescue plasmid pAd5Δ24 with the locations of the kanamycin resistance gene (green arrow) and origin of replication (yellow arrow). The plasmid map was made in SnapGene Viewer.

6.2 Cells

Bacteria and mammalian cells were employed in the study. Three *Escherichia coli* (*E. coli*) strains were utilized during the cloning process while a mammalian cell line was required for the virus production. The competent *E. coli* JM109, BJ5183, and XL10-Gold were all purchased from Agilent Technologies and stored at -80 °C only to be thawed on ice briefly preceding transformation. In culture, all *E. coli* were grown in Luria-Bertani medium (LB, Media Kitchen) and incubated at 37 °C and shaking (200-250 rpm) in 14 ml Falcon® round bottom snap cap tubes (Corning®, cat no: 352059).

The JM109 cells (Agilent Technologies, cat no: 200235) are chemically competent recombination proficient *E. coli* and in this instance utilized solely for the stock production and amplification of pAd5Δ24 and pTHSN at the very beginning of the study. The other recombination proficient *E. coli* was the BJ5183 cells (Agilent Technologies, cat no: 200154) that are electroporation competent cells. The BJ5183 cells were utilized in the homologous recombination. The only recombination deficient *E. coli* strain in the study was the XL10-Gold ultracompetent cells (Agilent Technologies, cat no: 200315). This strain was utilized for plasmid preservation and amplification for potentially recombined plasmids in homologous recombination and Gibson Assembly®. Aside from retaining the integrity of transformed plasmids, the XL10-Gold are also well suited for large constructs.

The only mammalian cell line in the study was the A549 cells (ATCC). These are adherent human lung carcinoma epithelial cells suitable for virus production and amplification. The culture conditions for the A549 cells are 37 °C and 5% CO_2 in complete Dulbeccos Modified Eagle's Medium (DMEM) 1 g/L glucose (Lonza, cat no: BE12-707F/12) supplemented with 10% heat-inactivated fetal bovine serum (Gibco™, cat no: 10500064), 1X (2mM) L-glutamine (GlutaMAX™ supplement, Gibco™, cat no: 35050061), and 1X penicillin-streptomycin (100 U and 0.1 µg/µl respectively) antibiotics (Pen Strep, Gibco™, cat no: 15140122).

6.3. Cloning

A large part of the study pertains to the cloning process and the screening for the recombined plasmid (pAd5Δ24-CD40L). The two methods utilized in the cloning were homologous recombination and Gibson Assembly®. All generated clones underwent the same screening process for the detection of the positive recombined clone. During the cloning, other methods such as electrophoresis and spectrophotometry were repeatedly employed.

Spectrophotometry is utilized for concentration measurement of DNA after for example plasmid isolation and purification or DNA precipitation. For this, the SPECTROstar® Nano (BMG LABTECH) was utilized. The DNA concentration could be determined by nucleic acid quantitation based on nucleic acids absorption of UV light. The concentrations were measured on an LVis Plate with solvent as a blank, which as a rule was sterile water (MQ). Spectrophotometry was also used for determining the purity of the samples by measuring the ratio between absorbance at the wavelengths 260 nm and 280 nm, i.e. 260/280 value.

Electrophoresis is the separation and visualization of DNA fragments. The method is based upon the negative charge of DNA that generates migration through the mesh of the gel from the negative to the positive node when an electric current is applied. The rate and ease with which this movement occurs depends on the size and conformation of the fragment. Smaller fragments and supercoiled (SC) DNA can move forward with more ease whereas larger circular fragments and linearized DNA are retained longer in the network of the gel, thereby creating a band pattern. In this study, the electric currents ranged between 60 and 100 volts (though generally 70 volts) and were applied for 1-2 hours, depending on the samples.

Generally, the analysis gels consist of either agarose or polyacrylamide, the latter providing a more pronounced separation of fragments close in size. The gels used in this project were made from agarose in different concentrations. The tighter gels (1.5% and 2%) were utilized when separating smaller fragments and the looser gels (0.6% and 0.8%)

for larger fragments. The different percentages were attained by dissolving TopVision agarose tablets (Thermo Fisher Scientific™, cat no: R2801) in 1X Tris-acetate-EDTA (TAE) buffer diluted in MQ (50XTAE, Media Kitchen), which was also used as the running buffer during electrophoresis.

For DNA visualization SYBR® Safe DNA Gel Stain (Thermo Fisher Scientific™, cat no: S33102) was mixed into the melted agarose and DNA Gel Loading Dye (Thermo Fisher Scientific™, cat no: R0611) added to the samples for a final concentration of 1X, which facilitated sample loading into the wells of the gel. Two size markers were primarily used: λ DNA-Mono Cut Mix (New England Biolab®, cat no: N3019S) for bands over 35,000 bp and GeneRuler 1 kb (Thermo Fisher Scientific™, cat no: SM0314) for bands under 10,000 bp. The size marker GeneRuler DNA ladder mix (Thermo Fisher Scientific™, cat no: SM0331) was used together with BlueJuice™ loading buffer (Thermo Fisher Scientific™ cat no: 10816015) for the first two gel runs.

6.3.1 Homologous recombination

Homologous recombination is the traditional way for cloning adenoviral vectors. In this method, the transgene is transferred to the desired location in the rescue plasmid with the help of homologous regions flanking the transgenes in pTHSN and E3-gp19k in pAd5Δ24. These homologous regions are identical sequences that can be used to essentially switch the transgene into the pAd5Δ24 by replicating bacteria. The general concept of the method is displayed in Figure 11 below.

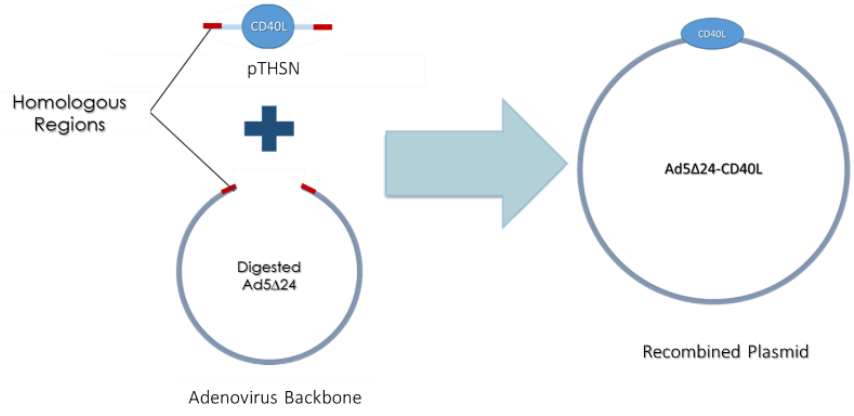

Figure 11: A schematic representation of the homologous recombination using the homologous regions.

In the first attempt, all four pTHSN-CD40L were used separately in the recombination with pAd5Δ24. To begin with, all plasmids needed to be linearized prior to transformation. The restriction enzyme EcoRI (New England Biolab®, cat no: R0101S) was used for pAd5Δ24, excising a part of the E3 region from the backbone, and SpeI (New England Biolab®, cat no: R0133S) for pTHSN-CD40L. The amount of pTHSN-CD40L DNA digested of each plasmid was 20 µg in a 50 µl reaction volume with 2 µl SpeI. Conversely, 2 µl EcoRI enzyme was added to a 100 µl reaction with 10 µg pAd5Δ24 DNA. After confirming successful digestion of the plasmids with electrophoresis on a 0.6% agarose gels (Thermo Fisher Scientific™, cat no: R2801), the 5' end of pAd5Δ24 was dephosphorylated with calf-intestine phosphatase (CIP, New England Biolab®, cat no: M0290S) to minimize the extent of the background due to recircularization. The reaction conditions were for all enzymes incubation in a 37 ˚C water bath for generally one hour in their respective buffers.

To desalt the cleaved plasmids and remove the enzymes, the DNA was precipitated with ethanol. Adding 0.1 volumes of 3 M sodium acetate (pH 5.2, Media Kitchen) to each digested plasmid, the mixtures were briefly vortexed before adding 2.5 volumes of -20 °C 100% ethanol. After another quick vortex, the mixtures were incubated at -20 °C for at least an hour. Centrifuging the mixture at 16,000XG and 4 °C for 20 minutes, the precipitated DNA became visible as small slightly opaque pellets. Carefully decanting the supernatants, the pellets were washed at least once with 1 ml cold 70% ethanol before repeating the centrifugation at 16,000XG for 5 minutes. Removing the supernatants, the pellets were air-dried ca 10 minutes before dissolution in suitable volumes of MQ.

In the electroporation, the linearized pTHSN-CD40L and pAd5Δ24 were transformed to BJ5183 cells with a short electric shock to permeabilize the bacterial membrane. As recommended by the cell manufacturer, 1 µg pTHSN-CD40L and 0.1 µg pAd5Δ24 was added to 40 µl bacteria. Transferring the mixtures into chilled Gene Pulser®/MicroPulser™ cuvettes with a 0.2 cm gap (Bio-Rad, cat no:1652086), the cells were pulsed once in the MicroPulser™ Electroporator (Bio-Rad). The program for *E. coli* cells in a 0.2 cm cuvette was the Ec 2 which delivers a shock of 2.50 kilovolts.

After the electroporation, the cells were grown in LB broth without antibiotics at 37 °C and shaking to allow their metabolism to commence. An hour later, the bacteria were plated in suitable amounts (100 µl, 300 µl, and any remaining volume) onto LB plates containing 25 µg/ml kanamycin (Media Kitchen). Following incubation at 37 °C for 48 hours, ten of the smallest colonies of each construct were plated onto fresh LB-kanamycin plates and incubated for another two nights before transferring them to 4 °C for storage.

In the second attempt, only the mouse variants of pTHSN-CD40L were applied (soluble and full-length). This time, the pTHSN-mCD40L plasmids were digested with the restriction endonucleases SpeI and NdeI (20 µg pTHSN-mCD40L DNA and á 2 µl enzyme in one 50 µl reaction). Performing the rest of the protocol as previously described for the first attempt, the colonies were grown for 72 hours at 30 °C after which they were analyzed directly instead of streaking them onto new plates. Aside from an optimization of the screening, the cloning process was otherwise largely the same as described for the first attempt.

6.3.2 Gibson Assembly®

In Gibson Assembly®, a polymerase chain reaction (PCR) amplified fragment with the human full-length CD40L was transferred into the linearized pAd5Δ24 with the use of designed overlap regions that should preferably be between 15 to 80 bp long. The two DNA strands can be recombined in the presence of select enzymes, which are: exonuclease, DNA polymerase, and ligase. These are introduced with the Gibson Assembly® Master mix.

The Gibson Assembly® reaction can be divided into three steps according to the functions of the different enzymes. First, the exonuclease cleaves the DNA strands from their 5’ end, one nucleotide at a time. The subsequently exposed 3’ strand of the backbone and the insert anneal with the aid of overlaps. Second, DNA polymerase repairs any remaining gaps before, third, the two DNA strands are sealed together with ligase, simultaneously removing potential nicks. Applying the reagents and positive control from the Gibson Assembly® Cloning Kit (New England Biolabs®, cat no: E5510), the reactions were run

at 50 °C for a duration of 15 minutes in a thermal cycler (T100™ Thermal Cycler, Bio-Rad). The idea behind the Gibson Assembly® and the functions of the different enzymes are depicted below in Figure 12.

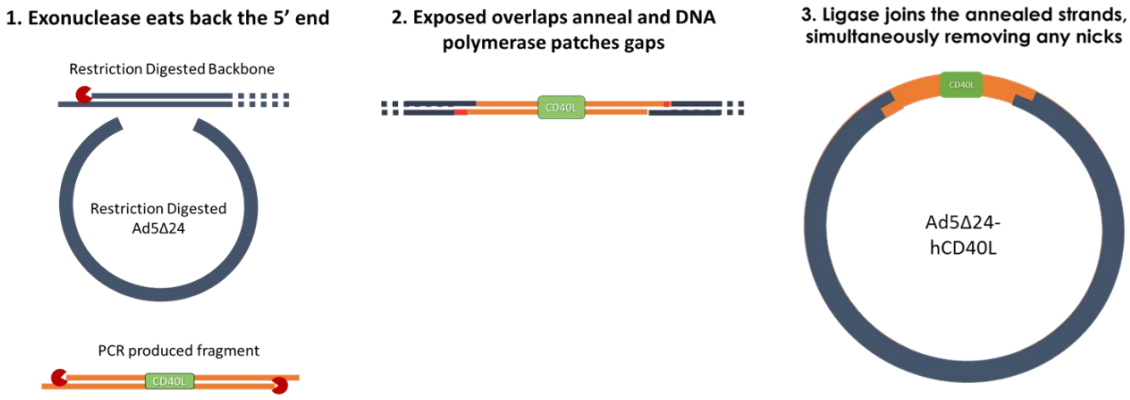

Figure 12: The three main steps in the Gibson Assembly® reaction employing the use of exonuclease, DNA polymerase, and ligase to join two DNA strands together. The approach enables recombination without the need of bacteria, requiring only incubation at 50 °C for at least 15 minutes.

To begin with, an insert with the CD40L transgene was amplified with PCR to incorporate the overlaps to insure correct orientation during annealing and ligation of the PCR fragment into the backbone. The hCD40L-FL was chosen for the pilot run of this method, the primer sets designed to create the different overlaps gathered in Table 4. Per the manufacturers instruction, a high-fidelity DNA polymerase was chosen for the insert amplification, the Phusion DNA polymerase (Thermo Fisher Scientific™, cat no: F530S). As DNA template, 1 ng of pTHSN-hCD40L-FL.

Table 4: The two primer sets used for the PCR amplification of CD40L inserts with varying overlaps of 18 to 34 bp. The T_m for the forward primer I is calculated from the highlighted area while for the other sequences the T_m is calculated for the whole primer.

Primers	Orientation	Sequence	T_m	Overlap
Gibson Reaction I Primer Set	Forward	5'- AAT ACT GCG CGC TGA CTC TTA AGG **ACT AGT TTC GCG CCC TTT C** -3'	57 °C	24 bp
	Reverse	5'- GTA AAT TTC ATA ATT AAA GAA TTC TAA GAA GCT C –3'	56 °C	34 bp
Gibson Reaction II Primer Set	Forward	5'- GCC CAC CGA AAC CGA ATT -3'	56 °C	18 bp
	Reverse	5'- GTA AAT TTC ATA ATT AAA GAA TTC TAA GAA GCT C –3'	56 °C	34 bp

There was a total of three Gibson Assembly® reactions in the study. The first two applied backbones that were digested using either EcoRI or SpeI and EcoRI-HF (High Fidelity, New England Biolab®, cat no: R3101S) restriction endonucleases and corresponding inserts. The third approach was intended as a control, the single digested backbone combined with an insert designed for the double digested backbone. The double digested pAd5Δ24 reaction was named Gibson Reaction 1 and the single digested Gibson Reaction 2.

Because of the previously designed flanking homologous regions, the overlap was generated automatically for almost all the primers. However, in the Gibson Reaction I a 24 bp sequence needed to be added to the 5' end of the forward primer to generate the left-hand overlap. In the initial polymerase reaction, only the 19 bp long highlighted area in Table 4 will attach to the pTHSN-hCD40L, integrating this new sequence which will thereafter be replicated as part of all the following amplified insert fragments. A detailed recounting of the components of the master mix and the PCR cycle are presented in APPENDIX 2. The amplification of the CD40L containing fragment was confirmed with electrophoresis on a 0.8% agarose gel from which the DNA amount was estimated with the GeneRuler 1 kb size marker.

The backbone digestions were done with 10 µg plasmid DNA in a 50 µl reaction with 2 µl of each enzyme in the double-digestion and 2 µl in the single-digestion. The high fidelity EcoRI restriction enzyme was applied in the double digestion to enable the addition of both enzymes to the same reaction (100% activity of SpeI and EcoRI-HF in CutSmart® buffer). As controls, the backbone was also digested with the SpeI and EcoRI-HF separately.

Following successful digestion of the pAd5Δ24, heat-inactivation of the enzymes, and dephosphorylation with CIP, the differently digested backbone DNA were precipitated with ethanol as described previously (page 34). Details regarding the backbone preparation for the Gibson Assembly® are recounted in APPENDIX 2. The DNA was resuspended in MQ and the concentration determined with spectrophotometry.

The optimal DNA quantities were calculated according to Equation 1 per the kit manufacturer's instructions. The quantities ultimately used were 0.05 pmol PCR fragment, 0.02 pmol of the SpeI and EcoRI-F digested backbone, and 0.03 pmol of the EcoRI digested backbone. Less of the double-digested backbone was used to minimize the introduction of disturbing elements from the digestion to the assembly reaction. Backbone and corresponding PCR fragments were added to 1X Gibson Assembly Master mix and MQ for a final volume of 20 µl. Loading the reactions onto eight tube strips from a FrameStar® Break-A-Way 96-well PCR plate (4titude) with flat capped removable strips, the assembly conditions were 50 °C for 15 minutes before being moved to -20 °C to await transformation. Aside from combining the single digested backbone with the wrong insert as a negative control, the positive control provided with the Gibson Assembly® kit was also utilized.

$$\text{pmols} = (\text{weight in ng}) \times 1{,}000 / (\text{base pairs} \times 650 \text{ Daltons})$$

Equation 1: The formula utilized in calculating the number of pmol for the fragments to ensure optimal assembly.

As recommended by the manufacturer, the Gibson Assembly® reaction was diluted 1:4 prior to transformation to XL10-Gold cells. The transformation to the recombination deficient ultracompetent bacteria XL10-Gold was accomplished with heat shock. Prechilling all equipment used to handle the bacteria prior to the transformation, the cells were thawed on ice and divided into 50 µl aliquots. After incubating the cells with β-mercaptoethanol to improve the transformation efficiency, 2 µl of the diluted Gibson Assembly® reaction was added to an aliquot of bacteria. Following a 30-minute incubation period to allow the DNA to attach to the outside of the bacteria, the DNA was internalized with a 42 ˚C heat-pulse lasting 30 seconds. Chilling the bacteria on ice for 2 minutes afterwards, prewarmed 42 ˚C NZY^{+} broth (Media Kitchen) was added and the bacterial solution incubated for an hour under shaking at 37 ˚C. Finally, the bacteria were plated on LB-kanamycin plates and incubated overnight at 37 ˚C.

6.4 The Screening Process

Whether after homologous recombination or Gibson Assembly®, identifying the correctly recombined plasmid was essential and therefore several control points were implemented throughout the cloning process. The three main screening methods employed served to confirm the presence of various critical elements of the final recombined plasmid, providing increasing confidence in that the final construct was the correct one, without the need for sequencing. First was the positive selection of transformed bacteria that carried either the backbone or recombined plasmid through antibiotic selection, second colony PCR to isolate the bacteria with the transgene, followed by the third and final control point, restriction analysis, to establish the presence of the transgene in the backbone as well as the retained integrity of vital areas of the construct.

The antibiotic selection during cloning is a standard procedure and was a process that underwent no modification during the presented study, the antibiotic resistance gene and placement being predetermined. The colony PCR was a protocol implemented and improved throughout the different cloning attempts and will be presented along with the restriction analysis in greater detail in the section below.

6.4.1 Colony Polymerase Chain Reaction

Colony PCR is a robust high capacity screening method employing the speed of PCR and the selectivity of the primers in the analysis of a large quantity of bacterial colonies for the desired insert. The process involves picking a single bacterial colony, adding it to the PCR reaction to provide a template, and then preserving the colony by inoculating it in 5 ml of LB with antibiotics. Inoculation allows for further expansion of the bacteria that give a positive signal, implicating them as possible carriers of the recombined plasmid; Figure 13 visualizes the colony PCR process.

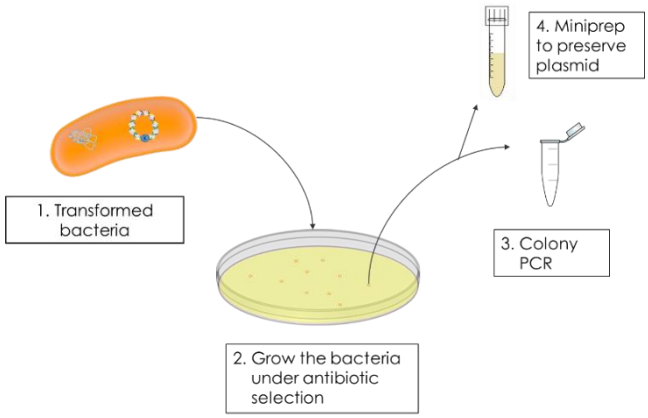

Figure 13: The steps in colony PCR from how the colony is analyzed to how the bacteria is preserved. Transformed bacteria are grown under antibiotic selection on an LB plate, after which the colonies are picked for colony PCR and the plasmid preserved by inoculation into 5 ml LB with antibiotics.

Forward and reverse primers were designed that bound to ca 20 bp long sequences flanking the transgenes. The location of the recognition sequences for the primers in relation to the transgenes enable the use of the same primers for all four intended constructs. Four primer sets were vetted, out of which two were chosen for the colony PCR (Table 5). As the protocol was optimized in the second homologous recombination attempt, only one primer set was ultimately used, consisting of the forward primer from Primer Set I and the reverse primer from Primer Set II. Furthermore, while initially the high-fidelity DNA polymerase Phusion was utilized in the screening, it was later replaced by DreamTaq DNA polymerase (Thermo Fisher Scientific™, cat no: EP0702). The latter polymerase lacks proof-reading abilities, but provided sufficient accuracy at a lower cost for this application.

Table 5: The primer sets used in colony PCR, first separate and later by combining the forward primer of Primer Set I and the reverse primer of Primer Set II.

Primers	Orientation	Sequence	Tm °C Phusion	Tm °C DreamTaq
Primer Set I	Forward	5'– ACG CGG AGG CTC TCT TCA GTA –3'	67.7	62.1
	Reverse	5'– CCG GAC GGA GAC CAA GCG –3'	71.9	63.8
Primer Set II	Forward	5'– CCC AGA CGG AGT GAG TCT AC –3'	61.9	58.5
	Reverse	5'– CCT GAC TTC AAG GTT GTA GCG–3'	64.1	57.3

Different approaches were tested for the addition of the bacterial template. Generally, the colony is analyzed by touching a pipette tip to it and then dipping the tip in the PCR master mix. The approach that proved most effective in this study was the inoculation of colonies in 5 ml of LB with 25 µg/ml kanamycin (Media Kitchen) and growing them under shaking overnight at 37 °C. In the morning, 30 µl of the inoculate was diluted in 70 µl MQ and then boiled for 10 minutes at 98 °C to ensure release of the plasmid. Finally, 20 µl of mixture was added to the prepared PCR reaction. The dilution was essential, both to reduce the inhibitory effect of the LB, as well as to reduce the amount of template added to the reaction. The amount of MQ was reduced from the final volume added to the master mix for a correct final concentration of the components.

All PCR reactions were pipetted on ice and the preparations for the PCR reactions were performed at a different site to the subsequent analysis of the PCR amplified products to avoid DNA cross-contamination. The reactions occurred on eight tube PRC strips with positive (pAd5Δ24 SC) and negative controls (MQ). A detailed description of the reagent concentrations in the master mix as well as the PCR cycle are found in APPENDIX 3. The colony PCR reactions were analyzed on a 2% agarose gel to determine the possible presence and size of PCR amplified product. The bacteria in the 5 ml inoculums for the colonies that gave positive signals were collected in 2 ml microcentrifuge tubes. The plasmid DNA was extracted with QIAGEN® Plasmid Minikit (ref no: 12123) following the instructions provided with the kit (APPENDIX 4). The formed plasmid DNA pellet was resuspended in MQ and transferred to -20 °C for storage until further analysis.

6.4.2 Restriction Analysis

Restriction analysis was employed to assess the presence of all desired elements in the recombined plasmid which would be needed for the subsequent virus production. In restriction analysis, it is presupposed that a plasmid has a definite number of restriction enzyme sites. When cleaved with their respective enzymes, the result will be a certain number of bands of a certain size that can then be separated on an analysis gel to give a band pattern. The band pattern can in turn be utilized in judging the presence of certain

components in the plasmid. In this study, the elements of special interest were the successful integration of the transgene and the retained integrity of the area by the ITRs.

Three different restriction enzymes were utilized in the study: PacI (New England Biolab®, cat no: R0547S), HindIII (High Fidelity, New England Biolab®, cat no: R3104S), and BamHI (High Fidelity, New England Biolab®, cat no: R3136S). The PacI digestion ascertained the integrity of the area by the ITRs which is crucial for the primary virus production. The BamHI and HindIII were, in turn, utilized in the detection of the transgene in the backbone, the BamHI for the mouse variants and the HindIII for the human variants. The expected restriction sites in the final recombined plasmid for all three restriction enzymes are displayed in Figure 14. A detailed account for reagent amount in each restriction digestion is gathered in APPENDIX 5.

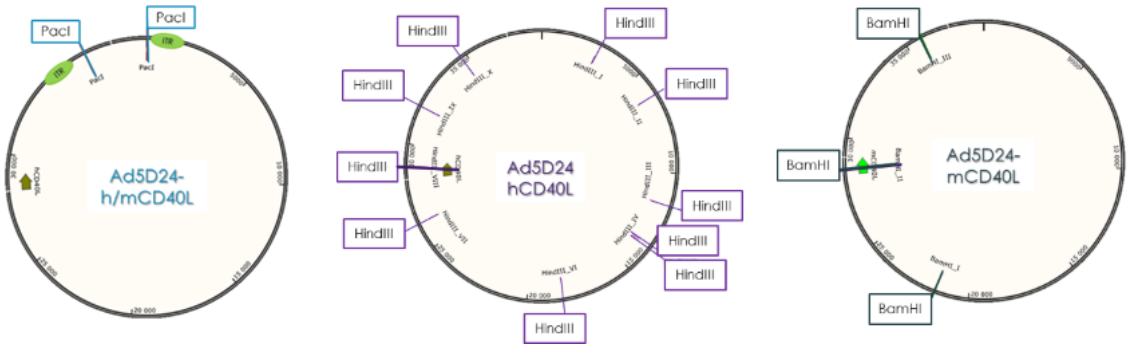

Figure 14: The restriction enzyme sites for (from left to right) PacI, HindIII, and BamHI in the recombined pAd5Δ24-CD40L.

All digestion reactions were prepared on ice and subsequently incubated at 37 °C for 1-2 hours before being moved onto ice. Cleaved plasmid DNA was added to the wells and separated according to size with electrophoresis on 0.8% agarose gels. The generated band patterns were compared to an expected pattern predicted based on the plasmid maps. The empty pAd5Δ24 was used as a control in all restriction reactions.

6.5 Transfection

In preparation for the transfection of the recombined plasmids to the A549 cells, sufficient plasmid DNA was needed. Therefore, the Gibson Assembly® generated plasmids and empty pAd5Δ24 were transformed to XL10-Gold cells with heat shock for plasmid

amplification. Following the transformation protocol provided by the manufacturer, the bacteria were afterwards grown under 25 μg/ml kanamycin selection on LB plates. Inoculating single bacterial colonies in 5 ml LB and 25 μg/ml kanamycin, the bacterial solutions were ultimately increased to 135 ml preparations. After growing the bacteria to an optical density at 600 nm of ca 4, the bacterial solutions were transferred for long-term storage in 1 ml 15% glycerol (99.5% glycerol stock, Media Kitchen) preparations.

The remaining bacteria were then harvested and the plasmids purified with the Nucleobond XtraMidi kit (Macherey-Nagel, cat no: 740410.50); a detailed account of the manufacturers protocol is provided in APPENDIX 6. Afterwards, all plasmids were cleaved using PacI restriction endonuclease in two separate reactions, each containing 5 μg DNA, followed by electrophoresis. After confirmed digestion, the two restriction reactions were purified. The A549 cells were taken into culture, grown in complete DMEM and split in the ratio 1:4 two to three times a week at around 80-90% confluency in T75 ventilated cap flask (Sarstedt order no: 83.3911.002). The transfection was first attempted with the ViraPack Transfection Kit (Agilent Technologies, cat no: 200488), followed by the QIAGEN® Effectene Transfection Reagent (QIAGEN®, cat no: 301425).

Prior to the ViraPack transfection, the duplicate DNA samples were pooled by running them through the QIAGEN-tip 20 from the QIAGEN® Plasmid Minikit. The recovery of DNA was tested prior with 20 μg pAd5Δ24 DNA which according to the user manual was the maximum preparation capacity of high-copy plasmid or cosmid DNA. For the DNA purification, the tips were equilibrated with 1 ml Buffer QBT, after which the DNA was applied dropwise in 50 μl aliquots. Washing the columns twice with 2 ml Buffer QC, the DNA was eluted with 65 ˚C warm 0.8 ml Buffer QF. Finally, the DNA was precipitated with 0.56 ml room temperature isopropanol by centrifugation at 4 ˚C at 16,000XG for 30 minutes. Washing the DNA with room temperature 70% ethanol, the DNA was precipitated anew before air drying and resuspension in 25 μl MQ. The purification method above was not repeated for the QIAGEN® Effectene transfection, where the DNA was simply precipitated with ethanol (see section 6.5.1 on page 44 for more details).

6.5.1 ViraPack Transfection

The ViraPack transfection kit user manual details that the kit utilizes the calcium orthophosphates method that enables transfection by increasing cell membrane adsorption and subsequent uptake of DNA by the cells. To begin with, A549 cells were grown to 80% confluency before trypzinizing them with 1X TrypLE™ Express Enzyme (Gibco™, cat no: 12604013) for 10 minutes. Gently tapping the sides of the bottle to ensure all the cells are dislodged, the enzyme is inactivated with addition of fresh complete DMEM media. Washing the cells slowly along the bottom of the flask, potential clusters of cells are resuspended before transferring a portion of the cells to a new T75 flask for continuation.

A 5-ml portion of the cell suspension was diluted 1:1 in fresh media and briefly vortexed to assure homogenous suspension of the cells. Mixing 10 µl of the dilution with an equal volume trypan blue, 10 µl was pipetted into a Countess® cell counting chamber slide (Thermo Fisher Scientific™, cat no: C10228). Details from the cell counting is gathered in APPENDIX 7. The transfection was done in T25 ventilated cap flasks (Greiner, cat no: 690175) at a cell density of 250,000 cells/flask, which amounted to 144 µl of the cell suspension to 5 ml complete media. The cells were then incubated overnight.

On the day of infection, around 1 µg DNA of two recombined Gibson plasmids, pAd5Δ24, pAd5/3Δ24, and a green fluorescent protein (GFP) plasmid were prepared for transfection in sterile BD Falcon® 5 ml polystyrene round bottom tubes (BD Biosciences, cat no: 352235) according to the ViraPack Transfection Kit instructions. The empty pAd5Δ24 and pAd5/3Δ24 (in-house) were controls for the virus production while the GFP plasmid functioned as a positive control for the transfection.

During the transfection, DMEM containing 1X glutamine and 6% modified bovine serum solution was used according to the manufacturers recommendations. After adding the DNA to the cells, the transfections were incubated for three hours at 37 °C and 5% CO_2. Removing the media, the cells were washed with 1X phosphate-buffered saline (PBS, Media Kitchen) thrice before ensuring the complete removal of DNA complex

precipitate. Exchanging the PBS with 5 ml complete DMEM the cells were incubated at 37 ˚C and 5% CO_2. The transfections were observed during a week for cytopathic effect (CPE), replenishing the growth medium as needed according to its color. The GFP transfected cells were monitored for fluorescence to determine the success of the DNA transfection. A detailed account of the protocol provided by the manufacturer can be found in APPENDIX 8.

6.5.2 QIAGEN® Effectene Transfection

The Effectene Transfection Reagent is described by QIAGEN® as a nonliposomal lipid formula that together with the DNA enhancer and DNA-condensation buffer offer a high transfection efficiency. The transfection is achieved by the Effectene reagent coating the enhancer condensed DNA molecules with cationic lipids, enabling the complex to transfer into the cell. The possibility of carrying out the transfection in the presence of serum provide low cytotoxicity, making the transfection highly suited for sensitive cell lines or primary cells. Furthermore, for most cell types there is no need to remove the transfection-complex.

To begin with, the A549 cells were cultured to around 80% confluency at which point they were trypsinized and counted in the same manner as described on page 44; details of the cell count are found in APPENDIX 7. With a desired cell density of 800,000 cells per T25 ventilated cap flasks (Sarstedt, order no: 83.3910.002), a volume of 364 µl was added per 5 ml complete DMEM. While incubating the flasks for 2 hours, DNA dilutions were prepared for the transfection with the QIAGEN® Effectene Transfection Reagent. Following the instructions provided by the manufacturer (see APPENDIX 9), the transfection was performed with the same plasmids as in the ViraPack transfection. Around 1 µg DNA was used for all constructs, except the second recombined plasmid where only 0.25 µg DNA was added. The cells were incubated in complete media at 37 ˚C and 5% CO_2 and monitored in the manner described for the ViraPack transfection for signs of GFP and CPE.

After QIAGEN® Effectene Transfection, the transfected A549 cells were harvested upon detection of sufficient CPE. Gently tapping the sides of the dishes to dislodge any attached cells, the cell suspension was transferred to 15 ml centrifuge tubes (Sarstedt, order no: 62.554.502). Separating the cells from the media by centrifugation at 500XG for 10 minutes at 4 °C, all but 2 ml of the supernatant was removed. Resuspending the cells by vortex, the cell suspensions were subjected to four freeze-thaw cycles to free the primary virus from within the cells. The freeze-thaw cycle consisted of freezing at -80 °C and rapid thawing in a 37 °C water bath. The centrifugation of the suspension was repeated at 500XG and 4 °C for 10 minutes after the fourth round. To amplify the primary viruses, the supernatants or viral lysates (á 2 ml for each virus) were pipetted to separate T75 flasks with A549 cells in complete DMEM at around 80-90% confluency and incubated between three to six days, depending on the development of CPE. Next, the presence of the virus and the expression of CD40L was confirmed with immunostaining.

6.6 Immunostaining

Following a round of virus amplification, the produced viruses were analyzed with immunostaining, using antibodies for the hexon and CD40L proteins. For this, A549 cells were seeded into the wells on a 12-well plate (Sarstedt, order no: 83.3921) at a cell density of 100,000 cells per well. Afterwards, the cells were allowed to adhere and divide for a final confluency of 50-60% on plastic cover slips (Ø 13 mm, no 1.5, VWR®, cat no: 631-0150). Performing the staining twice, in the first staining the cells were fixed with paraformaldehyde or methanol, providing the need for duplicate 12-well plates. In the second staining, only methanol fixed cells were used.

The recombined viruses (both Ad5Δ24-hCD40L), the Ad5Δ24, and two other in-house viruses (Ad5/3-hCD40L-CMV and Ad5/3-CD40L-h-TERT) were stained. The viruses were diluted 1:100 in complete DMEM and added 48 hours after seeding the A549 cells onto the coverslips. The layout of the 12-well plate is presented in Figure 15 on page 47. In the wells used as negative controls (-), the media was simply changed. In the first staining, the viruses were left to infect the cells for a period of 24 hours and extended to 48 hours for the second staining of methanol fixed cells.

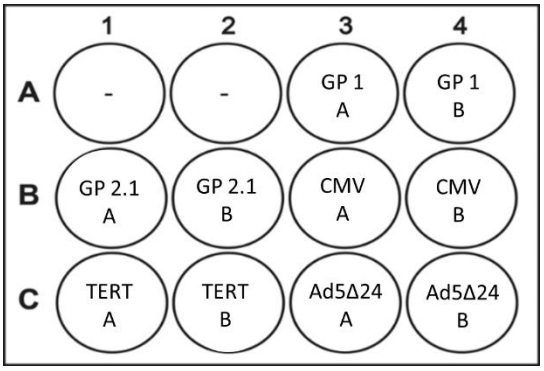

Figure 15: The mapping of the different samples for immunostaining on the 12-well plate. All samples were made in duplicates and included both constructed viruses Gibson Plasmid virus 1 (GP 1) and Gibson Plasmid virus 2.1 (GP 2.1). The positive controls were the Ad5/3-hCD40L-CMV (CMV), Ad5/3-CD40L-h-TERT (TERT), and Ad5Δ24 and mock (-).

In the paraformaldehyde fixation, the old media was removed and the cells washed twice with 1XPBS. Adding 3.5% paraformaldehyde in PBS to the cells, the cells were left for 20 minutes at room temperature, followed by three washes with 1XPBS. For blocking the cells, 3% bovine serum albumin (Media Kitchen) in 1XPBS was added to each well and left for 10 minutes. Diluting the primary antibodies for the CD40L (ab 231 rabbit-anti-CD40L) and the hexon protein (8C4 mouse-anti-adenovirus), both were added simultaneously and incubated for 1 hour. Washing the coverslips twice with 1XPBS, the secondary antibodies were added, goat anti-rabbit Alexa 488 for the CD40L and goat anti-mouse Alexa 594 for the hexon protein, and incubated in the dark for another hour. Washing the cells thrice with 1XPBS, the Hoechst reagent (in-house) was diluted 1:10 000 and after addition left for ca 1 minute. Washing the coverslips one last time in 1XPBS and MQ, they were mounted and imaged with EVOS FL Cell Imaging System.

Cells were fixed with methanol 24 hours and 48 hours after virus addition, at which point the old media was aspirated and the cells washed once with 1XPBS. Adding around 1 ml of -20 °C 100% methanol to each well, the plates were incubated in the freezer for ca 11 minutes. Removing the methanol, the cells were washed thrice with 1XPBS. The staining was done as previously described, with the exception that the 48-hours infected cells were incubated primary and secondary antibodies in the dark. After mounting, the cells were imaged with EVOS FL Cell Imaging System.

7 RESULTS

The results from the cloning, transfection, and immunostaining are recounted in the subsequent chapter. The results from the homologous recombination and Gibson Assembly® are presented chronologically with supplementary information provided in the appendices.

7.1 First Homologous Recombination

The homologous recombination was attempted in two rounds. In the first attempt, the shuttle plasmids with the four different transgenes were linearized with the restriction enzyme SpeI. The digestion was confirmed with electrophoresis, visualizing the cleaved pTHSN-CD40L plasmids as ca 6,600 bp bands; the ca 200 bp size difference between the plasmids generated by the varying lengths of the soluble and membrane bound transgenes are indiscernible on the 0.6% agarose gel presented in Figure 16.

SpeI digestion

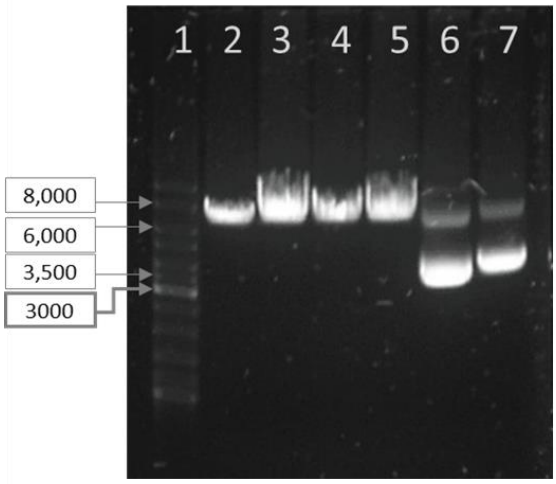

LANE	Sample
1	GeneRuler DNA Ladder mix
2	pTHSN-CD40L-S mouse
3	pTHSN-CD40L-S human
4	pTHSN-CD40L-FL mouse
5	pTHSN-CD40L-FL human
6	Control: pTHSN-CD40L-S human SC
7	Control: pTHSN-CD40L-FL human SC

Figure 16: The four SpeI digested pTHSN-CD40L of all four origins with two of the undigested pTHSN-CD40L as controls for the first homologous recombination. The amount of DNA loaded onto the gel amounts to 1 μg each.

The backbone plasmid was prepared by digestion with the dual cutter EcoRI, excising a ca 2,700 bp band where the plasmid would be inserted. The bands were separated on a

0.6% agarose gel following a one-hour incubation at 37 ˚C (Figure 17). The DNA amount loaded onto the gel was 0.5 µg (lane 3 and 5) and 1 µg (lane 2 and 4); the SC pAd5Δ24 was used as control.

EcoRI digestion

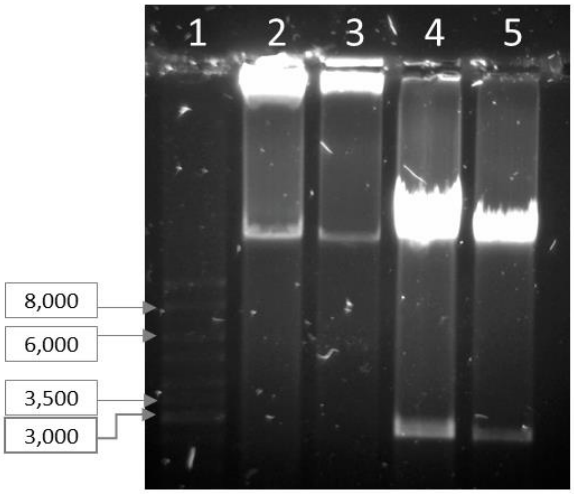

LANE	Sample
1	GeneRuler Ladder DNA mix
2	pAd5Δ24 SC
3	pAd5Δ24 SC
4	pAd5Δ24
5	pAd5Δ24

Figure 17: Determination of the successful cleavage of the pAd5Δ24, with the uncut backbones as controls. Two different DNA amounts were loaded of both plasmids, 0.5 µg (3 and 5) and 1 µg (lane 2 and 4).

After simultaneous transformation of á 1 µg pTHSN-CD40L of one of the four transgenes and 0.1 µg pAd5Δ24 to BJ5183 cells, the bacteria growing under kanamycin selection were screened with colony PCR. Ten colonies of each transgene were analyzed with two separate primer sets that had previously been verified for their functionality. The results for the testing of the four primer sets are gathered in APPENDIX 10. The screened colonies were visualized for potential PCR amplification product on 2% agarose gels. First, ten clones from the pTHSN-hCD40L-FL and pAd5Δ24 transformation were screened. The results from Primer Set I are presented in Figure 18 and Primer Set II, with the same colonies in the same order, in Figure 19.

Colony PCR Primer Set I: hCD40L-FL

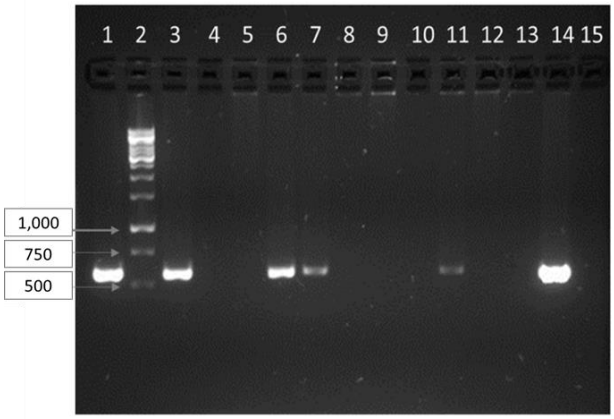

LANE	Sample
1	Control pAd5Δ24 PCR product
2	GeneRuler 1 kb Ladder
3-12	Single bacterial colonies
13	Control EcoRI-pAd5Δ24-CIP PCR product
14	Control pAd5Δ24 PCR product
15	Negative Control MQ

Figure 18: The gel run on a 2% agarose gel from the colony PCR of the ten hCD40L-FL transformed bacterial colonies. Here Primer Set I was used and four signals were observed.

Colony PCR Primer Set II: hCD40L-FL

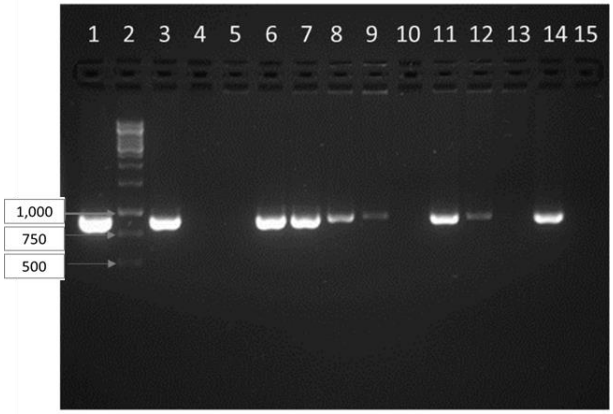

LANE	Sample
1	Control pTHSN-hCD40L-FL PCR product
2	GeneRuler 1 kb Ladder
3-12	Single bacterial colonies
13	Control EcoRI-pAd5Δ24-CIP PCR product
14	Control pTHSN-hCD40L-FL PCR product
15	Negative Control MQ

Figure 19: The results from the colony PCR with Primer Set II and ten hCD40L-FL transformed bacterial colonies, run on a 2% agarose gel. Seven signals were observed.

Ten bacterial colonies with the transformed hCD40L-S transgene were screened next. The colonies amplified with Primer Set I are in Figure 20 and those with Primer Set II in Figure 21. The corresponding mouse constructs (full-length and soluble) are found in APPENDIX 11.

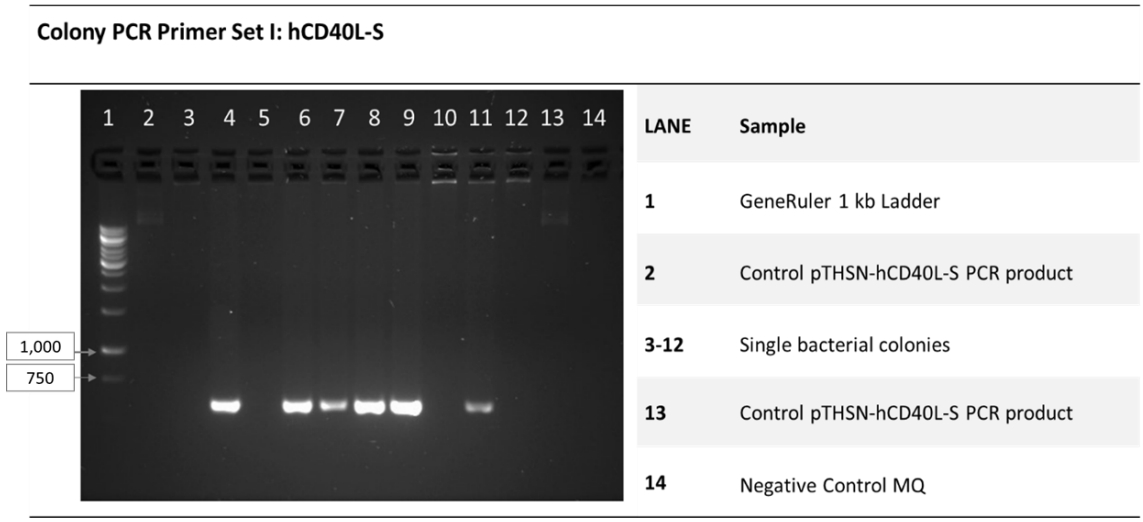

Figure 20: Colony PCR amplified product for ten hCD40L-S transformed colonies using Primer Set I. Six clear signals were observed on the 2% agarose gel.

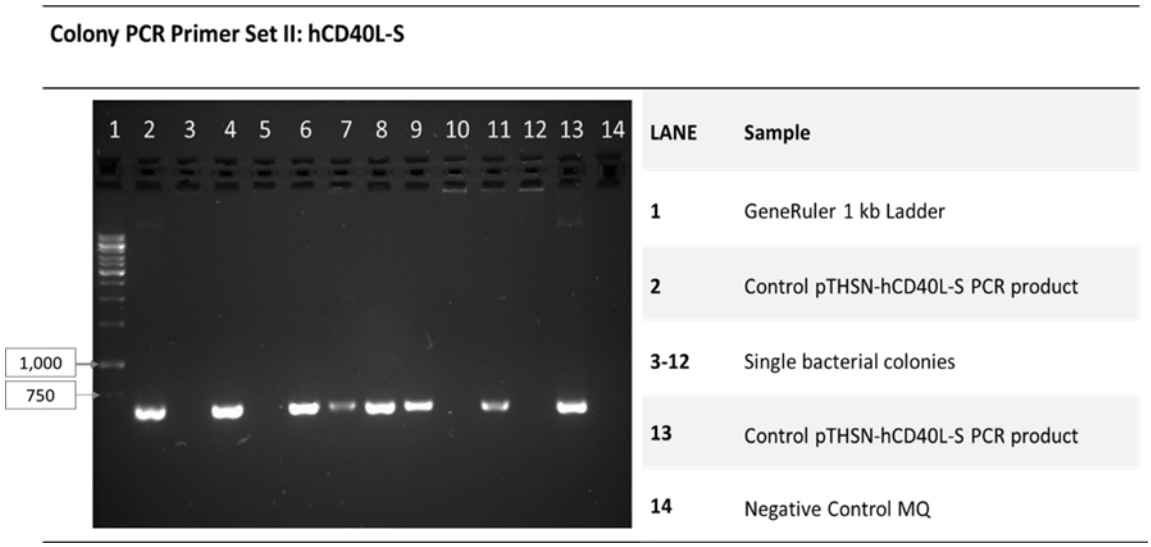

Figure 21: The amplified colony PCR products using the Primer Set II for ten hCD40L-S transformed colonies. Seven signals were observed on the 2% agarose gel.

A total of 40 bacterial colonies were screened in the first homologous recombination attempt, out of them, 18 were deemed positive. The two colonies with the strongest signals that emerged for both primer sets of each construct was initially chosen for continued analysis with restriction enzymes. The colonies in Table 6 were the first that underwent plasmid extraction and restriction analysis.

Table 6: Two colonies of each constructs, providing a PCR product with both Primer Set I and Primer Set II that were chosen for further analysis.

Construct	Colony
hCD40L-FL	1 and 4
hCD40L-S	2 and 4
mCD40L-FL	1 and 2
mCD40L-S	2 and 8

In restriction analysis, the expected band pattern from the digestion of PacI, HindIII, and BamHI are relayed in Table 7. Depending on whether the construct contains the soluble or full-length variant of the transgene, there may be small variations in the size of the bands; these differences would, however, often be indiscernible on an agarose gel. The results from the restriction analysis with PacI are presented in the Figure 22 and the results using HindIII and BamHI in Figure 23. All three digestion products were analyzed on 0.8% agarose gels. In the HindIII digestion, the ca 5,700 bp band in the empty pAd5Δ24 is cleaved into two bands, ca 2,600 bp and 3,100 bp in size, because of the introduction of an additional HindIII recognition sequence with the transgene.

Table 7: The calculated sizes based on the plasmid maps in SnapGene Viewer for the different fragments produced during restriction analaysis with PacI, HindIII, and BamHI of the recombined plasmids and the empty pAd5Δ24. The sizes are recounted as kilo base-pairs (kb).

Restriction Enzyme	Fragments of pAd5Δ24 (kb)	Fragments of a positive clone (kb)	
		Full-length	Soluble
PacI	2.9 36	2.9 36	2.9 35
HindIII	2.1 2.9 3.4 4.6 5.3 5.7 6.7 8.0	0.1 2.1 2.6 2.9 3.1 3.4 4.6 5.3 6.7 8.0	
BamHI	14 24	7.0 7.3 24	6.7 7.3 24

PacI Restriction Analysis

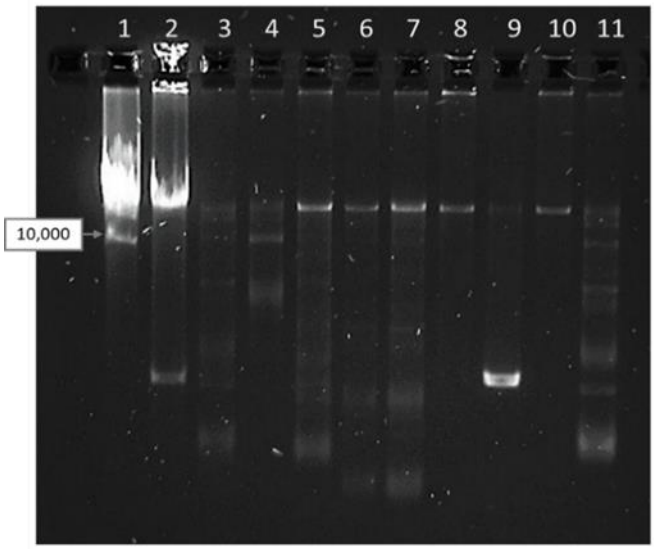

LANE	Sample
1	λ DNA-Mono Cut Mix Ladder
2	pAd5Δ24
3	hCD40L-FL-1
4	hCD40L-FL-4
5	hCD40L-S-2
6	hCD40L-S-4
7	hCD40L-S-4
8	mCD40L-FL-1
9	mCD40L-FL-2
10	mCD40L-S-2
11	mCD40L-S-8

Figure 22: The band pattern for the potential positive clones selected with colony PCR on a 0.8% agarose gel. The PacI digestion is expected to yield two bands, one ca 2,900 bp and the other ca 35,000 bp for mouse constructs and ca 36,000 bp for human constructs and the control, pAd5Δ24.

HindIII & BamHI Restriction Analysis

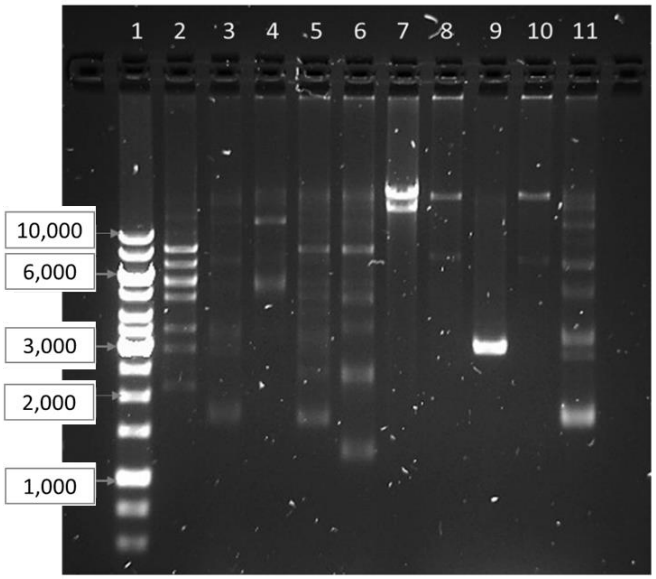

LANE	Sample
1	GeneRuler 1 kb Ladder
2	pAd5Δ24 HindIII
3	HindIII hCD40L-FL-1
4	HindIII hCD40L-FL-4
5	HindIII hCD40L-S-2
6	HindIII hCD40L-S-4
7	pAd5Δ24 BamHI
8	BamHI mCD40L-FL-1
9	BamHI mCD40L-FL-2
10	BamHI mCD40L-S-2
11	BamHI mCD40L-S-8

Figure 23: The results from the HindIII and BamHI of the suspected positive clones of all four constructs on a 0.8% agarose gel. For the BamHI digested constructs carrying the mouse transgenes, a band would be cleaved, the same for the HindIII digested plasmids carrying the human transgenes.

Upon separation of the products from the restriction analyses with PacI, BamHI, and HindIII, the background was substantial with the appearance of superfluous bands at varying intensity. Most notably, none of the PacI digestions presented the successful excision of a 2,900 bp band. This implied loss of structural integrity precluded the generation of operational viruses, requiring the cloning to be attempted anew.

7.2 Second Homologous Recombination

In the second attempt, only the mouse CD40L constructs were used, being double digested with SpeI and NdeI. The digestions were, as previously, confirmed on a 0.8% agarose gel (Figure 24) before proceeding with cotransformtion to BJ5183 cells; digested backbone from the first attempt at homologous recombination was utilized. The double-digested plasmids should yield bands approximately 4,300 bp and 3,000 bp in size for pTHSN-mCD40L-FL and 4,000 bp and 3,000 bp for the pTHSN-mCD40L-S.

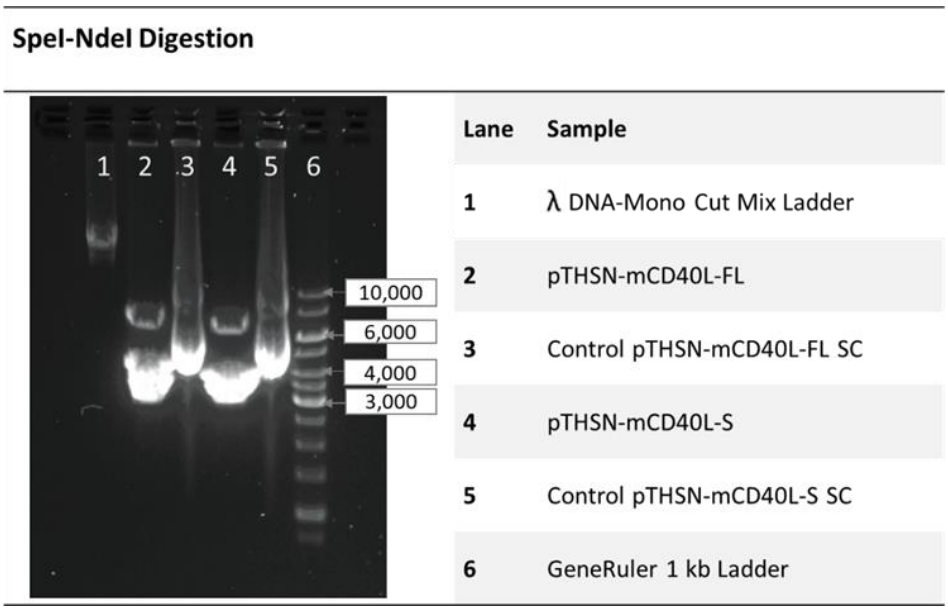

Figure 24: The NdeI and SpeI double digested pTHSN-mCD40L-FL and pTHSN-mCD40L-S on a 0.8% agarose gel. The controls were the same undigested constructs.

With the optimized combined primer set in the second attempt, a PCR fragment would be produce for both the empty pAd5Δ24 and all pAd5Δ24-CD40L. The different constructs would yield different sized PCR products: pAd5Δ24 a ca 2,400 bp band, pAd5Δ24-CD40L-FL a ca 2,200 bp band, and pAd5Δ24-CD40L-S a ca 1,900 bp band. Out of the 25 screened pAd5Δ24-mCD40L-FL clones, three were positive (Figure 25

lanes 3 and 5, Figure 26 lane 2) and out of the 45 screened pAd5Δ24- mCD40L-S colonies, one was positive (Figure 26 lane 8). The other samples screened yielded no PCR product and were empty as, for example, lane 6 through 12 in Figure 25. The colony PCR gel run of these samples are not included.

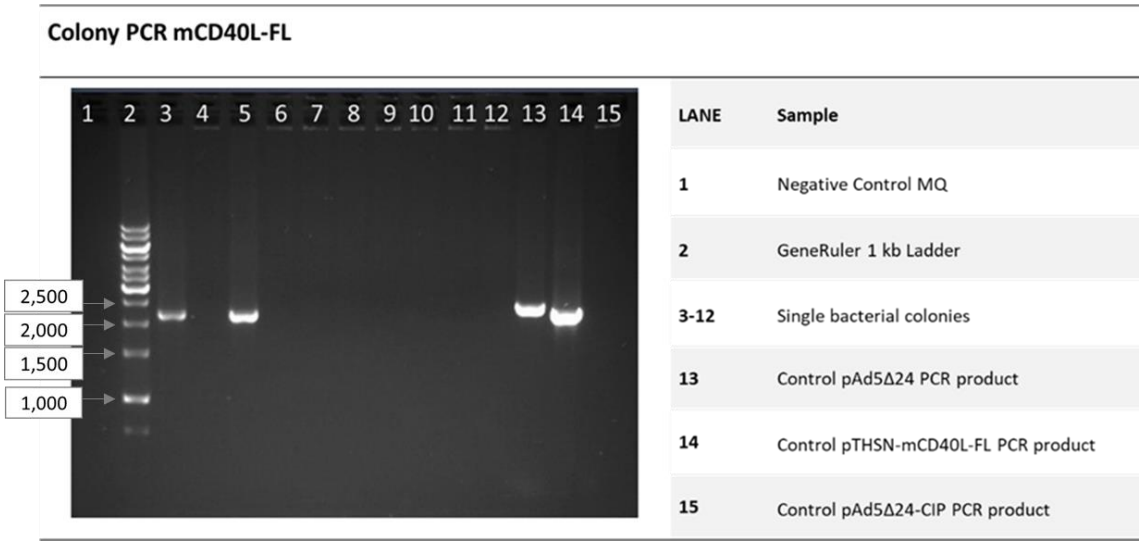

Figure 25: The gel run of the pAd5Δ24-mCD40L-FL colony PCR. The samples were run on a 1.5% agarose and two were potential positives.

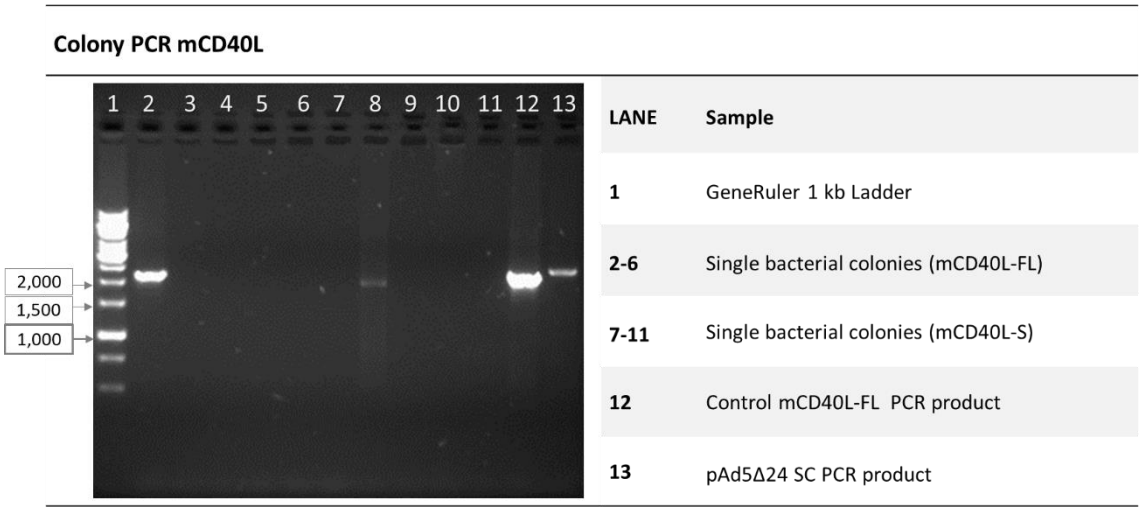

Figure 26: The results from the colony PCR of bacteria transformed with full-length and soluble mCD40L after electrophoresis on a 1.5% agarose gel. One mCD40L-FL and one mCD40L-S were deemed potential positive clones.

Isolating the plasmids from the potential positive clones (three pAd5Δ24-mCD40L-FL and one pAd5Δ24-mCD40L-S) they were transformed to XL10-Gold cells for plasmid

preservation and propagation. After isolating the plasmids from 135 ml preparations, exceptionally 6 µg DNA was digested with PacI or BamHI for restriction analysis to ensure visibility. The digestion products were separated on 0.8% agarose gels (Figures 27 and Figure 28).

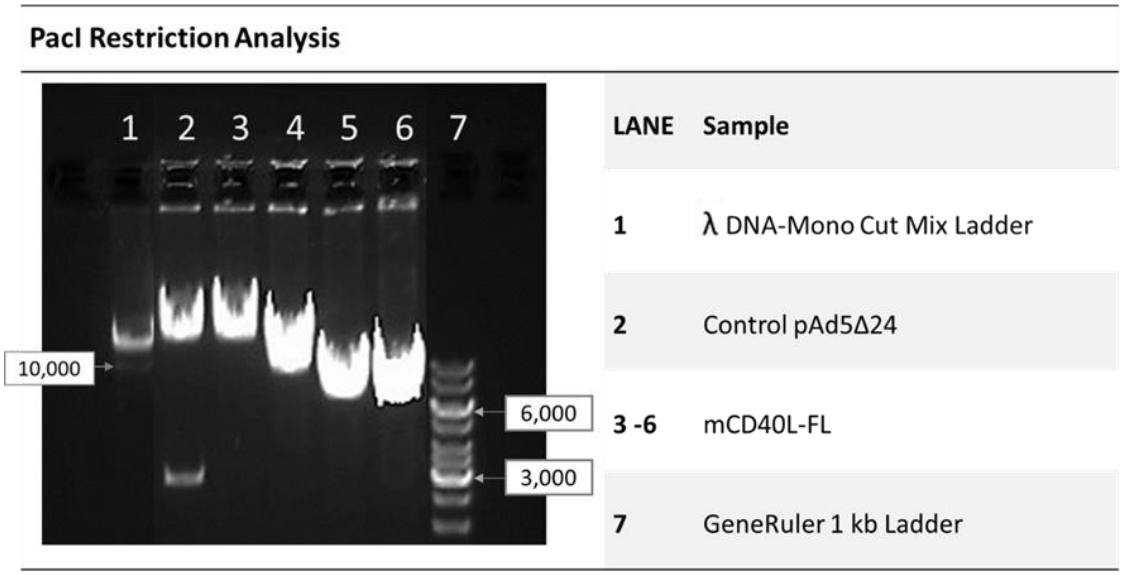

Figure 27: The PacI digested potential positive clones carrying mCD40L-FL run on a 0.8% agarose gel. The expected band pattern for positive clones is two bands, approximately 2,900 bp and 36,000 bp in size.

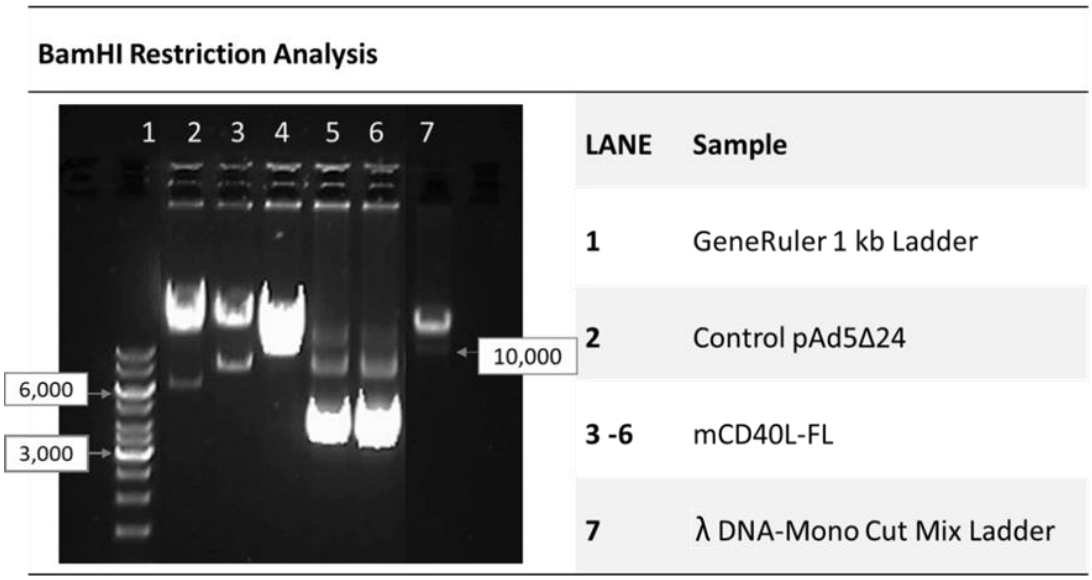

Figure 28: The BamHI digested potential positive clones run on a 0.8% agarose gel to confirm the presence of the mCD40L-FL transgene. Successfully recombined constructs will present as three bands, ca 7,000 bp, 7,300 bp, and 24,000 bp in size.

The resolution of the products from the restriction analyses was significantly improved compared to the first attempt (Figures 22 and 23 on page 53). Still, the issue of the PacI digestion persisted in proving the current protocols failure to retain the structural integrity to vital areas of the assembled product. In the subsequent attempt, a novel *in vitro* recombination method was exchanged for the traditional homologous recombination.

7.3 Gibson Assembly®

In Gibson Assembly®, the backbones were digested with either SpeI and EcoRI-HF restriction endonucleases or EcoRI alone. The digestions were confirmed on 0.8% agarose gels (Figure 29 and 30). For the transgene inserts, the amplification was done for both soluble and full-length hCD40L, using 1 ng and 10 ng of pTHSN-hCD40L as template. The reaction with 1 ng pTHSN-hCD40L-FL DNA initially added was ultimately applied to the assembly reaction. The verification of insert production is seen in Figure 31. Primer set I (for SpeI and EcoRI-HF digested) yielded bands ca 2,800 bp for the hCD40L-FL or ca 2,500 bp for the hCD40L-S. Primer Set II (EcoRI digested) generated bands either ca 2,600 bp bands for the hCD40L-FL and 2,300 bp bands for the hCD40L-S.

EcoRI-SpeI Digestion

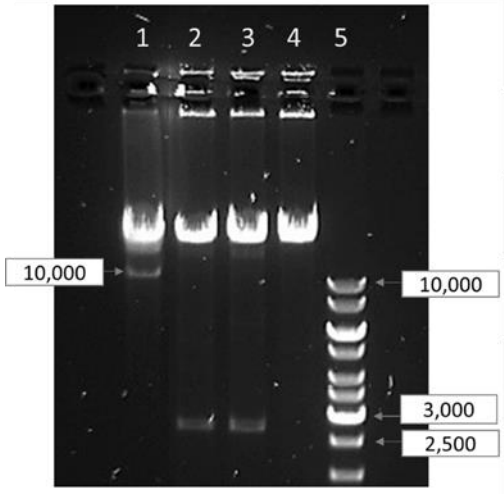

LANE	Sample
1	λ DNA-Mono Cut Mix Ladder
2	pAd5Δ24-SpeI-EcoRI-HF
3	pAd5Δ24-EcoRI-HF
4	pAd5Δ24-SpeI
5	GeneRuler 1 kb Ladder

Figure 29: The single and double digested pAd5Δ24 using SpeI and/or EcoRI-HF in preparation for Gibson Assembly® on a 0.8% agarose gel. The SpeI digested vector is linearized into a ca 38,800 bp band while the SpeI and EcoRI-HF restriction analyzed vectors present as primarily two bands, ca 35,900 bp and 2,700 bp in size.

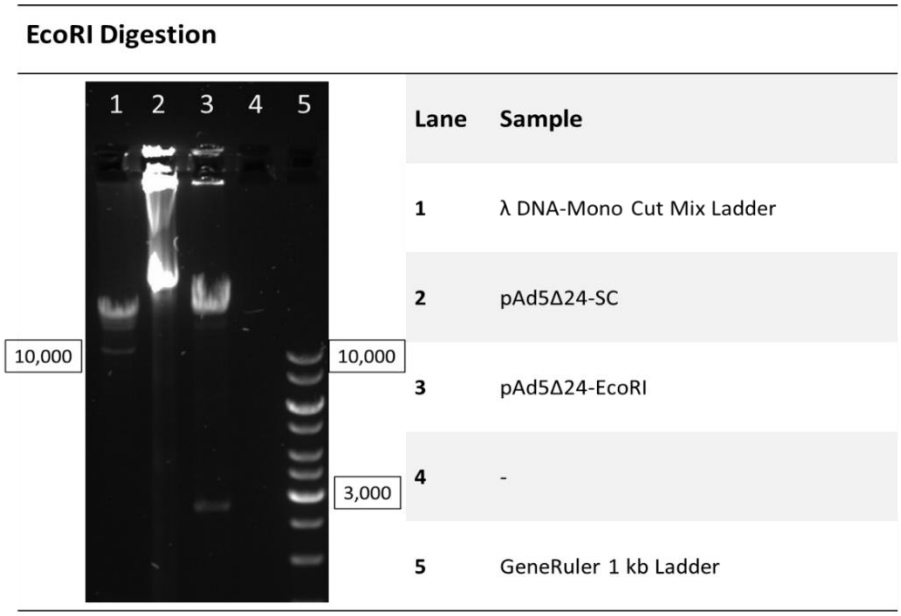

Figure 30: The gel run of the EcoRI digested pAd5Δ24 for Gibson Assembly®. The samples were run on a 0.8% gel. Bands ca 2,700 bp and ca 35,900 bp confirmed successful digestion.

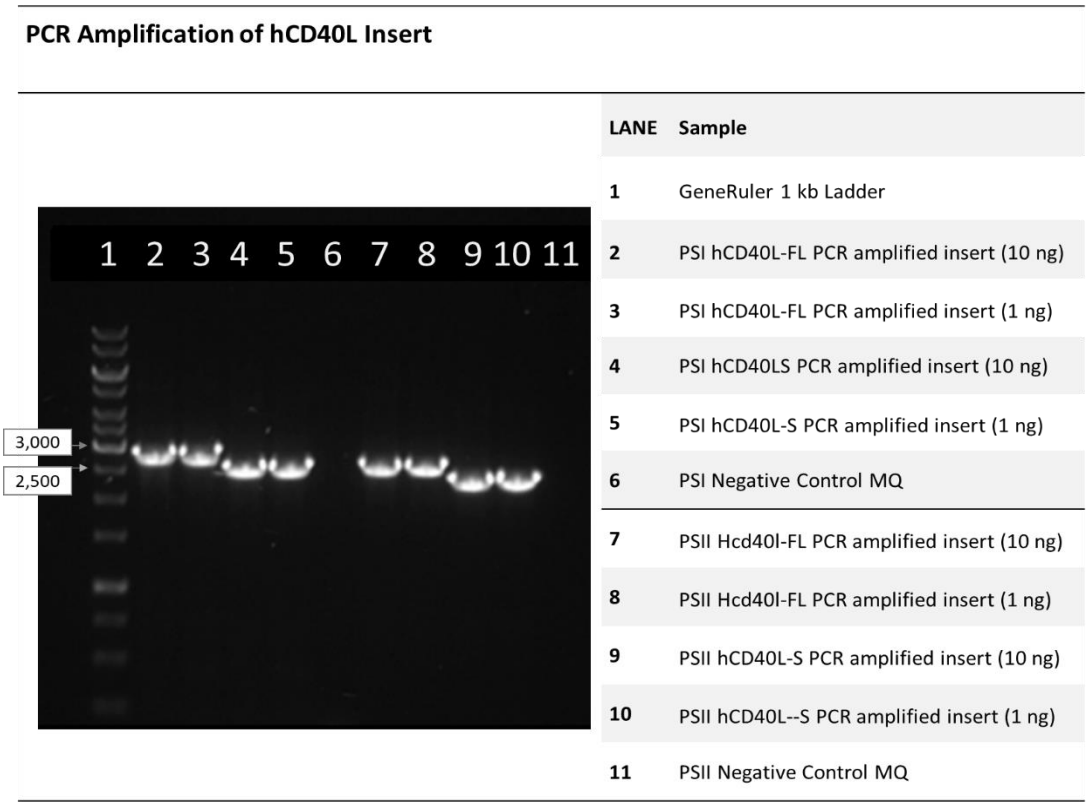

Figure 31: Production of the transgene insert for Gibson Assembly® using 1 and 10 ng of either pTHSN-hCD40L-FL or pTHSN-hCD40L-S as template separated on a 0.8% agarose gel. Primer set I (PSI) yielded bands ca 2,800 bp (hCD40L-FL) or ca 2,500 bp (hCD40L-S), and primer Set II (PSII) ca 2,600 bp bands (hCD40L-FL) and 2,300 bp bands (hCD40L-S).

After the transformation of the diluted Gibson Assembly® reaction product, 78 colonies were analyzed with colony PCR out of which three positives were found (see lanes 2, 7, and 10 in Figure 32). According to estimations made from the plasmid maps, the PCR should generate a band ca 2,200 bp for pAd5Δ24-hCD40L-FL and a band ca 2,400 bp for the pAd5Δ24 with these primers. The remaining 75 screened colonies gave no signal. The plasmids were named Gibson plasmid 1, Gibson plasmid 2.1, Gibson Plasmid 2.2. The Gibson Plasmid 1 was made with the SpeI and EcoRI-HF digested backbone and corresponding insert while the Gibson Plasmid 2 were made with the EcoRI digested backbone and corresponding insert.

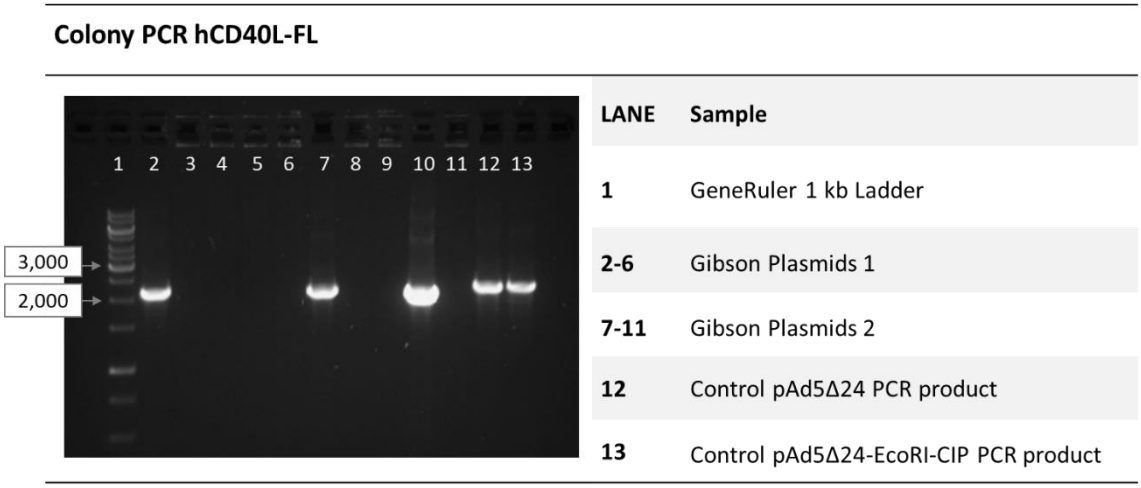

Figure 32: Results from the colony PCR with three potential positive clones produced with Gibson Assembly®.

The restriction analysis with HindIII and PacI fragments were separated on 0.8% gels as seen in Figure 33 on the following page; the controls were for both enzyme reactions the empty pAd5Δ24. The HindIII digestion were run on lanes 2 through 6, and the PacI digestion run on lanes 8 through 11. All desired bands were seen with both enzymes for all constructs, albeit with less DNA for of the Gibson Plasmid 2.2. For further confirmation of successful transgene insertion, the PCR amplified products from the colony PCR for Gibson Plasmid 1, Gibson Plasmid 2.1, and Gibson Plasmid 2.2 were also digested with HindIII. Separating these fragments on 2% agarose gels, the successful cleaving was confirmed (Figure 34). Based on the restriction analyses, Gibson Plasmid 1 and Gibson Plasmid 2.1 were ultimately chosen for transfection.

HindIII and PacI Restriction Analysis

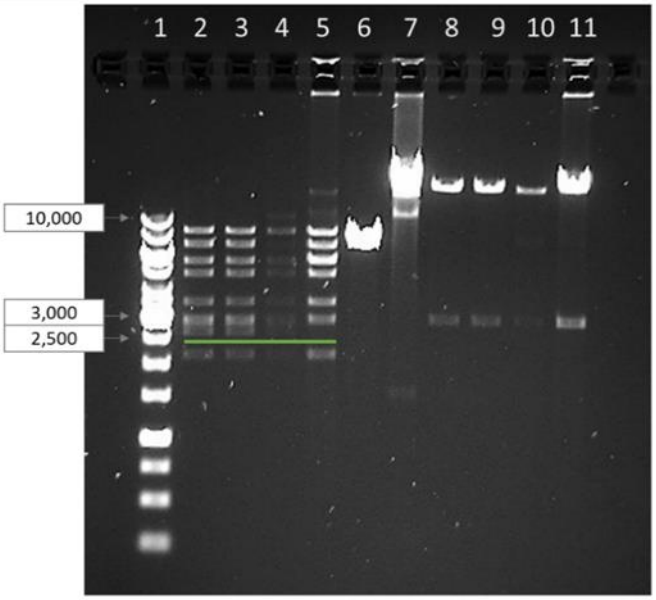

LANE	Sample
1	GeneRuler 1 kb Ladder
2	Gibson Plasmid 1
3	Gibson Plasmid 2.1
4	Gibson Plasmid 2.2
5	Control pAd5Δ24
6	pTHSN-hCD40L-FL
7	λDNA-Mono Cut Mix Ladder
8	Gibson Plasmid 1
9	Gibson Plasmid 2.1
10	Gibson Plasmid 2.2
11	Control pAd5Δ24

Figure 33: Restriction analysis for the Gibson Plasmids with HindIII and PacI restriction enzymes. The presence of the transgene can be judge by an emerging band above the green line, ca 2,600 bp in size, in the HindIII digestion. PacI digestions should yield bands approximately 2,900 bp and 36,000 bp large.

HindIII Digested Colony PCR Products

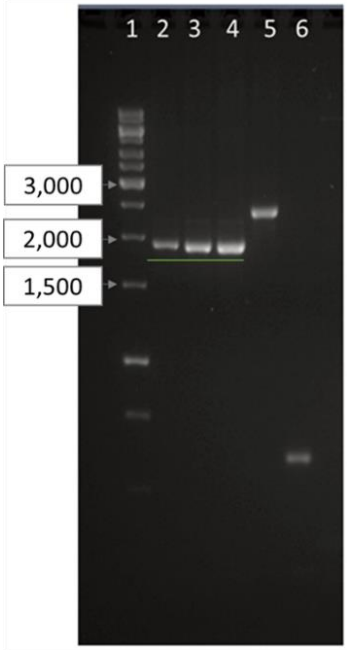

Lane	Sample
1	GeneRuler 1 kb Ladder
2	Gibson Plasmid 1 PCR product
3	Gibson Plasmid 2.1 PCR product
4	Gibson Plasmid 2.2 PCR product
5	pAd5Δ24 PCR product
6	pTHSN-hCD40L-FL PCR product

Figure 34: The HindIII digested colony PCR amplified products on a 2% agarose gel. A band was expected to appear at the area above the thin green line in the event of transgene incorporation into the virus genome.

With the application of the Gibson Assembly® method, plasmids were constructed encoding the CD40L that retained important structural sequences, as confirmed by the HindIII and PacI digestions. The freeing of the ITRs following PacI digestion, enabled the study to proceed to transfection and primary virus assembly,

7.4 Transfection

Following a round of plasmid propagation in XL10-Gold cells, transfection was attempted with ViraPack transfection kit and QIAGEN® Effectene Transfection Reagent. For both experiments, around 1 μg of PacI digested plasmids were required of Gibson Plasmid 1, Gibson Plasmid 2.1, GFP plasmid, pAd5Δ24, and pAd5/3Δ24 found in-house. The confirmed digestion of the linearized plasmids used in the ViraPack transfection are gathered in Figure 35 and similarly the ones for the QIAGEN® Effectene transfection in Figure 36. Only 0.25 μg Gibson Plasmid 2.1 DNA could be added due to low yield after digestion and purification. The measured DNA concentrations for the digestions are summarized in Table 8. The purity of the samples is also accounted for, the ratio of which preferably should be around 1.8 for DNA to be considered pure.

PacI Digestions - ViraPack

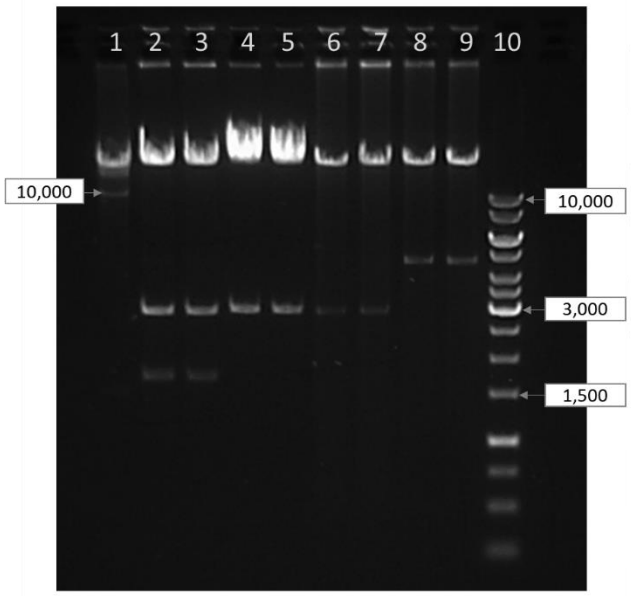

LANE	Sample
1	λ DNA-Mono Cut Mix Ladder
2	Gibson Plasmid 1
3	Gibson Plasmid 1
4	Gibson Plasmid 2.1
5	Gibson Plasmid 2.1
6	Control pAd5Δ24
7	Control pAd5Δ24
8	Control pAd5/3Δ24
9	Control pAd5/3Δ24
10	GeneRuler 1 kb Ladder

Figure 35: The PacI digestion of the plasmid DNA used for the ViraPack transfection.

PacI Digestions – Effectene Reagent

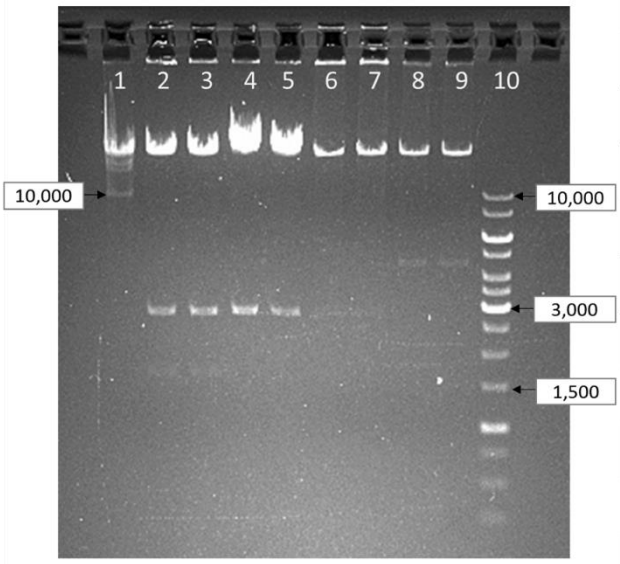

LANE	Sample
1	λ DNA-Mono Cut Mix Ladder
2	Gibson Plasmid 1
3	Gibson Plasmid 1
4	Gibson Plasmid 2.1
5	Gibson Plasmid 2.1
6	Control pAd5Δ24
7	Control pAd5Δ24
8	Control pAd5/3Δ24
9	Control pAd5/3Δ24
10	GeneRuler 1 kb Ladder

Figure 36: The PacI digested Gibson Plasmid 1 and 2.1 in preparation for transfection, separated on a 0.8% agarose gel. The plasmids were transfected to A549 cells in T25 flasks.

Table 8: The measured concentration for the PacI digested DNA for the ViraPack and QIAGEN® Effectene reagent transfections after ethanol precipitation.

DNA	Concentration (ng/µl)	260/280 Ratio
ViraPack Transfection		
Gibson Plasmid 1	68.01	1.54
Gibson Plasmid 2.1	44.87	1.68
Ad5Δ24	53.27	1.61
Ad5/3Δ24	20.92	1.61
QIAGEN® Effectene Transfection Reagent		
Gibson Plasmid 1	648.25	1.47
Gibson Plasmid 2.1	13.88	1.78
Ad5Δ24	184.44	1.47
Ad5/3Δ24	385.78	1.45

There are no images for the ViraPack transfection, however, after a week there was still no perceivable development of fluorescence in the GFP transfection control nor CPE in

the virus plasmid transfection. In the QIAGEN® Effectene reagent transfection, progressing fluorescence was observed one day after transfection in the GFP control (Figure 37). The GFP transfected cells were the only ones monitored for the first five days, leaving the cells transfected with viral plasmids in the incubator to minimize cells disruption.

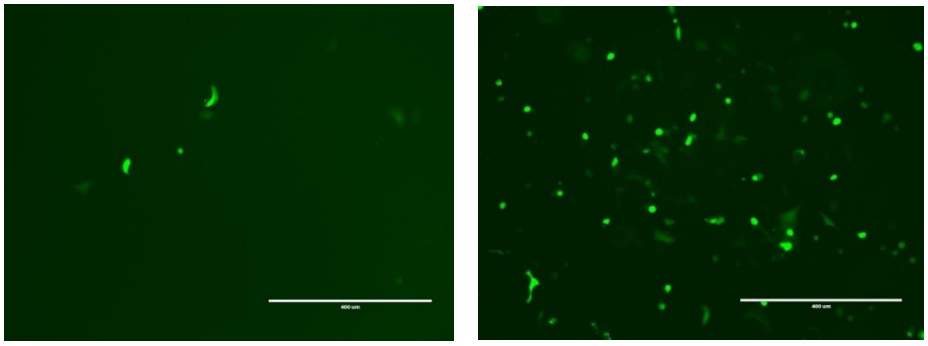

Day 1 Day 3

Figure 37: The green fluorescent protein plasmid transfected A549 cells using the Effectene transfection reagent, one and three days after transfection.

After careful monitoring, sufficient CPE was observed in the A549 transfected cells in the controls and Gibson plasmids on day 13, whereupon they were harvested. The visual state of the cells in the four transfections can be observed at 10X and 20X magnification in Figure 38 on page 64. In spite of apparent CPE, recently divided cells can be observed in the background of all transfection.

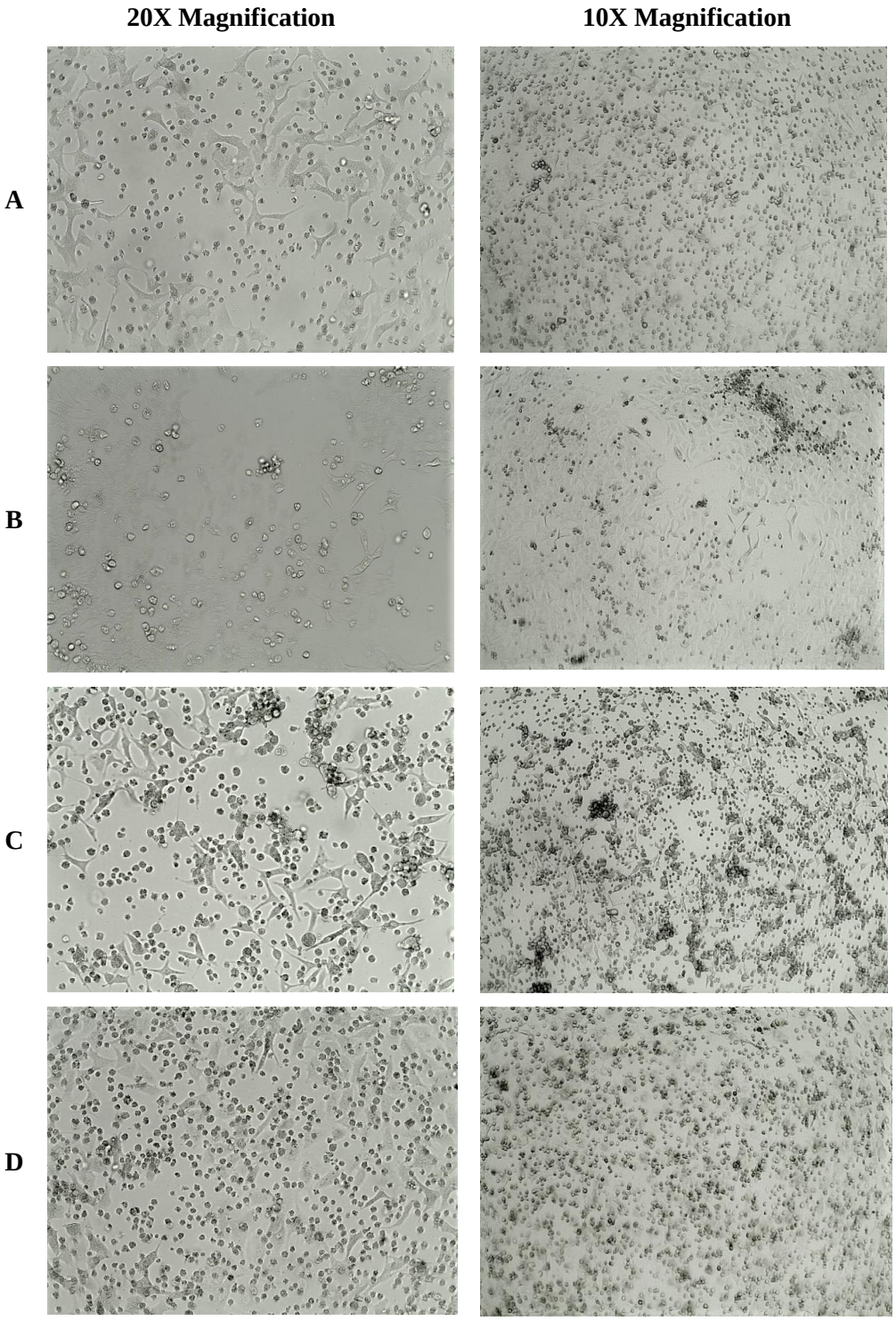

Figure 38: The state of the transfected A549 cells on the day of harvest, 13 days post transfection, in 20X and 10X magnification. Row A: Gibson Plasmid 1 virus, B: Gibson Plasmid 2.1 virus, C: Ad5Δ24, and D: Ad5/3Δ24.

7.5 Immunostaining

Following an amplification round, the virus infected cells were stained using primary and secondary antibodies. Infecting the cells with the Gibson Plasmid 1 virus, Gibson Plasmid 2.1 virus, Ad5/3-hCD40L-CMV, Ad5/3-CD40L-h-TERT, and Ad5Δ24, the A549 were fixed using both paraformaldehyde and methanol, 24 and 48 hours after infection. Upon staining, the primary antibodies bound to the hexon and CD40L proteins. The proteins were finally visualized with secondary antibodies attached with either Alexa 488 or Alexa 594.

The paraformaldehyde fixed cell stains (24-hour infection) are found in Figure 39 and the methanol fixed cells in Figure 40 (24-hour infection) and Figure 41 (48-hour infection). In all three figures, the cells are colored blue, green, or red depending on the staining. The blue cells are stained with Hoechst to localize the cell nuclei, the green with Alexa 488 for the CD40L, and the red with Alexa 594 to detect the hexon protein of the Ad capsid.

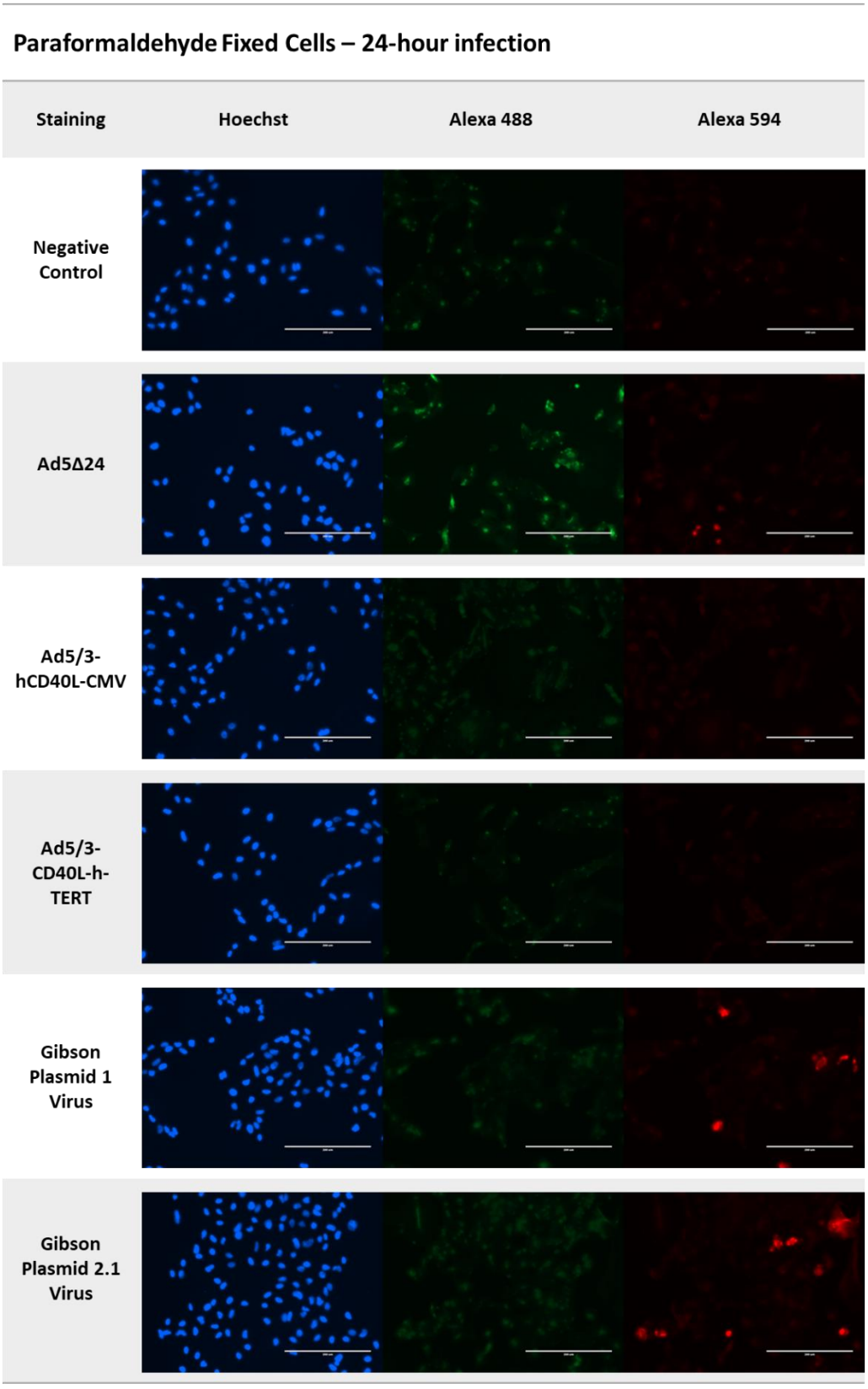

Figure 39: Stained A549 cells fixed with paraformaldehyde 24 hours after infection. The Hoechst stained cells locate the cell nuclei, Alexa 488 the CD40L protein, and Alexa 594 the hexon Ad protein.

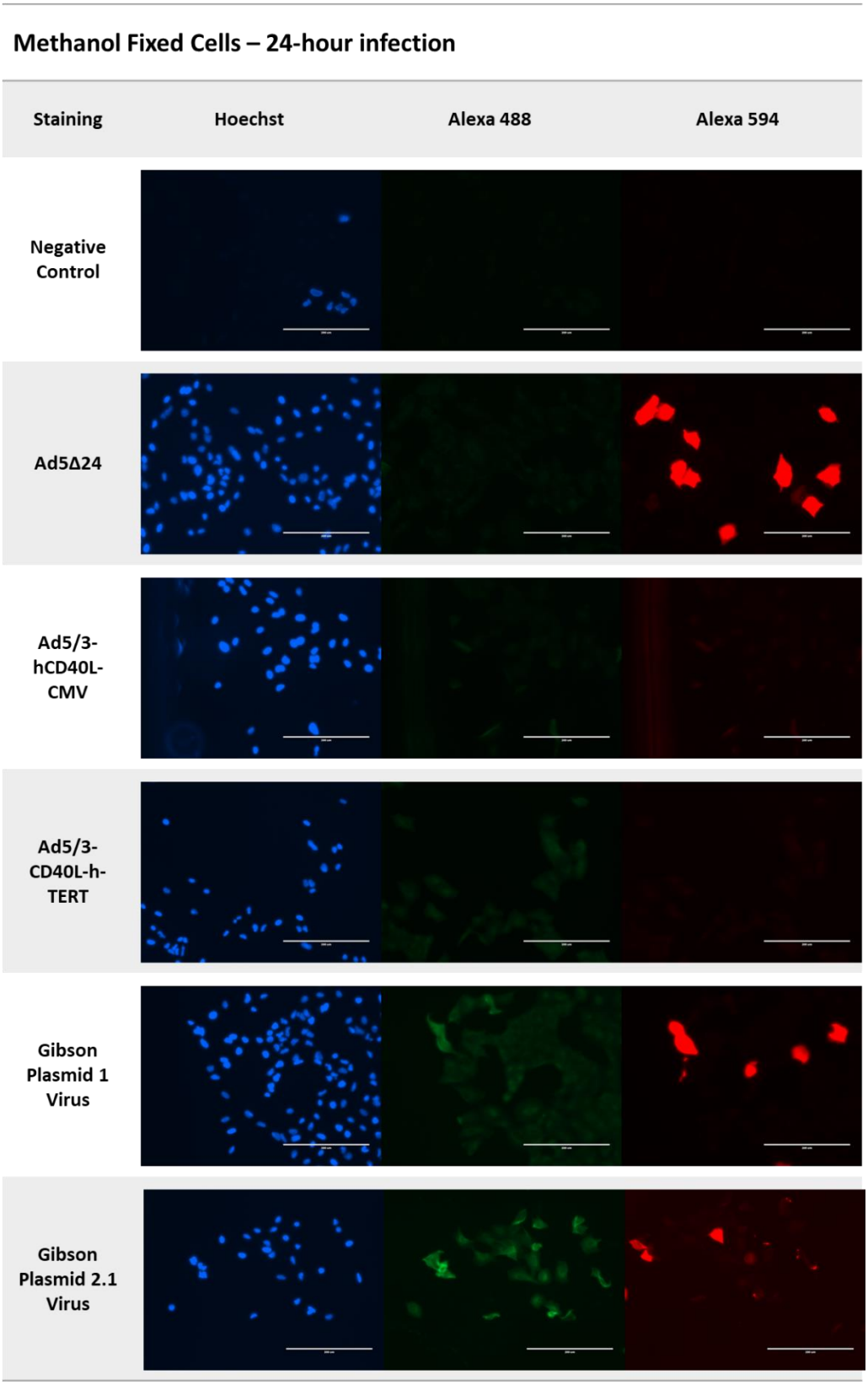

Figure 40: Methanol fixed A549 cells stained after a 24-hour infection period. The cells are located with the Hoechst reagent and the CD40L and hexon protein with the Alexa 488 and 594, respectively.

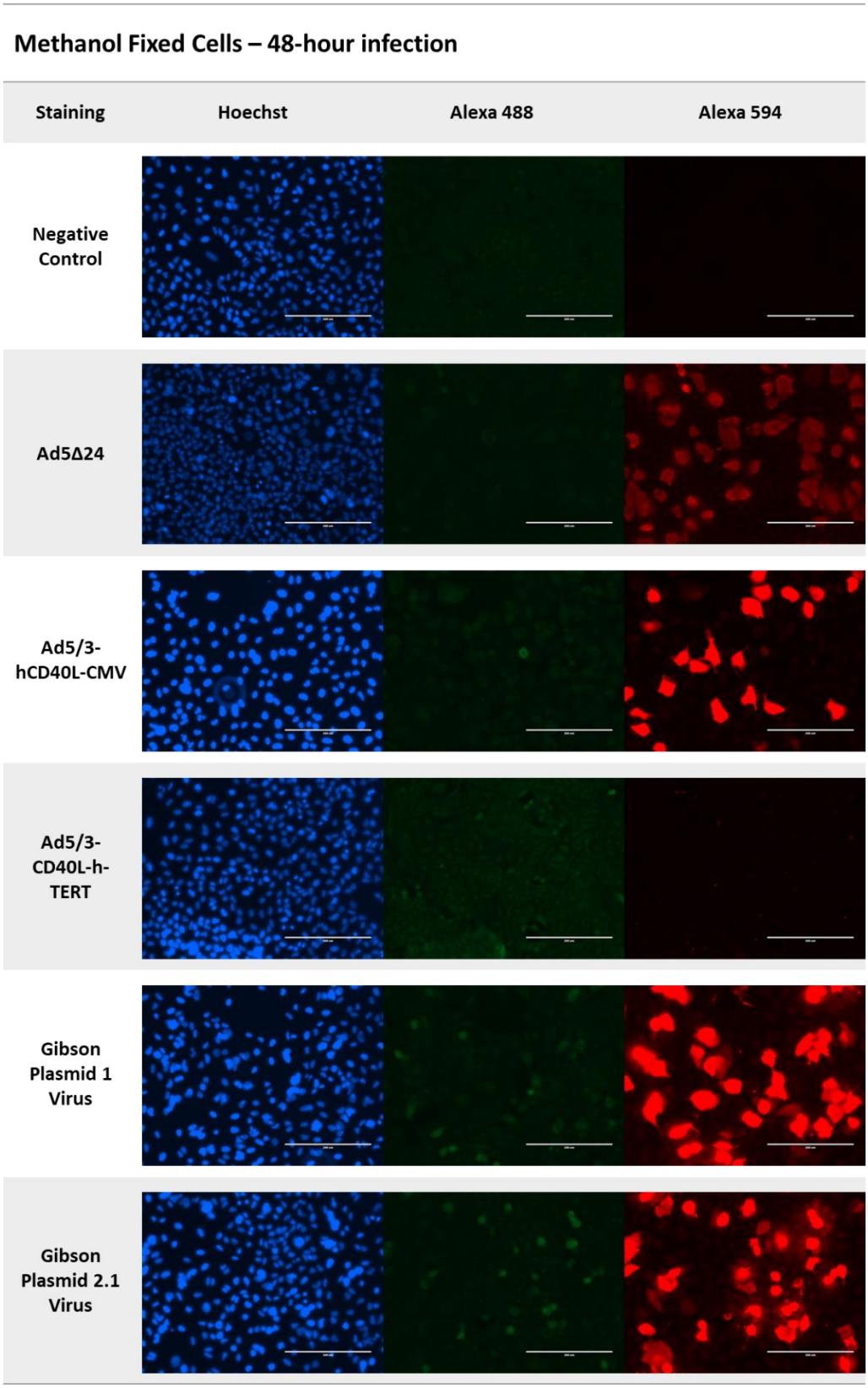

Figure 41: The methanol fixed A549 cells after a 48-hour infection period. The cell nuclei are visualized with Hoechst staining, the CD40L with Alexa 488, and the hexon protein with Alexa 594.

8 DISCUSSION

The study was a process of trial and error that in the end bore fruit. In the aftermath, a template had been established for arming OAds with desirable transgenes. Only one of the intended four constructs were successfully generated into a functional virus, however, with the established vetted protocols, the remaining constructs are estimated to be generated with relative ease. In the following chapter the results and challenges will be discussed and compared to available literature in the order of study progression. Possible reasons for the failure of the initial method of choice are debated as well as general inherent obstacles analyzed. Finally, improvements to the protocol will be contemplated and further perspectives for the study considered.

8.1 Genetic Arming of an Oncolytic Adenovirus with CD40L

CRAds have successfully been designed carrying varying transgenes with immune system effects. The thesis was planned predicated by encouraging results from previous studies proving an antitumor immune response when encoding CD40L into an Ad genome, e.g. Ad5/3-hTERT-E1A-hCD40L (Diaconu *et al*. 2012; Pesonen *et al*. 2012), Ad5-E1/E3-mCD40L (Loskog *et al*. 2004; Liljenfeldt *et al*. 2014), and AdEHCD40L (Gomes *et al*. 2009). Additionally, the CD40L has been incorporated alongside other transgenes in OVs for co-expression as, for example, in Ad-CCL20-hCD40L which possesses several gene expression cassettes: CMVp-CCL20, TERTp-E1A, and E1Bp-CD40L-IRES-E1B55K (Liu *et al*. 2015).

The AdEHCD40L was the first study where the CD40L transgene was successfully integrated into an OAd vector, utilizing a hypoxia inducing factor (HIF) for selective virus activities in HIF-1α–expressing human breast cancer cells (Gomes *et al*. 2009). The Ad5/3-hTERT-E1A-hCD40L has undergone preclinical and clinical studies. The preclinical studies proved significant antitumor effects in two syngeneic mouse models, whereas the clinical studies provided confirmation of the safety of the virus as well as signs of antitumor immunity and efficacy in human patients (Diaconu *et al*. 2012; Pesonen *et al*. 2012)

The novelty of the study was introduced with the soluble CD40L, which to current knowledge, has not been encoded in and successfully expressed by an OAd vector. Since the full-length CD40L naturally can be cleaved into this soluble form, theoretically there would be some present in the previously mentioned studies. However, since this was not an object of scrutiny, the extent of cleavage and the consequent ratio between the soluble form and full-length remains unknown. In the wake of the thesis, it is still uncertain whether the designed soluble CD40L would be excreted from the host cell and whether the produced protein folds into the required trimeric form to be biologically active. The issue will be addressed in future studies that have been planned as continuations to the one presented here.

Homologous recombination is a DNA repair mechanism that has become the preferred method generating recombined Ads. Another traditional approach has been to cleave the shuttle plasmid and backbone plasmid with restriction enzymes and joining them through ligation (He *et al.* 1998). However, this has proven to have low efficiency for larger constructs and is made further difficult by the few suitable unique restriction sites. In the generation of recombined OAds with homologous recombination, the AdEasy cloning system by Agilent Technologies is widespread and aside from direct application, the protocol has been used as a template in the development of other protocols by e.g. Hoffmann and Wildner (2006) and Liu and colleagues (2009).

The differences of the plasmids in this study to those in the AdEasy system, as well as the chosen area for transgene insertion, prevented complete adherence. Still, the main attributes of the commercial protocol could be used as guidelines. The reason(s) as to why the widespread approach of homologous recombination failed to yield a recombined plasmid in this instance will be explored in further detail in section 8.2.1 on page 72.

8.2 Cloning

Initially, the cloning of the desired virus construct was planned with homologous recombination. In the end, the method needed to be switched to Gibson Assembly® for

successful transgene insertion, ultimately generating three recombined plasmids though slightly varying approaches.

The challenges of the cloning can be traced primarily to the fundamental features of the utilized plasmids. Firstly, the sheer size of the final construct constitutes a challenge for *E. coli*. Plasmids below 20,000 bp in size are generally regarded as convenient in cloning. Additionally, there is a linear correlation between plasmid size and transformation probability in *E. coli* whereby when the plasmid size increases, the probability decays (Hanahan 1983). The final size of the virus construct in this instance would be close to 40,000 bp, making the laboriousness of recombining the pAd5Δ24-CD40L evident.

There are, however, ways by which the consequences of the construct size can be utilized. He and colleagues (1998) reported in their paper that the smaller colonies generally represented recombinants. This may be attributed to the fact that the growth of the positive colonies is slowed by the size of the recombinant plasmid. This was an approach applied to this study, however, the correspondence is uncertain as this potential marker was not studiously documented. Consequently, while the ultimately positive colonies were of smaller size, they were not necessarily the smallest.

Furthermore, on the issue of size, it has been proposed that the length of the Ad5 genome limits the transformation efficiency, a notion promoted by *E. coli* transformation being inhibited by increasing the amount of DNA (Chartier *et al*. 1996). To enable maintenance of a plasmid nearly twice the size of plasmids normally processed, a sufficient incentive must be conferred with the large viral plasmid. This is generally achieved by inclusion of an antibiotic resistance gene.

Secondly, the plasmids utilized and the location for transgene insertion made a change of antibiotic resistance impossible. Altering the antibiotic resistance of the recombined plasmid would have considerably facilitated the screening process by reducing the amount of background. Instead the subjugation of background colonies was attempted to be restrained by plasmid linearization and dephosphorylation which presented its own challenges.

The pAd5Δ24 was cleaved with EcoRI which was not unique in this plasmid but rather caused the excision of a ca 2,700 bp band that was not removed prior to transformation. This could enable both the realignment and base-pairing of the band into the vector or the recirculation of the digested vector. While the subsequent incubation of the vector with CIP enzyme should ameliorate the extent of colonies without the transgene, complete CIP digestion cannot be guaranteed, hence the presence of background. Gel purification of the vector was an option consciously left unexplored as it was deemed to confer no significant advantage as even without it there ought to be some positive clones. Double digestion with SpeI and EcoRI was later applied to improve on this aspect of the protocol.

Thirdly and finally, an issue relevant for the failed homologous recombination was the presence of superfluous homologous regions aside from the ones flanking the E3-gp19K. Generating a risk for erroneous recombination and the potential loss of critical elements in the rescue plasmid, this constituted a major obstacle for successful recombination. This problem will be explored in detail in section 8.2.1 on page 74.

The three aforementioned challenges were perceived at the beginning of the project and were in the extent possible accommodated, e.g. with the use of an *E. coli* strain with larger construct capacity (XL10-Gold) and CIP enzyme incubation with the backbone plasmid. Other aspects of the study which could not be altered involved changing the backbone plasmid and the location of transgene insertion. Ultimately, the only major component which could be modified would be to exchange the pTHSN for another shuttle plasmid, an option that will be explored further at a later point in this chapter.

Regarding the XL10-Gold bacteria, the application of the strain was later debated as a bacteriophage contamination was discovered upon sequencing of the backbone plasmid near the end of the study. In a letter to the editor, Kamal *et al*. (2013) describe a similar issue, however, no other mentions were found on the matter. Therefore, it was also considered that the contamination could have stemmed from the working environment. In terms of impact on the study, a contamination would at least be a disturbing element, at worst cause the destruction of bacteria carrying the recombined plasmid. The matter would require further investigation and the possible application of another bacterial strain.

8.2.1. Homologous Recombination

The principle for the AdEasy system was published by He and colleagues in the year 1998. The study details a strategy that enables recombination of SC Ad vectors by utilizing the inherent homologous recombination machinery in *E. coli*, allowing the inclusion of a maximum of 10,000 bp foreign DNA as well as multiple transgene expression. Prior to the publication of the study, manipulation of the Ad genome required utilization of restriction enzyme sites for gene insertion and mammalian cells for recombination, an approach that aside from being time-consuming and laborious was also hindered by the few applicable restriction enzyme sites in the Ad genome. The development of the strategy by He and colleagues (1998) additionally provided a means for facilitated direct evaluation of transfection and infection efficiency by the incorporation of a GFP gene into the Ad backbone sequence. The principles of the developed double-transformation, or cotransformation, technique presented in their study is echoed to an extent in this study.

Almost a decade later, Luo *et al.* (2007) introduced a modification to the protocol by He *et al*. (1998) whereby the Ad vector is first transformed into BJ5183 cells with electroporation. Growing the bacteria in the presence of antibiotics, the Ad vector transformed bacterial colonies are identified and cultured. Afterward, the bacteria are made chemically competent before transformation of the linearized shuttle plasmid into the cells with heat shock. Finally, the transgene is transferred into the virus backbone with the aid of homologous regions.

The main differences in the studies by He *et al.* (1998) and Luo *et al*. (2007) to the one presented here, was the insertion of the whole shuttle plasmid into the backbone vector. Aside from the gene of interest, the shuttle plasmid provides altered antibiotic resistance, origin of replication, the left ITR, and two PacI restriction enzyme sites. The change in antibiotic resistance eliminates the need for linearization and CIP digestion of the backbone plasmid, instead enabling its transformation in SC form, which has improved transformation probability (Hanahan 1983).

The method in the AdEasy cloning system could not be directly applied as it fails to allow targeted insertion of the gene of interest into the E3 region of the Ad genome, a crucial requirement for this study. The transgene insertion into the backbone also prevents the utilization of other potential markers for positive clones, such as the lacZ gene. Additionally, transforming pAd5Δ24 to the BJ5183 cells first, the linearized pTHSN-CD40L confers no added benefit to the bacteria, therefore providing no incentive for the bacteria to recombine the transgene into the virus backbone, thus failing to improve upon the situation.

An important fact to consider in contemplating the failure of the homologous recombination was the presence of superfluous homologous regions, which was briefly touched upon previously. A sequence comparison with the Basic Local Alignment Search Tool developed by Altschul and colleagues (1997) of the empty pTHSN and the pAd5Δ24 revealed that there are four regions with moderate to high alignment. The results of the search are presented in Figure 42.

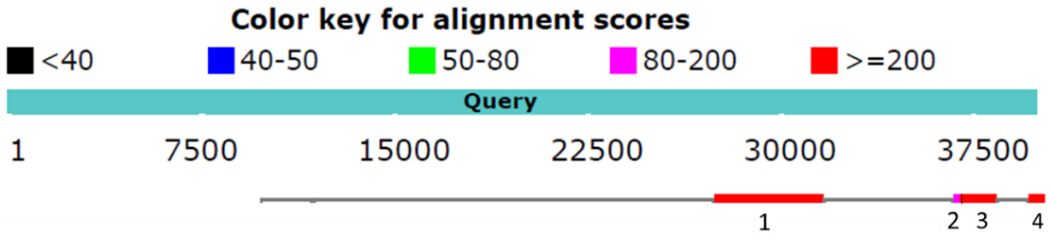

Figure 42: The results from Basic Local Alignment Search Tool by Altschul and colleagues (1997) of the pAd5Δ24 and pTHSN. According to the color key alignment scores, there are three areas with high alignment between pAd5Δ24 and empty pTHSN (1, 3, and 4), and one small visible area (2) that has a slightly lower alignment score.

The location of these homologous regions in relation to other vital elements of the pAd5Δ24 genome is presented in Figure 43. As is depicted, the largest homologous region is in the E3 transcription unit. From this area a ca 2,700 bp fragment is excised with EcoRI digestion, leaving homology regions around 250 bp and 1,000 bp in size in the middle of which the transgene will be inserted. The remaining three areas are all located close to the PacI digestion sites and ITRs.

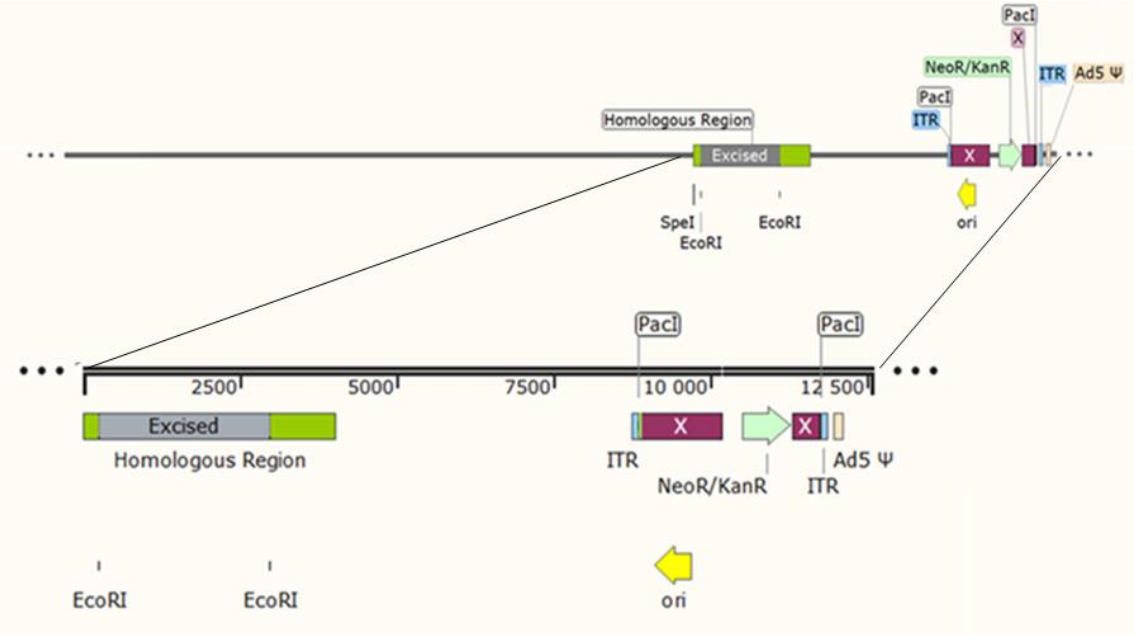

Figure 43: The pAd5Δ24 genome linearized and magnified. The homologous region marked in green was the area into which the transgene would be inserted. The wine-red areas marked with an 'X' adjacent to the PacI sites are superfluous regions with homology between the pTHSN and the pAd5Δ24. The image was made in SnapGeneViewer.

The recognition sequences for both PacI digestion sites by the ITRs are separated by ca 15 bp from the superfluous regions with homology. Restriction analysis of potential positive clones from homologous recombination proved that one PacI site was retained in this area since the vector was successfully cleaved, though the absence of an excised band indicated the incomplete freeing of the ITRs. Narrowing down which of the two sites might have undergone sequential changes can be aided by the BamHI restriction enzyme reactions.

One BamHI recognition site is located closed to the PacI site by the left ITR. Changes to the sequence affecting PacI digestion are likely to also impact BamHI digestion and can therefore be used as a marker. On two of the gel run samples (Figure 23 on page 58, lane 8 and 10) there are two visible bands. Upon comparing them with the controls and the size marker, the bands appear to be around 24,000 bp and 7,000 bp in size. Successful integration of the transgene should yield three bands ca 7,000 bp, 7,300 bp, and 24,000 bp in size. Due to the two smaller bands being relatively close in size and the weak intensity of the band on the gel, it may be that the final band is simply not visible, or overlapping with the ca 7,000 bp band. In the end, it remains inconclusive whether the

BamHI site, and consequently the closest PacI site, has disappeared. Aside from the four major homologous regions, an additional nine areas were identified that albeit small (the largest of them 51 bases, not shown) may cumulatively have disturbed the vector integrity to the extent that a functional virus would have been unable to be constructed.

It was acknowledged that the prolonged maintaining of the plasmids in the BJ5183 cells was a mistake during the first homologous recombination attempt. While the metabolism and inner machinery of the bacteria should be reduced when the LB plates were stored at 4 ˚C, it is possible that the bacteria continued to modify a potentially recombined plasmid. This is further validated by the extensive background and disproportion of the bands in the PacI, BamHI, and HindIII digestions in Figure 22 and 23 (page 55). It is likely, that the bacteria have modified the pTHSN (a much more manageable plasmid) by utilizing the homologous sequences flanking the kanamycin resistance gene, either switching the antibiotic resistance gene into the shuttle plasmid or generating an intermediate between the recue and shuttle plasmid with only the most essential elements for survival.

To remedy this issue, the duration between transformation and screening was reduced during the second attempt, along with double digestion of the pTHSN with SpeI and NdeI. As a result of the double digestion, the transgene, and the flanking homologous regions would be excised from the shuttle plasmid. However, no further isolation or purification of the fragment from remaining pTHSN was done aside from ethanol precipitation. This upon the advice of the article by Luo *et al.* (2007), according to whom gel purification of the cleaved shuttle should be avoided in order to prevent nicking the DNA as well as the reduction of transformation efficiency. While the pTHSN fragments may not in themselves constitute a major background component after transformation, it nonetheless brings a disturbing element to the transformation and recombination, reducing efficiency.

In the end, the one major change that might have considerably improved the outcome of homologous recombination would have been the changing of shuttle vectors to one without superfluous homology. Other minor changes suggested by Luo *et al.* (2007) not implemented would be reduction of incubation time post transformation from over an hour to 30 minutes or even excluding it all together and an increase of the kanamycin

concentration from 25 μg/ml to 50 μg/ml, at least for the LB-plates. Furthermore, while the authors recommend abstaining from gel purification, the shuttle plasmid conferring could be purified with alkaline lysis miniprep procedure in the event of too many colonies following transformation, a suggestion which could be attempted for the rescue plasmid in this study.

8.2.2 Gibson Assembly®

Gibson Assembly® is an alternative to recombination proficient bacteria. A simplified *in vitro* approach, principle for this isothermal recombinant DNA method was first presented in a 2008 paper by Gibson and colleagues titled "Complete Chemical Synthesis, Assembly, and Cloning of a *Mycoplasma genitalium* Genome". Later, the method for the isothermal single-reaction was published separately (Gibson *et al*. 2009). The idea that the Gibson Assembly® reaction builds upon is very simple and while the approach may be very straightforward it still has its own challenges.

The most relevant challenges for the approach presented here is, once more, the size of the construct. With the Gibson Assembly® DNA fragments as large as ca 150,000 bp was successfully cloned in *E. coli* in a two-step reaction (Gibson *et al.* 2008). The method has also been successfully applied in the synthesis of artificial bacterial cells (Gibson *et al.* 2010). Depending on the size of the fragments, the Synthetic Genomics, Inc Company Gibson Assembly® cloning guide, recommends either a one- or two-step reaction. For DNA ranging between 500 bp to 32,000 bp in a reaction of at most five fragments, the maximum construct size is 100,000 bp in multi-stage reactions. No published studies could be found where an OAd vector had previously been cloned in the manner reported here where an almost 40,000 bp construct has been generated in a single two fragment reaction.

The protocol with Gibson Assembly®, while successful, still left room for optimization. Currently, the success rate was at 4%, calculated from the number of positive colonies to the total number screened. Two major changes have been planned for future reactions, the first one being creating longer overlaps. Primers with 40 bp, 60 bp, and 80 bp overlaps

have already been designed for future use, their length providing a higher specificity. The second change would be the incubation period of the reaction. According to Gibson and colleagues (2009), 60 minutes was deemed an optimal duration, and in this instance prolonging the time from 15 minutes to 60 minutes would enable more of the desired construct to form.

After transformation to XL10-Gold cells, the study reactions and controls were plated onto LB plates with either kanamycin or ampicillin. The positive control provided with the Gibson Assembly® kit yielded expected results in the form of bacterial colonies growing on LB-ampicillin plates. However, the intended negative control behaved unexpectedly by also producing bacterial colonies. It was assumed that the mismatched transgene containing fragment would prevent plasmid propagation. Based on the apparent survival of bacteria under kanamycin selection, either the EcoRI restriction digestion or the dephosphorylation must have been incomplete. Despite this, the correct construct was still able to form in the Gibson reaction combining the EcoRI digested backbone with the correct corresponding PCR fragment (Gibson Reaction 2).

8.2.3 Screening of Colonies

Aside from improvements to the methods applied in the presented study, the screening and verification process of the clones was another object of scrutiny. The restriction analyses were always performed with internal controls to confirm the correct function of the enzymes in use and there was no doubt as to their functionality at the employed conditions. The lack of selection markers placed increased significance on an efficient screening method.

Overall, the established colony PCR protocol performed consistently and robustly with appropriate adjustments and optimizations made during the study. The primers utilized were designed to bind to DNA outside the transgene sequence, enabling the employment of the same primer pair for all intended constructs. The CD40L transgenes is in full-length around 200 bp smaller than the E3-gp19k it displaces, 786 bp (human) or 783 bp (mouse) and 986 bp respectively. The soluble CD40L is even smaller, only 510 bp. Since the

empty and recombined pAd5Δ24 both produce a signal, a way to distinguish between them is by comparing the sizes of the PCR fragments. With a sufficiently high agarose content, the size differences between the recombined and empty backbone plasmids should be discernable. Another approach would be to design primers where one binds to the transgene sequences. This provides more substantial proof that any positive colony contains the transgene and reduces the risk for false positives.

Incorporating colony PCR into the screening process was advocated by the method having a high throughput capacity, allowing for the analysis of a large number of colonies in a relatively short time-frame. Colony PCR is a staple in molecular cloning as an efficient and robust screening method of transformed and selected bacteria. One advantage of colony PCR the possibility to screen bacteria without the need for further bacterial amplification. In fact, less is more regarding DNA in colony PCR. The colony PCR reactions were always run alongside positive and negative controls that performed consistently according to expectations. The functionality of the primers was even at one point studied with a gradient PCR to affirm the correct annealing temperature for the PCR cycle (Figure 44). For this experiment, the bacterial solution was diluted 1:3 in MQ, adding 20 µl of the dilution to the master mix.

Gradient Colony PCR

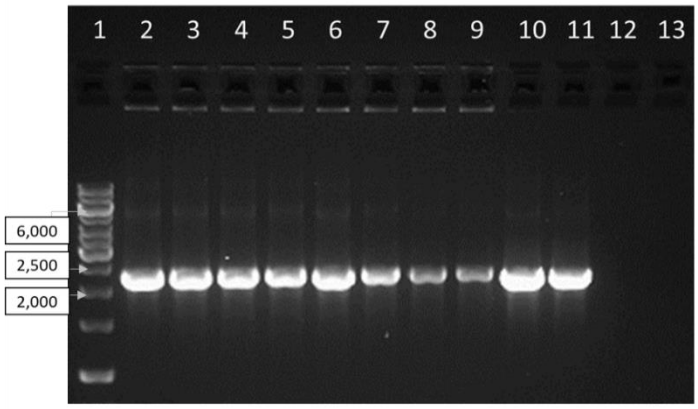

LANE	Sample	T (˚C)
1	GeneRule 1 kb	-
2	Colony pAd5Δ24 A	58.0
3	Colony pAd5Δ24 B	57.2
4	Colony pAd5Δ24 C	56.0
5	Colony pAd5Δ24 D	54.2
6	Colony pAd5Δ24 E	51.9
7	Colony pAd5Δ24 F	49.9
8	Colony pAd5Δ24 G	48.7
9	Colony pAd5Δ24 H	48.0
10	pAd5Δ24 SC	57.2
11	pAd5Δ24 EcoRI-CIP	56.0
12	XL10-Gold	48.7
13	MQ	54.2

Figure 44: Gradient colony PCR results using pAd5Δ24 transformed XL10-Gold as template. The temperature ranged from 54.2 ˚C to 58.0 ˚C.

Utilizing DreamTaq DNA polymerase, the calculated annealing temperature was 53 ˚C which corresponded quite well with the PCR analysis which suggested the maximum PCR product being generated at ca 51.9 ˚C (lane 6). The bacteria carrying the screened pAd5Δ24 plasmid, XL10-Gold, was also added to the screen to provide unequivocal proof that there was nothing in the bacteria to which the primers could bind and produce a PCR product. The gradient PCR echoed previous results gained with gradient PCR using isolated plasmid DNA as template (results not shown).

The gradient PCR also highlighted an issue with the dephosphorylated and cut pAd5Δ24 vector. Theoretically, there should be no signal from the control since successful enzyme digestion would remove the binding site for the reverse primer (Primer Set II reverse). A religated EcoRI digested pAd5Δ24 would similarly lack the binding site for the reverse primer, hence generating no PCR amplified product. However, this was not the case and instead either a PCR fragment was observed (pAd5Δ24 SC and pAd5Δ24-EcoRI-CIP) in substantial quantities or nothing was generated as was the case for the majority of the screened colonies. LB has the ability to inhibit the PCR process, but insufficient dilution was excluded as a reason since it was verified to function with positive controls (the empty pAd5Δ24 SC). This result does, nonetheless, confirm earlier suspicions of incomplete vector digestion and/or dephosphorylation as previously discussed regarding the “negative” control to the Gibson Assembly® (page 78).

In the colonies transformed with the Gibson Assembly® products, the lack of signal can also be explained by the fact that the exonuclease has simply eaten away the area to which the primers would bind, hence no product being formed. To reduce this type of background, it was considered that the reaction volume may be too large (100 µl) in the EcoRI digestion. In this case, the digestion could benefit from reducing the volume to multiple 50 µl reactions, similarly halving the DNA amount and enzyme amount to 1 µl of enzyme and 5 µg DNA. This approach was adopted for the PacI digestion prior to transfection, afterwards pooling two 5 µg reactions into one. It was also attempted for the EcoRI digestion of 10 µg of the backbone plasmid in the 50 µl reaction volume. Since the primers produced signals for the digested and dephosphorylated backbone, a reduction in DNA may generate more complete digestion of all DNA.

8.3 Transfection

In the *in vitro* propagation of viruses, there are certain cell lines that are used (Wold & Ison 2013). The cell line regarded as perhaps the most ideal host for all human Ad is the primary human embryonic kidney (HEK) cells. However, because of sequence homology, a low frequency of recombination has been identified in HEK293 cells between the DNA of the Ad in the cell line and transfected E1-deleted vectors. Consequently, replication-competent Ads will be generated in replication-deficient stock. By utilizing the A549 cell line, the risk of generating Ad5 with a fully intact E1 region should not be an issue.

In the transfection with the ViraPack kit, the experiment was deemed a failure when there was no development of GFP after six days of incubation aside from the auto-fluorescence of dead cells. While the CPE can take longer to manifest, the fluorescence should develop during the first couple of day. An explanation for the negative result may be the insufficient amount of DNA, which was something that constituted a challenge. While 10 μg DNA was digested in two 5 μg reactions before pooling them and precipitating the DNA with ethanol, the DNA concentrations as well as the purity of the DNA solutions were low which would have impacted the chances of successful transfection (Table 8, page 62).

The AdEasy system presents a modified protocol for transfection with the ViraPack kit where after DNA addition the cells are incubated for 3 hours before aspiration. The replacing media is supplemented with 25 μM chloroquine and incubated anew for an additional 6-7 hours before removal and addition of complete medium. Other optimization steps to the protocol is changing the concentration of the modified bovine serum. In the transfection performed during this study, the culture medium contained 6% bovine serum which was the recommended starting point by the manufacturer (APPENDIX 8) in a concentration range of 4-7%. Due to time constraints, it was decided to abandon optimization of the protocol in favor of trying the QIAGEN® Effectene Transfection Reagent.

8.4 Immunostaining

The QIAGEN® Effectene Transfection Reagent transfected cells were initially seeded into the wells of a 12-well plate. Curiously, the cells seemed to be dying and were adhering poorly to the surface of the coverslips, even after a 24-hour incubation. While no viable cause was found, it was speculated that the coverslips may have been coated with an agent that was harmful to the cells such as residual alcohol that had failed to evaporate. The cells, visibly recuperated after the changing of the media (complete DMEM) of the same batch that they had previously been in and the event was deemed inconsequential to the outcome of the staining.

In the first round the cells were fixed 24 hours after infection with paraformaldehyde and methanol. Upon comparison of the different fixation methods, it became apparent that the methanol fixed cells were stained better than the paraformaldehyde fixed cells. This may be attributed to the fact that the methanol was more successful at permeabilizing the cells, allowing for better binding of the subsequent primary and secondary antibodies. Throughout, the perhaps hardest stains to elucidate were those of the CD40L. To differentiate between auto-fluorescence and the actual expression of the CD40L transgene, the location of the observed fluorescence was scrutinized. Auto-fluorescence from e.g. dead cells would appear as bright fluorescing patches of the same intensity allover. The CD40L being a transmembrane protein led to the assumption that the antibodies would concentrated to the outer rim of the cell and to the nucleus. This was confirmed with the visualization of the Alex 488 in the methanol permeabilized cells infected for 48 hours with the viruses from Gibson Reaction 1 and 2 (Figure 41 page 68).

In an attempt to further enhance the signal for the CD40L, the infection was prolonged from 24 hours to 48 hours. While this did successfully enhance the fluorescence, it was still not as clear as the hexon staining. As can be seen in Figure 45 on the following page, there is a unique “halo effect” without a filter that occurs for some of the double positive stained cells. This effect as not observed for the Ad5Δ24 or other controls and may be a marker for cells expressing the CD40L. However, this would require further studies to confirm.

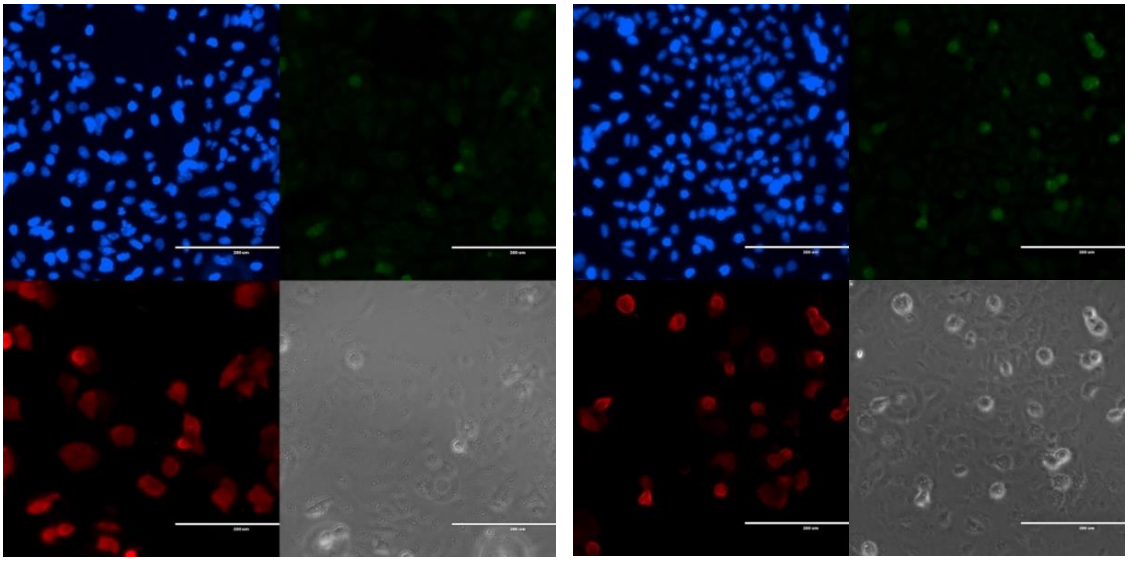

Figure 45: Cells infected with the Gibson Plasmid 1 virus (left) and Gibson Plasmid 2.1 virus (right) fixed with methanol 48 hours after infection. A peculiar halo effect seems to appear for some of the cells positive for both Ad hexon and CD40L protein. The same effect was absent from the other control infections.

Generally, the weakness of the CD40L staining can be attributed to several reasons that ascribe to either the antigen or antibody. Low expression of the CD40L would result in lower levels of antigen for the antibodies to bind to. Similarly, the concentration of the antibody may be too dilute. The cause deemed the most credible was the secondary antibody not being ideal for use with this primary antibody. Still, with the lack of a functional positive control for the CD40L, the functionality of the antibodies could not be reliably evaluated in this experiment. Unequivocal proof of the presence of the CD40L protein could be obtained by Western blot or an ELISA assay. For the Ad5Δ24-CD40L of the soluble variants, Ramos-Blue™ cells were intended to be applied for the determination of levels of e.g. CD40L.

Another issue warranting speculation was the stained cells that showed high levels of the hexon protein and thus the OAd but were not positive for the CD40L. The virus capsid component production occurs during the late stages of the virus proliferation around the same time the encoded transgene protein should be expressed. The negative controls were clean in all instances while the Ad5Δ24 virus control gave a clear signal which coincided with the signal found for the two generated viruses. However, the positive controls for the CD40L, i.e. Ad5/3-hCD40L-CMV and Ad5/3-CD40L-h-TERT, were lackluster.

Since the behavior of these viruses was consistent, it is highly possible that there was a problem with these vials or the batch of viruses.

8.5 Future Perspectives

Upon revisiting the initial aims laid out for the thesis, all three were largely fulfilled, albeit only for one virus. The construction of the remaining viruses will hopefully proceed without major complications, after which, the objective would be virus amplification and cesium chloride or kit purification. Regarding determination of the virus titer, while not addressed in the study, the titer for the produced Ad5Δ24-hCD40L-FL viruses was performed with spectrophotometry. However, since the reliability of the results could not be verified in the allotted time, the results were not included. Therefore, future efforts would entail the reliable determination of the virus titer for all the generated viral preparations with plaque assay.

In contemplating other future perspectives of the designed viruses, the first priority would be to gather sufficient evidence of functionality and efficacy of the generated viruses *in vitro*. This includes the verification of the CD40L expression and functionality as costimulatory molecules, particularly for the soluble CD40L. How well the soluble and full-length CD40L constructs stimulate the immune system and whether one is more effective than the other, is particularly interesting.

In the event that the soluble CD40L encoded construct proves more adapt at eliciting a strong antitumor response, the next major step would be proceeding to *in vivo* studies with humanized mice carrying melanoma tumors. Having mice with a human immune system is preferable as it is as close to a human test subject the viruses can be studied in at this point of development. Melanoma enables easy intratumoral injection because of its palpable tumor mass. Because of it is a more immunogenic form of cancer, it is also a suitable model for therapies wherein immune stimulation is a fundamental aspect of the study. The experiment would further be critical in determining the potential of the Ad5Δ24-mCD40L viruses, since if the treatment fails in this model, there is little hope of them working on any other cancer.

9 CONCLUSIONS

Cancer persistently afflicts a growing part of the world population, with several million people being diagnosed annually. In the search of new and efficient treatments, the oncolytic viruses have emerged as a field in oncology beginning to yield results. The study presented here delves into traditional and novel methods of cloning to generate a CD40L armed oncolytic adenovirus with the intent to enhance the elicitation of systemic antitumor immunity. Ultimately, a functional Ad5Δ24-hCD40L-FL virus was generated with confirmed transgene expression using Gibson Assembly® in manner previously unreported. Consequently, protocols were successfully established to the laboratory for future purposes, encompassing the main steps from cloning to primary virus production. The protocols can be further be applied for the construction of an Ad5Δ24 with insertion of transgenes aside from the CD40L. Considering the discussed improvements to the protocols, future perspectives of the presented study encompass the generation of the remaining viruses, including the viruses encoding the novel soluble CD40L transgenes. After *in vitro* validation of expression and functionality of all the transgenes as well as virus stock production and titer determination, the study will hopefully proceed to *in vivo* testing.

REFERENCES

Aloui C, Prigent A, Sut C, Tariket S, Hamzeh-Cognasse H, Pozzetto B, Richard Y, Cognasse F, Laradi S, Garraud O: The Signaling Role of CD40 Ligand in Platelet Biology and in Platelet Component Transfusion. Int. J. Mol. Sci 15(12): 22342-22364, 2014

Altschul SF, Madden TL, Schäffer AA, Zhang J, Zhang Z, Miller W, Lipman DJ: Gapped BLAST and PSI-BLAST: a new generation of protein database search programs. Nucleic Acids Res 25: 3389-3402, 1997

Ancrile BB, O'Hayer KM, Counter CM: Oncogenic Ras–Induced Expression of Cytokines in Cancer. Mol Interv 8(1): 22–27, 2008

Appledorn DM, Kiang A, McBride A, Jiang H, Seregin S, Scott JM, Stringer R, Kousa Y, Hoban M, Frank MM, Amalfitano A: Wild-type adenoviruses from groups A–F evoke unique innate immune responses, of which HAd3 and SAd23 are partially complement dependent Gene Ther 15, 885–901, 2008

Bergelson JM, Cunningham JA, Droguett G, Kurt-Jones E, Krithivas A, Hong JS, Horwitz MS, Crowell RL, Finberg RW: Isolation of a Common Receptor for Coxsackie B Viruses and Adenoviruses 2 and 5. Science 275(5304): 1320-1323, 1997

Berk A: Adenoviridae. In Fields virology, p. 1704-1728, 6th edition. Editors-in-Chief Knipe DM, Howley PM, Wolters Kluwer/Lippincott Williams & Wilkins Health, Philadelphia 2013

Bett AJ, Prevec L, Graham FL: Packaging capacity and stability of human adenovirus type 5 vectors. J Virol. 67(10): 5911-5921, 1993

Bischoff JR, Kirn DH, Williams A, Heise C, Horn S, Muna M, Ng L, Nye JA, Sampson-Johannes A, Fattaey A, McCormick F: An Adenovirus Mutant That Replicates Selectively in p53-Deficient Human Tumor Cells. Science 274(5286): 373-376, 1996

Bos JL: ras Oncogenes in Human cancer: a review Cancer Res 49: 4682-4689, 1989

Boyer GS, Denny FW Jr, Ginsberg HS: Sequential Cellular Changes Produced By Types 5 And 7 Adenoviruses In Hela Cells And In Human Amniotic Cells. J Exp Med 110(5): 827-844, 1959

Bramson JL, Hitt M, Gauldie J, Graham FL: Pre-existing immunity to adenovirus does not prevent tumor regression following intratumoral administration of a vector expressing IL-12 but inhibits virus dissemination. Gene Ther. 4(10): 1069-1076, 1997

Bray F: Transitions in Human Development and the Global Cancer Burden. In World Cancer Report 2014, p 65. Edited by Wild CP, Stewart BW, International Agency for Research on Cancer, Lyon 2014.

Buckwalter SP, Teo R, Espy MJ, Sloan LM, Smith TF, Pritt BS: Real-Time Qualitative PCR for 57 Human Adenovirus Types from Multiple Specimen Sources. J Clin Microbiol 50(3): 766-771, 2012

Buijs PRA, Verhagen JHE, van Eijck CHJ, van den Hoogen BG: Oncolytic viruses: From bench to bedside with a focus on safety Hum Vaccin Immunother 11(7): 1573-1584, 2015

Cancer (online) Fact Sheet. World Health Organization, February 2017, (referenced 31.3.2017), Available online: www.who.int

Capasso C, Hirvinen M, Garofalo M, Romaniuk D, Kuryk L, Sarvela T, Vitale A, Antopolsky M, Magarkar A, Viitala T, Suutari T, Bunker A, Yliperttula M, Urtti A, Cerullo V: Oncolytic adenoviruses coated with MHC-I tumor epitopes increase the antitumor immunity and efficacy against melanoma. Oncoimmunology 5(4): e1105429, 2016

Cerullo V, Pesonen S, Diaconu I, Escutenaire S, Arstila PT, Ugolini M, Nokisalmi P, Raki M, Laasonen L, Särkioja M, Rajecki M, Kangasniemi L, Guse K, Helminen A, Ahtiainen L, Ristimäki A, Räisänen-Sokolowski A, Haavisto E, Oksanen M, Karli E, Karioja-Kallio A, Holm SL, Kouri M, Joensuu T, Kanerva A, Hemminki A: Oncolytic adenovirus coding for granulocyte macrophage colony-stimulating factor induces antitumoral immunity in cancer patients. Cancer Res 70: 4297-4309, 2010

Chartier C, Degryse E, Gantzer M, Dieterle A, Pavirani A, Mehtali M: Efficient generation of recombinant adenovirus vectors by homologous recombination in Escherichia coli. J Virol 70(7): 4805-4810, 1996

Chen D, Mellman I: Oncology Meets Immunology: The Cancer-Immunity Cycle. Immunity 39(1): 1-10, 2013

Chen F, Zhuang X, Lin L, Yu P, Wang Y, Shi Y, Hu G, Sun Y: New horizons in tumor microenvironment biology: challenges and opportunities. BMC Med 13(45): 2015

Danthinne X, Imperiale MJ: Production of first generation adenovirus vectors: a review Gene Ther 7(20): 1707-1714, 2000

Davison AJ, Benkő M, Harrach B: Genetic content and evolution of adenoviruses, J Gen Virol 84(Pt 11): 2895–2908, 2003

DeNardo DG, Barreto JB, Andreu P, Vasquez L, Tawfik D, Kolhatkar N, Coussens LM: CD4(+) T cells regulate pulmonary metastasis of mammary carcinomas by enhancing protumor properties of macrophages. Cancer Cell 16(2): 91–102, 2009

DeWeese TL, van der Poel H, Li S, Mikhak B, Drew R, Goemann M, Hamper U, DeJong R, Detorie N, Rodriguez R, Haulk T, DeMarzo AM, Piantadosi S, Yu DC, Chen Y, Henderson DR, Carducci MA, Nelson WG, Simons JW: A phase I trial of CV706, a replication-competent, PSA selective oncolytic adenovirus, for the treatment of locally recurrent prostate cancer following radiation therapy. Cancer Res 61(20): 7464-7472, 2001

Diaconu I, Cerullo V, Hirvinen ML, Escutenaire S, Ugolini M, Pesonen SK, Bramante S, Parviainen S, Kanerva A, Loskog AS, Eliopoulos AG, Pesonen S, Hemminki A: Immune response is an important aspect of the antitumor effect produced by a CD40L-encoding oncolytic adenovirus. Cancer Res 72(9): 2327-2338, 2012

Downward J: Targeting RAS signalling pathways in cancer therapy. Nat Rev Cancer 3(1): 11-22, 2003

Echavarría M: Adenoviruses in Immunocompromised Hosts. Clin Microbiol Rev 21(4): 704-715, 2008

European Medicines Agency (EMA) Press release "First oncolytic immunotherapy medicine recommended for approval" October 23rd 2015 Available online: www.ema.europa.eu

Farkona S, Diamandis EP, Blasutig IM: Cancer immunotherapy: the beginning of the end of cancer? BMC Med 14: 73, 2016

Ferlay J, Soerjomataram I, Dikshit R, Eser S, Mathers C, Rebelo M, Parkin DM, Forman D, Bray F: Cancer incidence and mortality worldwide: sources, methods and major patterns in GLOBOCAN 2012. Int J Cancer 136(5): E359-386, 2015

Finnish Cancer Registry Cancer statistics (referenced 26.4.2017) Available online: https://cancerregistry.fi

Food and Drug Administration (FDA) Press Announcement October 27th 2015 "FDA approves first-of-its-kind product for the treatment of melanoma" (referenced 26.4.2017) Available online: www.fda.gov

Frantz, C, Stewart, KM, Weaver VM: The extracellular matrix at a glance. J Cell Sci 123(24), 4195–4200, 2010.

Fueyo J, Gomez-Manzano C, Alemany R, Lee PSY, McDonnell TJ, Mitlianga P, Shi Y-X, Levin VA, Yung WKA, Kyritsis AP: A mutant oncolytic adenovirus targeting the Rb pathway produces anti-glioma effect in vivo. Oncogene 19(1): 2-12, 2000

Garber K: China approves world's first oncolytic virus therapy for cancer treatment. J Natl Cancer Inst 98: 298–300, 2006

Giacca M, Zacchigna S: Virus-mediated gene delivery for human gene therapy. J Control Release 161(2): 377–388, 2012

Gibson DG, Benders GA, Andrews-Pfannkoch C, Denisova EA, Baden-Tillson H, Zaveri J, Stockwell TB, Brownley A, Thomas DW, Algire MA, Merryman C, Young L, Noskov VN, Glass JI, Venter JC, Hutchison CA 3rd, Smith HO: Complete chemical synthesis, assembly, and cloning of a *Mycoplasma genitalium* genome. Science 319(5867): 1215-1220, 2008

Gibson DG, Glass JI, Lartigue C, Noskov VN, Chuang RY, Algire MA, Benders GA, Montague MG, Ma L, Moodie MM, Merryman C, Vashee S, Krishnakumar R, Assad-Garcia N, Andrews-Pfannkoch C, Denisova EA, Young L, Qi ZQ, Segall-Shapiro TH, Calvey CH, Parmar PP, Hutchison CA 3rd, Smith HO, Venter JC: Creation of a bacterial cell controlled by a chemically synthesized genome. Science 329(5987): 52-56, 2010

Gibson DG, Young L, Chuang R-Y, Venter J C, Hutchison CA 3rd, Smith HO: Enzymatic assembly of DNA molecules up to several hundred kilobases. N Meth 6(5): 343-345, 2009

Giberson AN, Davidson AR, Parks RJ: Chromatin structure of adenovirus DNA throughout infection. Nucleic Acids Res 40(6): 2369-2376, 2012

Gomes EM, Rodrigues MS, Phadke AP, Butcher LD, Starling C, Chen S, Chang D, Hernandez-Alcoceba R, Newman JT, Stone MJ, Tong AW: Antitumor activity of an oncolytic adenoviral-CD40 ligand (CD154) transgene construct in human breast cancer cells. Clin Cancer Res 15(4): 1317-1325, 2009

Greaves M, Maley CC: Clonal evolution in cancer. Nature 481(7381): 306–313, 2012

Greber UF, Suomalainen M, Stidwill RP, Boucke K, Ebersold MW, Helenius A: The role of the nuclear pore complex in adenovirus DNA entry. EMBO J 16(19): 5998-6007, 1997

Grivennikov SI, Greten FR, Karin M: Immunity, inflammation, and cancer. Cell 140(6): 883-899, 2010

Hanahan D: Studies on transformation of *Escherichia coli* with plasmids. J Mol Biol 166(4): 557-580, 1983

Hanahan D, Weinberg RA: The hallmarks of cancer. Cell 100(1): 57–70, 2000

Hanahan D, Weinberg R A: Hallmarks of cancer: the next generation. Cell 144(5): 646-674, 2011

Hawkins LK, Johnson L, Bauzon M, Nye JA, Castro D, Kitzes GA, Young MD, Holt JK, Trown P, Hermiston TW: Gene delivery from the E3 region of replicating human adenovirus: evaluation of the 6.7 K/gp19 K region. Gene Ther 8(15): 1123-1131, 2001

He TC, Zhou S, da Costa LT, Yu J, Kinzler KW, Vogelstein B: A simplified system for generating recombinant adenoviruses. Proc Natl Acad Sci U S A 95(5): 2509-2514, 1998

Helleday T, Eshtad S, Nik-Zainal S: Mechanisms underlying mutational signatures in human cancers Nat Rev Genet 15(9): 585-598, 2014

Henn V, Steinbach S, Büchner K, Presek P, Kroczek RA: The inflammatory action of CD40 ligand (CD154) expressed on activated human platelets is temporally limited by coexpressed CD40. Blood 98(4):1047-1054, 2001

Hilleman MR, Werner JH: Recovery of new agent from patients with acute respiratory illness. Proc Soc Exp Biol Med 85(1): 183-188, 1954.

Hirvinen M, Rajecki M, Kapanen M, Parviainen S, Rouvinen-Lagerström N, Diaconu I, Nokisalmi P, Tenhunen M, Hemminki A, Cerullo V: Immunological Effects of a Tumor Necrosis Factor Alpha-Armed Oncolytic Adenovirus. Hum Gene Ther 26(3): 134-144, 2015

Hoffmann D, Wildner O: Efficient generation of double heterologous promoter controlled oncolytic adenovirus vectors by a single homologous recombination step in *Escherichia coli*. BMC Biotechnol 6: 36, 2006

Huang JL, aRocca CJ, Yamamoto M: Showing the Way: Oncolytic Adenoviruses as Chaperones of Immunostimulatory Adjuncts. Biomedicines 4(3): 23, 2016

Joyce JA, Pollard JW: Microenvironmental regulation of metastasis. Nat Rev Cancer 9(4): 239-252, 2009

Kamal F, Zhang L, Reha-Krantz LJ: *Escherichia coli* XL10-Gold Bacteria Produce Bacteriophage. J Clin Microbiol 51(2): 727, 2013

Kaufman HL, Kohlhapp FJ, Zloza A: Oncolytic viruses: a new class of immunotherapy drugs. Nat Rev Drug Discov 14(9): 642-662, 2015

Kelly E, Russell SJ: History of oncolytic viruses: genesis to genetic engineering. Mol Ther 15(4): 651-659, 2007

Kennedy MA, Parks RJ: Adenovirus Virion Stability and the Viral Genome: Size Matters. Mol Ther 17(10): 1664-1666, 2009

Kenny PA, Lee GY, Bissell MJ: Targeting the tumor microenvironment. Front Biosci 12: 3468-3474, 2007

Knaul F M, Arreola-Ornelas H, Méndez O, Alsan M, Seinfeld J, Marx A, Atun R: The Global Economic Burden of Cancer, In World Cancer Report 2014. p. 581, edited by Wild CP, Stewart BA, International Agency for Research on Cancer, Lyon 2014

Kremer EJ, Nemerow GR: Adenovirus Tales: From the Cell Surface to the Nuclear Pore Complex. Spindler KR, ed. PLoS Pathogens 11(6): e1004821, 2015

Krilov LR: Adenovirus Infections in the Immunocompromised host. Pediatr Infect Dis J 24: 555-556, 2005

Lapenna S, Giordano: A Cell cycle kinases as therapeutic targets for cancer. Nat Rev Drug Discov 8(7): 547-566, 2009

Law LK, Davidson BL: What does it take to bind CAR? Mol Ther 12(4): 599-609, 2005

Lechner RL, Kelly TJ Jr: The structure of replicating adenovirus 2 DNA molecules. Cell 12(4): 1007-1020, 1977

Liljenfeldt L, Dieterich LC, Dimberg A, Mangsbo SM, Loskog AS: CD40L gene therapy tilts the myeloid cell profile and promotes infiltration of activated T lymphocytes. Cancer Gene Ther 21(3): 95-102, 2014

Liu, HY, Han BJ, Zhong YX, Lu ZZ: A three-plasmid system for construction of armed oncolytic adenovirus. J Virol Methods 162(1-2): 8-13, 2009

Liu GY, Li ZJ, Li QL, Jin Y, Zhu YH, Wang YH, Liu MY, Li YG, Li Y: Enhanced growth suppression of TERT-positive tumor cells by oncolytic adenovirus armed with CCL20 and CD40L. Int Immunopharmacol 28(1): 487-493, 2015

Loskog A: Immunostimulatory Gene Therapy Using Oncolytic Viruses as Vehicles. Lamfers MLM, Chiocca EA, eds. Viruses 7(11): 5780-5791, 2015

Loskog A, Dzojic H, Vikman S, Ninalga C, Essand M, Korsgren O, Totterman TH: Adenovirus CD40 ligand gene therapy counteracts immune escape mechanisms in the tumor Microenvironment. J Immunol 172(11):7200-7205, 2004

Lu P, Weaver VM, Werb Z: The extracellular matrix: a dynamic niche in cancer progression. J Cell Biol 196: 395–406 2012

Luo J, Deng ZL, Luo X, Tang N, Song WX, Chen J, Sharff KA, Luu HH, Haydon RC, Kinzler KW, Vogelstein B, He TC: A protocol for rapid generation of recombinant adenoviruses using the AdEasy system. Nat Protoc 2(5): 1236-1247, 2007

Malmström PU, Loskog AS, Lindqvist CA, Mangsbo SM, Fransson M, Wanders A, Gårdmark T, Tötterman TH: AdCD40L immunogene therapy for bladder carcinoma-the first phase I/IIa trial. Clin Cancer Res 16(12): 3279-3287, 2010

Marusyk A, Almendro V, Polyak K: Intra-tumour heterogeneity: a looking glass for cancer? Nat Rev Cancer 12(5): 323-334, 2012

Mazzei GJ, Edgerton MD, Losberger C, Lecoanet-Henchoz S, Graber P, Durandy A, Gauchat JF, Bernard A, Allet B, and Bonnefoy JY: Recombinant soluble trimeric CD40 ligand is biologically active. J Biol Chem 270(13): 7025-7028, 1995

Mclellan AD, Heiser A, Hart DNJ: Induction of dendritic cell costimulator molecule expression is suppressed by T cells in the absence of antigen-specific signalling: role of cluster formation, CD40 and HLA-class II for dendritic cell activation. Immunology 98(2): 171-180, 1999

Meier O, Greber UF: Adenovirus endocytosis. J Gene Med 6 Suppl 1: S152-163, 2004

Melcher A, Parato K, Rooney CM, Bell JC: Thunder and Lightning: Immunotherapy and Oncolytic Viruses Collide. Mol Ther 19(6): 1008-1016, 2011

Monteiro J, Fodde R: Cancer stemness and metastasis: Therapeutic consequences and perspectives European Journal of Cancer 46(7): 1198-1203, 2010

Nevins JR, Ginsberg HS, Blanchard JM, Wilson MC, Darnell JE: Regulation of the Primary Expression of the Early Adenovirus Transcription Units. J Virol 32(3): 727-733, 1979

O'Shea CC, Johnson L, Bagus B, Choi S, Nicholas C, Shen A, Boyle L, Pandey K, Soria C, Kunich J Shen Y, Habets G, Ginzinger D, McCormick F: Late viral RNA export, rather than p53 inactivation, determines ONYX-015 tumor selectivity Cancer Cell 6(6): 611-623, 2004

Pattabiraman DR, Weinberg RA: Tackling the cancer stem cells – what challenges do they pose? Nat Rev Drug Discov 13(7): 497-512, 2014

Pickup MW, Mouw JK, Weaver VM: The extracellular matrix modulates the hallmarks of cancer EMBO Rep 15(12): 1243-1253, 2014

Pesonen, S, Diaconu I, Kangasniemi L, Ranki T Kanerva A, Pesonen SK, Gerdemann U, Leen AM, Kairemo K, Oksanen, M, Haavisto, E, Holm SL, Karioja-Kallio A, Kauppinen, S, Partanen K, Laasonen L, Joensuu T, Alanko T, Cerullo V, Hemminki A: Oncolytic Immunotherapy of Advanced Solid Tumors with a CD40L-Expressing Replicating Adenovirus: Assessment of Safety and Immunologic Responses in Patients. Cancer Res 72(7): 1621-1631, 2012

Plummer M, de Martel C, Vignat J, Ferlay J, Bray F, Franceschi S: Global burden of cancers attributable to infections in 2012: a synthetic analysis. The Lancet Global Health 4(9): e609-e616, 2016

Pollard JW: Tumour-educated macrophages promote tumour progression and metastasis. Nat Rev Cancer 4(1): 71-78, 2004

Rodriguez R, Schuur ER, Lim HY, Henderson GA, Simons JW, Henderson DR: Prostate attenuated replication competent adenovirus (ARCA) CN706: a selective cytotoxic for prostate-specific antigen-positive prostate cancer cells. Cancer Res 57(13): 2559-2563, 1997

Roelvink PW, Lizonova A, Lee JG, Li Y, Bergelson JM, Finberg RW, Brough DE, Kovesdi I, Wickham TJ: The coxsackievirus-adenovirus receptor protein can function as a cellular attachment protein for adenovirus serotypes from subgroups A, C, D, E, and F. J Virol 72(10): 7909–7915, 1998

Rowe WP, Huebner RJ, Gilmore LK, Parrott RH, Ward TG: Isolation of a cytopathogenic agent from human adenoids undergoing spontaneous degeneration in tissue culture. Proc Soc Exp Biol Med 84(3): 570–573, 1953

Russell SJ, Peng KW, Bell JC: Oncolytic virotherapy. Nat Biotechnol 30(7): 658-670, 2012

Salone B, Martina Y, Piersanti S, Cundari E, Cherubini G, Franqueville L, Failla C, Boulanger P, Saggio I: Integrin α3β1 Is an Alternative Cellular Receptor for Adenovirus Serotype 5. J Virol 77(24): 13448–13454, 2003

Schulz O, Edwards AD, Schito M, Aliberti J, Manickasingham S, Sher A, Reis e Sousa C: CD40 triggering of heterodimeric IL-12 p70 production by dendritic cells in vivo requires a microbial priming signal. Immunity 13(4): 453-462, 2000

Shashkova EV, May SM, Barry MA: Characterization of human adenovirus serotypes 5, 6, 11, and 35 as anticancer agents Virology 394(2): 311–320, 2009

Sherr CJ, McCormick F: The RB and p53 pathways in cancer. Cancer Cell 2(2):103-112, 2002

Shiver JW, Fu TM, Chen L, Casimiro DR, Davies ME, Evans RK, Zhang ZQ, Simon AJ, Trigona WL, Dubey SA, Huang L, Harris VA, Long RS, Liang X, Handt L, Schleif WA, Zhu L, Freed DC, Persaud NV, Guan L, Punt KS, Tang A, Chen M, Wilson KA, Collins KB, Heidecker GJ, Fernandez VR, Perry HC, Joyce JG, Grimm KM, Cook JC, Keller PM, Kresock DS, Mach H, Troutman RD, Isopi LA, Williams DM, Xu Z, Bohannon KE, Volkin DB, Montefiori DC, Miura A, Krivulka GR, Lifton MA, Kuroda MJ, Schmitz JE, Letvin NL, Caulfield MJ, Bett AJ, Youil R, Kaslow DC, Emini EA: Replication-incompetent adenoviral vaccine vector elicits effective anti-immunodeficiency-virus immunity. Nature 415(6869): 331-335, 2002

Smith JG, Wiethoff CM, Stewart PL, Nemerow GR: Adenovirus. Curr Top Microbiol Immunol 343: 195-224, 2010

Sun Y: Translational horizons in the tumor microenvironment: harnessing breakthroughs and targeting cures. Med Res Rev 35(2): 408-436, 2015

Stratton MR, Campbell PJ, Futreal PA: The cancer genome. Nature 458(7239): 719-724, 2009

Thaiss CA, Semmling V, Franken L, Wagner H, Kurts C: Chemokines: A New Dendritic Cell Signal for T Cell Activation. *Front Immunol* 2: 31, 2011

Turley SJ, Cremasco V, Astarita JL: Immunological hallmarks of stromal cells in the tumour microenvironment. Nat Rev Immunol 15(11): 669-682, 2015

Vartiainen E, Karjalainen S, Pylkkänen L, Vertio H Jalava K, Järvisalo J, Koivuranta-Vaara P, Malila N, Nurminen R, Pajari A-M, Reijula K, Remes K, Rosenberg-Ryhänen L, Tammela T, Jarmo V: Syöpätautien asiantuntijaryhmä. Syövän ehkäisyn varhaisen toteamisen ja kuntoutumisen tuen kehittäminen vuosille 2014–2025 osana kansallista syöpäsuunnitelmaa [Development of cancer prevention, early detection and rehabilitative support 2014–2025. National Cancer Plan, Part II]. p. 13, National Institute for Health and Welfare Directions 6/2014 Juvenes Print – Suomen Yliopistopaino Oy, Tampere 2013

Veglia F, Gabrilovich DI: Dendritic cells in cancer: the role revisited. Curr Opin Immunol 45: 43–51, 2017

Vogelstein B, Papadopoulos N, Velculescu VE, Zhou S, Diaz LA Jr, Kinzler KW: Cancer genome landscapes. Science 339(6127): 1546-1558, 2013

Wiethoff CM, Wodrich H, Gerace L, Nemerow GR: Adenovirus Protein VI Mediates Membrane Disruption following Capsid Disassembly. J Virol 79(4): 1992-2000, 2005

Wold W, Ison M: Adenoviruses. In Fields virology, p. 1732-1762, 6th edition. Editors-in-Chief Knipe DM, Howley PM, Wolters Kluwer/Lippincott Williams & Wilkins Health, Philadelphia 2013

Wold WS, Toth K: Adenovirus vectors for gene therapy, vaccination and cancer gene therapy. Curr Gene Ther 13(6): 421-433, 2013

Yamamoto M, Curiel DT: Current Issues and Future Directions of Oncolytic Adenoviruses. Mol Ther 18(2): 243-250, 2010

Yamamoto Y, Nagasato M, Yoshida T, Aoki K: Recent advances in genetic modification of adenovirus vectors for cancer treatment. Cancer Sci 108(5): 831-837, 2017

Zhang Y, Bergelson JM: Adenovirus receptors. J Virol 79(19): 12125–12131, 2005

APPENDICIES

APPENDIX 1: The CD40L amino acid sequences and design

The CD40L was designed in a membrane bound and soluble form. The intra-, trans-, and extracellular domain of the membrane bound form are depicted by the three different colors utilized: blue (extracellular), yellow (transcellular), and brown (extracellular). The total length of the membrane bound form is 261 (human) or 260 (mouse) amino acids.

After the molecular processing, the 149 aminoacid sequence for the soluble CD40L is generated. To ensure the secretion of this soluble form, a 20 amino acids long signal peptide was added to the N-terminal.

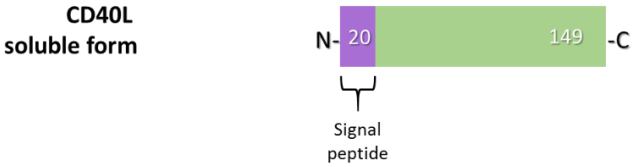

UniProtKB

Homo sapiens (Human) CD40L_HUMAN Length 261

A. Topology

Feature key	Position(s)	DescriptionActions	Length
Topological domain	1 – 22	Cytoplasmic	22
Transmembrane	23 – 46	Helical; Signal-anchor for type II membrane protein	24
Topological domain	47 – 261	Extracellular	215

B. Immature sequence

Length 261 Mass (Da) 29,274

```
   10         20         30         40         50
MIETYNQTSP RSAATGLPIS MKIFMYLLTV FLITQMIGSA LFAVYLHRRL
         60         70         80         90        100
DKIEDERNLH EDFVFMKTIQ RCNTGERSLS LLNCEEIKSQ FEGFVKDIML
        110        120        130        140        150
NKEETKKENS FEMQKGDQNP QIAAHVISEA SSKTTSVLQW AEKGYYTMSN
        160        170        180        190        200
NLVTLENGKQ LTVKRQGLYY IYAQVTFCSN REASSQAPFI ASLCLKSPGR
        210        220        230        240        250
FERILLRAAN THSSAKPCGQ QSIHLGGVFE LQPGASVFVN VTDPSQVSHG
        260
TGFTSFGLLK L
```

C. Molecule processing

Position(s)	Description Actions	Length
1 – 261	CD40 ligand, membrane form	261
113 – 261	CD40 ligand, soluble form	149

Mus musculus (Mouse) CD40L_MOUSE Length 260

A. Topology

Feature key	Position(s)	Description Actions	Length
Topological domain	1 – 22	Cytoplasmic	22
Transmembrane	23 – 46	Helical; Signal-anchor for type II membrane protein	24
Topological domain	47 – 260	Extracellular	214

B. Immature sequence

Length 260 Mass (Da) 26,370

```
         10         20         30         40         50
MIETYSQPSP RSVATGLPAS MKIFMYLLTV FLITQMIGSV LFAVYLHRRL
         60         70         80         90        100
DKVEEEVNLH EDFVFIKKLK RCNKGEGSLS LLNCEEMRRQ FEDLVKDITL
        110        120        130        140        150
NKEEKKENSF EMQRGDEDPQ IAAHVVSEAN SNAASVLQWA KKGYYTMKSN
        160        170        180        190        200
LVMLENGKQL TVKREGLYYV YTQVTFCSNR EPSSQRPFIV GLWLKPSSGS
        210        220        230        240        250
ERILLKAANT HSSSQLCEQQ SVHLGGVFEL QAGASVFVNV TEASQVIHRV
        260
GFSSFGLLKL
```

C. Molecule processing

Position(s)	Description Actions	Length
1 – 260	CD40 ligand, membrane form	260
112 – 260	CD40 ligand, soluble form	149

APPENDIX 2: Preparation for Gibson Assembly®

The transgene insert production

The PCR cycle and master mix composition for amplification of the PCR insert in Gibson Assembly®

PCR cycle:
98 °C 20 s
98 °C 10 s
57 °C 20 s
72 °C 90 s
} 30 cycles
72 °C 5 min
12 °C ∞

FINAL CONC.	REAGENT
to 50 µl	MQ
1x	5x Phusion HF Buffer
0.5 µM	Gibson Reaction Forward primer
0.5 µM	Gibson Reaction Reverse primer
1 ng	pTHSN-CD40L-human
0.2 mM	10 mM dNTPs mix
3%	DMSO
0.02 U/µl	Phusion DNA Polymerase

Backbone digestion

The backbone was single (EcoRI-HF) and double digested (SpeI and EcoRI)

MQ to 50 µl
5 µl 10x Cutsmart buffer
10 µg pAd5D24
2 µl EcoRI HF/ SpeI

Incubate at 37 °C for 1 hr. Confirm digestion on 0.8 % agarose gel run at 70 V for 1 hr. Heat-inactivate the digestions for 20 minutes at a minimum of 80 °C

APPENDIX 3: Colony Polymerase Chain Reaction

The day after the transformation, pick colonies for minipreps and grow them overnight. The following morning, the template can be processed in two ways:

1) Take 5 µl of the bacterial solution and dilute it in 95 µl MQ before boiling it at 98 °C for 10 minutes in the thermal cycler. 20 µl of the dilution is then used for the PCR.
2) Add 30 µl bacterial culture to 70 µl MQ and use 20 µl of this dilution for the PCR.

In both cases, add 30 µl of the master mix with half the volume of MQ to compensate for the MQ added with the template.

DreamTaq

PCR cycle:
95 °C 2 min
95 °C 30 s
58 °C 30 s
72 °C 2 min
} 30 cycles
72 °C 5 min
4 °C ∞

FINAL CONC.	REAGENT
to 50 µl x 0,5	MQ
1x	10X DreamTaq Buffer
0.5 µM	Forward Primer
0.5 µM	Reverse Primer
0.2 mM	10 mM dNTP Mix
1.25 U	DreamTaq DNA Polymerase
20 µl	Template in MQ

Run the PCR amplified products on 1.5 % agarose gels for 1 hr at 70 V.

Phusion HF

PCR cycle:
98 °C 3 min
98 °C 10 s
66 °C 20 s
72 °C 30 s
} 35 cycles
72 °C 5 min
6 °C ∞

FINAL CONC.	REAGENT
to 50 ul x 0,5	MQ
1x	5X Phusion HF Buffer
0.5 µM	Forward Primer
0.5 µM	Reverse Primer
0.2 mM	10 mM dNTP Mix
0.02 U/µl	Phusion DNA Polymerase
20 µl	Template in MQ

APPENDIX 4: Protocol for QIAGEN® Plasmid Mini Kit

This is the plasmid extraction protocol as provided by the manufacturer for the QIAGEN® Plasmid Minikit (ref no: 12123).

Procedure

1. Pick a single colony from a freshly streaked selective plate and inoculate a starter culture of 2–5 ml LB medium containing the appropriate selective antibiotic. Incubate for approximately 8 h at 37°C with vigorous shaking (approx. 300 rpm). Use a tube or flask with a volume of at least 4 times the volume of the culture.

2. Dilute the starter culture 1/500 to 1/1000 into 3 ml selective LB medium. Grow at 37°C for 12–16 h with vigorous shaking (approx. 300 rpm). Use a flask or vessel with a volume of at least 4 times the volume of the culture. The culture should reach a cell density of approximately 3–4 x 109 cells per milliliter,
which typically corresponds to a pellet wet weight of approximately 3 g/liter medium.,

3. Harvest the bacterial cells by centrifugation at 6000 x *g* for 15 min at 4°C.
If you wish to stop the protocol and continue later, freeze the cell pellets at –20°C.

4. Resuspend the bacterial pellet in 0.3 ml of Buffer P1.
Ensure that RNase A has been added to Buffer P1. If LyseBlue reagent has been added to Buffer P1, vigorously shake the buffer bottle before use to ensure LyseBlue particles are completely resuspended. The bacteria should be resuspended completely by vortexing or pipetting up and down until no cell clumps remain.

5. Add 0.3 ml of Buffer P2, mix thoroughly by vigorously inverting the sealed tube 4–6 times, and incubate at room temperature (15–25°C) for 5 min.
Do not vortex, as this will result in shearing of genomic DNA. The lysate should appear viscous. Do not allow the lysis reaction to proceed for more than 5 min. After use, the bottle containing Buffer P2 should be closed immediately to avoid acidification from CO2 in the air. If LyseBlue has been added to Buffer P1, the cell suspension will turn blue after addition of Buffer P2. Mixing should result in a homogeneously colored suspension. If the suspension contains localized colorless regions or if brownish cell clumps are
still visible, continue mixing the solution until a homogeneously colored suspension is achieved.

6. Add 0.3 ml of chilled Buffer P3, mix immediately and thoroughly by vigorously inverting 4–6 times, and incubate on ice for 5 min.
Precipitation is enhanced by using chilled Buffer P3 and incubating on ice. After addition of Buffer P3, a fluffy white material forms and the lysate becomes less viscous. The precipitated material contains genomic DNA, proteins, cell debris, and KDS. The lysate should be mixed thoroughly to ensure even potassium dodecyl sulphate precipitation. If the mixture still appears viscous, more mixing is required to completely neutralize the solution. If LyseBlue reagent has been used, the suspension should be mixed until all

trace of blue has gone and the suspension is colorless. A homogeneous colorless suspension indicates that the SDS has been effectively precipitated.

7. Centrifuge at maximum speed in a microcentrifuge for 10 min. Remove supernatant containing plasmid DNA promptly.
Before loading the centrifuge, the sample should be mixed again. Centrifugation should be performed at maximum speed in 1.5 ml or 2 ml microcentrifuge tubes (e.g., 10,000–13,000 rpm in a microcentrifuge). Maximum speed corresponds to 14,000–18,000 x *g* for most microcentrifuges. After centrifugation, the supernatant should be clear. If the supernatant is not clear, a second, shorter centrifugation should be carried out to avoid applying any suspended or particulatematerial to the column. Suspended material (which causes the sample to appear turbid) will clog the column and reduce or eliminate flow.

Optional: Remove a 50 µl sample from the cleared lysate and save it for an analytical gel (sample 1).

8. Equilibrate a QIAGEN-tip 20 by applying 1 ml Buffer QBT, and allow the column to empty by gravity flow.
PlaceQIAGEN-tips into aQIArack over the waste tray or use the tip holders provided with each kit (see "Setup of QIAGEN-tips" page 13). Flow of buffer will begin automatically by reduction in surface tension due to the presence of detergent in the equilibration buffer. Allow the QIAGEN-tip to drain completely. QIAGEN-tips can be left unattended, since the flow of buffer will stop when the meniscus reaches the upper frit in the column.

9. Apply the supernatant from step 7 to the QIAGEN-tip 20 and allow it to enter the resin by gravity flow.
The supernatant should be loaded onto the QIAGEN-tip promptly. If it is left too long and becomes cloudy due to further precipitation of protein, it must be centrifuged again before loading to prevent clogging of the QIAGEN-tip.

Optional: Remove a 50 µl sample of the flow-through and save for an analytical gel (sample 2).

10. Wash the QIAGEN-tip 20 with 2 x 2 ml Buffer QC.
Allow Buffer QC to move through the QIAGEN-tip by gravity flow.

Optional: Remove a 220 µl sample of the combined wash fractions and save for an analytical gel (sample 3).

11. Elute DNA with 0.8 ml Buffer QF.
Collect the eluate in a 1.5 ml or 2 ml microcentrifuge tubes (not supplied).
Note: For constructs larger than 45–50 kb, prewarming the elution buffer to 65°C may help to increase yield.
Optional: Remove a 45 µl sample of the eluate and save for an analytical gel (sample 4).

12. Precipitate DNA by adding 0.7 volumes (0.56 ml per 0.8 ml of elution volume) of room-temperature isopropanol to the eluted DNA. Mix and centrifuge immediately at ≥15,000 x *g* rpmfor 30min in amicrocentrifuge. Carefully decant the supernatant.
All solutions should be at room temperature to minimize salt precipitation. Isopropanol pellets have a glassy appearance and may be more difficult to see than the fluffy, salt-containing pellets that result from ethanol precipitation. Marking the outside of the tube before centrifugation allows the pellet to be easily located. Isopropanol pellets are also more loosely attached to the side of the tube, and care should be taken when removing the supernatant.

13. Wash DNA pellet with 1 ml of 70% ethanol and centrifuge at 15,000 x *g* for 10 min. Carefully decant the supernatant without disturbing the pellet.
The 70% ethanol removes precipitated salt and replaces isopropanol with the more volatile ethanol, making the DNA easier to redissolve.

14. Air-dry the pellet for 5–10min, and redissolve the DNA in a suitable volume of buffer (e.g., TE buffer, pH 8.0, or 10mM Tris·Cl, pH 8.5)
Redissolve the DNA pellet by rinsing the walls to recover the DNA. Pipetting the DNA up and down to promote resuspension may cause shearing and should be avoided. Overdrying the pellet will make the DNA difficult to redissolve. DNA dissolves best under slightly alkaline conditions; it does not easily dissolve in acidic buffers.

APPENDIX 5: Restriction analysis and digestions

pTHSN-CD40L, all constructs
MQ to 50 µl
20 µg pTHSN-CD40L DNA
5 µl Cutsmart buffer
2 µl SpeI/NdeI

pAd5Δ24
MQ to 100 µl
10 µg pAd5Δ24 DNA
10 µl Cutsmart buffer
2 µl EcoRI

Dephosphorylation
Dilute the CIP enzyme 1:10 with MQ for 10 ul CIP-diluted
1 ul CIP-diluted
5 ul 10X Cutsmart buffer
The EcoRI digested sample

Restriction analysis
MQ to 50 ul
3 ug DNA /5 ul DNA
5 ul 10x Cutsmart buffer
1 ul PacI/HindIII/BamHI

Digestion of PCR samples
MQ to 30 ul
10 ul PCR sample
2 ul 10X Cutsmart Buffer
2 ul HindIII

The digestions were incubated at 37°C for 1-2 hour and separated on a 0.8% agarose or 0.6% (PacI) gel at 70 volts for 1 hour.

APPENDIX 6: NucleoBond® Xtra plasmid purification

The plasmid purification instructions for the NucleoBond® Xtra kit (Macherey-Nagel, cat no: 740410.50).

1 Preparation of starter culture
Inoculate a 3–5 mL starter culture of LB medium with a single colony picked from a freshly streaked agar plate. Make sure that plate and liquid culture contain the appropriate selective antibiotic to guarantee plasmid propagation (see section 4.3 for more information). Shake at 37 °C and ~ 300 rpm for ~ 8 h.

2 Preparation of large overnight culture
Note: To utilize the entire large binding capacity of the NucleoBond® Xtra Columns it is important to provide enough plasmid DNA. If the culture is known to grow poorly or the plasmid does not quite behave like a high-copy plasmid, please consult section 4.6 for larger culture volumes. If you are not sure about the plasmid copy number and growth behavior of your host strain, increase the culture volume and decide later in step 3 how much cells to use for the preparation. The recommended culture volumes below are calculated for a final OD_{600} of around 4 (see section 4.5).

Inoculate an overnight culture by diluting the starter culture 1 / 1000 into the given volumes of LB medium also containing the appropriate selective antibiotic. Grow the culture overnight at 37 °C and ~ 300 rpm for 12–16 h.

Midi Volume: 100 mL

3 Harvest of bacterial cells
Measure the cell culture OD_{600} and determine the recommended culture volume.
V [mL] = 400 / OD_{600}
Pellet the cells by centrifugation at **4,500–6,000 x *g*** for **≥ 10 min** at **4 °C** and discard the supernatant completely.

4 Resuspension (Buffer RES)
Resuspend the cell pellet completely in **8 mL Resuspension Buffer RES + RNase A** by pipetting the cells up and down or vortexing the cells. For an efficient cell lysis it is important that no clumps remain in the suspension.

Note: Increase RES buffer volume proportionally if more than the recommended cell mass is used (see section 4.8 for information on optimal cell lysis and section 4.9 regarding difficult-to-lyse strains).

5 Cell lysis (Buffer LYS)
Add **8 mL Lysis Buffer LYS** to the suspension. Mix gently by **inverting** the tube **5 times**. **Do not vortex** as this will shear and release contaminating chromosomal DNA from cellular debris into the suspension. **Incubate** the mixture at room temperature (18–25 °C) for **5 min**.

Warning: Prolonged exposure to alkaline conditions can irreversibly denature and degrade plasmid DNA and liberate contaminating chromosomal DNA into the lysate.
Note: Increase LYS buffer volume proportionally if more than the recommended cell mass is used (see section 4.8 for information on optimal cell lysis).

6 Equilibration (Buffer EQU)
Equilibrate a NucleoBond® Xtra Column together with the inserted column filter with **12 mL Equilibration Buffer EQU**. Apply the buffer onto the rim of the column filter as shown in the picture and make sure to wet the entire filter. Allow the column to empty by gravity flow. The column does not run dry.

7 Neutralization (Buffer NEU)
Add **8 mL Neutralization Buffer NEU** to the suspension and immediately mix the lysate gently by **inverting** the tube **until blue samples turns colorless completely! Do not vortex**. The flask or tube used for this step should not be filled more than two thirds to allow homogeneous mixing. Make sure to neutralize completely to precipitate all the protein and chromosomal DNA. The lysate should turn from a slimy, viscous consistency to a low viscosity, homogeneous suspension of an off-white flocculate. In addition, LyseControl should turn completely colorless without any traces of blue. Immediately proceed with step 8. **An incubation of the lysate is not necessary**.

Note: Increase NEU buffer volume proportionally if more than the recommended cell mass is used (see section 4.8 for information on optimal cell lysis).

8 Clarification and loading
Make sure to have a homogeneous suspension of the precipitate by **inverting the tube 3 times** directly before applying the lysate to the equilibrated NucleoBond® Xtra Column Filter to avoid clogging of the filter. The lysate is simultaneously cleared and loaded onto the column. Refill the filter if more lysate has to be loaded than the filter is able to hold. Allow the column to empty by gravity flow.

Alternative: The precipitate can be removed by centrifugation at ≥ 5,000 x *g* for at least 10 min, for example if more than double the recommended cell mass was used. If the supernatant still contains suspended matter transfer it to a new tube and repeat the centrifugation, preferably at higher speed, or apply the lysate to the equilibrated NucleoBond® Xtra Column Filter. This clarification step is extremely important since residual precipitate may clog the NucleoBond® Xtra Column. To load the column you can either apply the cleared lysate to the equilibrated filter or remove the unused filter beforehand. Allow the column to empty by gravity flow.

Note: You may want to save all or part of the flow-through for analysis (see section 8.1).

9 1st Wash: Column filter and column (Buffer EQU)
Wash the NucleoBond® Xtra Column Filter and NucleoBond® Xtra Column with **5 mL Equilibration Buffer EQU**. Apply the buffer to the funnel shaped rim of the filter and make sure it is washing out the lysate which is remaining in the filter. Omitting this step or just pouring the buffer directly inside the funnel may reduce plasmid yield.

10 Filter removal
Either pull out the NucleoBond® Xtra Column Filter or discard it by turning the column upside down.

11 2st Wash: Column only (Buffer WASH)
Wash the NucleoBond® Xtra Column with **8 mL Wash Buffer WASH**. It is important to remove the column filter before applying the washing buffer to avoid low purity.

12 Elution (Buffer ELU)
Elute the plasmid DNA with **5 mL Elution Buffer ELU**. Collect the eluate in a 15 mL or 50 mL centrifuge tube (not provided).

Note: Preheating Buffer ELU to 50 °C prior to elution may improve yields for large constructs such as BACs.

13 Precipitation
Add **3.5 mL room-temperature isopropanol** to precipitate the eluted plasmid DNA. **Vortex thoroughly!** Centrifuge at **≥ 4,500 x *g*** for **≥ 15 min** at **≤ room temperature**, preferably at **15,000 x *g*** for **30 min** at **4 °C**. Carefully discard the supernatant.

14 Washing and drying
Add **2 mL room-temperature 70 % ethanol** to the pellet. Centrifuge at **≥ 4,500 x *g***, preferably **≥ 15,000 x *g*** for **5 min** at **room temperature** (18–25 °C).
Carefully remove ethanol completely from the tube with a pipette tip. Allow the pellet to dry at **room temperature** (18–25 °C) **10–15 min.**

15 Reconstitution
Dissolve the DNA pellet in an appropriate volume of buffer TE or sterile H_2O. Depending on the type of centrifugation tube, dissolve under gentle pipetting up and down or constant spinning in a sufficient amount of buffer for 10–60 min (3D-shaker). Determine plasmid yield by UV spectrophotometry. Confirm plasmid integrity by agarose gel electrophoresis (see section 4.14).

APPENDIX 7: Cell Count for ViraPack and QIAGEN® Effectene Reagent Transfection

ViraPack
Total cells 9.1 * 10^5/ml
Alive cells 8.7*10^5/ml
Dead cells 4.0 * 10^4/ml
Viability 96%

870,000 * 2 = 1,740,000 cells/ml
250,000 / 1,740,000 = 0.1436 ca 144 µl

144 µl * 6 = 864 µl to 30 ml media

QIAGEN® Effectene Reagent
Live cells 1.1 x 106/ml
Dead cells 3.0 x 104/ml
Total 1.1 x 106/ml
Viabiliy 97%

800,000 / 5 ml
1,100,00 * 2 (dilution factor) =2,200,000 live cells
800,000/2,200,000/ml = 364 µl

364 µl * 6 = 2.2 ml cells to 27.8 ml media

APPENDIX 8: ViraPack Transfection kit protocol

The protocol for the ViraPack Transfection Kit (Agilent Technologies, cat no: 200488) utilized in the first transfection.

TRANSFECTION PROTOCOL

Note *Please read the entire transfection protocol before beginning. See the final page of this instruction manual for a condensed, quick-reference protocol that can be detached and used when detailed instructions are no longer required.*

This protocol outlines the procedure necessary for transient transfection using 60-mm tissue culture dishes. If using 100-mm tissue culture dishes, double the quantities and the volumes of the solutions included in the protocol.

1. Inoculate 60-mm tissue culture dishes with 1–5 × 10^5 exponentially growing cells per dish, 24 hours before the transfection.
2. Grow the cells overnight in 5 ml of the appropriate culture medium.

Important *Roswell Park Memorial Institute (RPMI) media cannot be used for $CaPO_4$ transfection. The excess positive charge in this media will cause formation of a dense precipitate that is toxic to the cells.*

Preparing the DNA Suspension for Transfection

The optimal amount of DNA must be determined for each plasmid and cell line separately. The recommended amount is between 1 and 10 µg of DNA per dish. Start with 5 µg of the pCMV β-gal control plasmid DNA per dish when preparing the DNA for the control transfection.

The amounts indicated in the following steps are for duplicate 60-mm tissue culture dishes (500 µl each).

1. For each duplicate transfection, dilute the optimal amount of DNA (2–20 µg) with sterile water to a final volume of 450 µl in a 5-ml BD Falcon polystyrene round bottom tube.

   Note *Polystyrene tubes yield superior results compared to tubes composed of polyethylene or polypropylene.*

2. Add 50 µl of solution 1 and 500 µl of solution 2. Mix the contents of the tube by gently tapping the sides.
3. Incubate the DNA suspension at room temperature for 10–20 minutes. During this incubation period, prepare the cells as indicated in the following section (see *Preparing the Cells for Transfection*).

Preparing the Cells for Transfection

1. Remove the standard culture medium from the tissue culture dishes by aspiration.
2. Wash the cells twice with phosphate-buffered saline (PBS).
3. Add 5 ml of culture medium containing 4–7% solution 3 (MBS).

   Note *The optimal concentration of MBS should be determined by titration. A good starting point for most cell lines is 6%.*

   The cells are now ready to receive the DNA.

Applying the DNA Suspension

1. ***Gently*** resuspend any precipitate in the DNA suspension by pipetting the suspension up and down with a pipettor set at 500 µl. The DNA suspension should appear clear to opaque.
2. Slowly add 500 µl of the DNA suspension to each tissue culture dish ***dropwise in a circular motion*** to distribute the DNA suspension evenly onto each tissue culture dish.
3. Swirl each tissue culture dish ***once***.

Incubating the Transfection Reactions

1. Incubate the dishes for 3 hours at 37°C under 5% CO_2.

   Note *Incubation at 37°C under 5% CO_2 works well; however, for optimal transfection efficiency, the 3-hour incubation should be performed at 35°C under 3% CO_2.*

2. After 3 hours, check the precipitate, which will vary in consistency from slightly perceptible to noticeably granular.
3. Remove the culture medium by aspiration and wash the tissue culture dishes three times with PBS, which should be added gently to avoid dislodging the cells. Check for residual precipitate by microscopic inspection. Add additional wash steps as required to ensure complete removal of the precipitate.
4. Add the appropriate volume of culture medium and incubate the dishes at 37°C under 5% CO_2. For the pCMV β-gal control plasmid, add 5 ml of medium per dish and incubate the cell cultures overnight–24 hours at 37°C under 5% CO_2. For the viral DNA transfection reactions, follow the manufacturer's recommendations for virus production and titering.
5. For the pCMV β-gal control plasmid, perform an assay to detect the β-galactosidase gene product in order to monitor the transfection efficiency. See either the *β-Galactosidase Activity Assay* section or the *β-Galactosidase Histochemical Staining Assay* section.

APPENDIX 9: QIAGEN® Effectene Transfection Reagent protocol

The instruction manual for the QIAGEN® Effectene Transfection Reagent (QIAGEN®, cat no: 301425) for use with adherent cells.

DNA (µg)	Ratio of DNA to Effectene Reagent 1:10	1:25	1:50
0.5	0.5 µg DNA 4.0 µl Enhancer 5.0 µl Effectene Reagent	0.5 µg DNA 4.0 µl Enhancer 12.5 µl Effectene Reagent	0.5 µg DNA 4.0 µl Enhancer 25.0 µl Effectene Reagent
1.0	1 µg DNA 8 µl Enhancer 10 µl Effectene Reagent	1 µg DNA 8 µl Enhancer 25 µl Effectene Reagent	1 µg DNA 8 µl Enhancer 50 µl Effectene Reagent
2.0	2 µg DNA 16 µl Enhancer 20 µl Effectene Reagent	2 µg DNA 16 µl Enhancer 50 µl Effectene Reagent	2 µg DNA 16 µl Enhancer 100 µl Effectene Reagent

Gibson Plasmid 1: 148.4 µl buffer EC + 1.5 µl DNA
Gibson Plasmid 2.1: 132 µl buffer EC + 18 µl DNA
GFP: 1:10 147.2 µl buffer EC + 2.7 µl DNA
pAd5Δ24: 144.6 µl buffer EC + 5.4 µl DNA
pAd5/3Δ24: 147.4 µl buffer EC + 2.6 µl DNA

8 µl enhancer to all except Gibson Plasmid 2.1 where 2 µl was added.

Protocol for Transient or Stable Transfection of Adherent Cells

The following protocol is for transfection of adherent cells in 60 mm dishes. As a starting point, use 1 µg DNA per 60 mm dish. **Although this DNA quantity may seem low, it is usually sufficient for transfection.** Starting points for optimizing transfection in other formats are listed in Table 3 on page 14. See Table 1 on page 9 for the recommended number of cells to seed. Optimal transfection conditions should be determined for every cell line if the highest transfection efficiency with Effectene Reagent is required. Please refer to the optimization guidelines on pages 9–11.

1. **The day before transfection, seed 2–8 x 10^5 cells (depending on the cell type) per 60 mm dish in 5 ml appropriate growth medium containing serum and antibiotics.**
2. **Incubate the cells under their normal growth conditions (generally 37°C and 5% CO_2). The dishes should be 40–80% confluent on the day of transfection.**
3. **The day of transfection, dilute 1 µg DNA dissolved in TE buffer, pH 7 to pH 8 (minimum DNA concentration: 0.1 µg/µl) with the DNA-condensation buffer, Buffer EC, to a total volume of 150 µl. Add 8 µl Enhancer and mix by vortexing for 1 s.**

   IMPORTANT: Always keep the ratio of DNA to Enhancer constant.

   Note: Plasmid DNA quality strongly influences several transfection parameters such as efficiency, reproducibility, and toxicity, as well as interpretation of results. Therefore only plasmid DNA of the highest purity should be used. DNA purified using HiSpeed, QIAfilter, and QIAGEN Plasmid Kits is well suited for transfection of most cell lines. For highest reproducibility and best results with all cell lines, we recommend DNA purified using the EndoFree Plasmid Kit. This kit quickly and efficiently removes bacterial endotoxins during the plasmid purification procedure, ensuring optimal transfection results.
4. **Incubate at room temperature (15–25°C) for 2–5 min then spin down the mixture for a few seconds to remove drops from the top of the tube.**
5. **Add 25 µl Effectene Transfection Reagent to the DNA-Enhancer mixture. Mix by pipetting up and down 5 times, or by vortexing for 10 s.**

   Note: It is not necessary to keep Effectene Reagent on ice at all times. 10–15 min at room temperature will not alter its stability.
6. **Incubate the samples for 5–10 min at room temperature (15–25°C) to allow transfection-complex formation.**
7. **While complex formation takes place, gently aspirate the growth medium from the plate, and wash cells once with 4 ml PBS. Add 4 ml fresh growth medium (can contain serum and antibiotics) to the cells.**
8. **Add 1 ml growth medium (can contain serum and antibiotics) to the tube containing the transfection complexes. Mix by pipetting up and down twice, and immediately add the transfection complexes drop-wise onto the cells in the 60 mm dishes. Gently swirl the dish to ensure uniform distribution of the transfection complexes.**

9. **Incubate the cells with the transfection complexes under their normal growth conditions for an appropriate time for expression of the transfected gene. The incubation time is determined by the assay and gene used.**

   Optional: In many cases, removal of transfection complexes is not necessary. However, if cytotoxicity is observed, remove the Effectene–DNA complexes after 6–18 h, wash the cells once with PBS, and add 5 ml fresh growth medium.

10. **For transient transfections, assay cells for expression of the transfected gene.**

    Cells transfected with *β-gal* or *cat* reporter constructs are typically incubated for 24–48 h post-transfection to obtain maximal levels of gene expression.

    For stable transfections, passage cells 1:5 to 1:10 into the appropriate selective medium 24–48 h after transfection. Maintain cells in selective medium until colonies appear.

    Note: We recommend establishing a kill curve (dose-response curve) with each combination of cell line and antibiotic used. It is important to bear in mind that the kill curve can be influenced by cell density.

    It may be necessary to plate the transfected cells into their normal growth medium (i.e., with no selective drug) and then incubate them for 1–2 days before addition of selective medium.

Table 3. Starting points for optimizing the transfection of adherent cells in different formats using Effectene Reagent. Volumes given apply to each well of multiwell plates.

Culture format	DNA (µg)	Enhancer (µl)	Final volume of DNA in Buffer EC (µl)	Volume of Effectene Reagent (µl)	Volume of medium to add to cells (µl)†	Volume of medium to add to complexes (µl)†
Protocol step	**3**	**3**	**3**	**5**	**7**	**8**
96-well plate	0.1	0.8	30	2.5*	100	0
48-well plate	0.15	1.2	50	4*	150	200
24-well plate	0.2	1.6	60	5	350	350
12-well plate	0.3	2.4	75	6	800	400
6-well plate	0.4	3.2	100	10	1600	600
60 mm dish	1.0	8.0	150	25	4000	1000
100 mm dish	2.0	16.0	300	60	7000	3000

** If transfections are performed in 96- or 48-well plates, dilute the Effectene Reagent with Buffer EC to a total volume of 20 µl or 50 µl, respectively, before addition to the diluted DNA–Enhancer mixture prepared in step 3.*

† Medium should contain the same percentage of serum as routinely used for culturing cells.

APPENDIX 10: The Primer Set Testing for colony PCR

The initial testing of the four primer sets intended for colony PCR. The primers were used with 0.01 µg DNA of each control together with the Phusion HF polymerase. The samples were run on a 2% agarose gel.

Primer Set I and Primer Set II

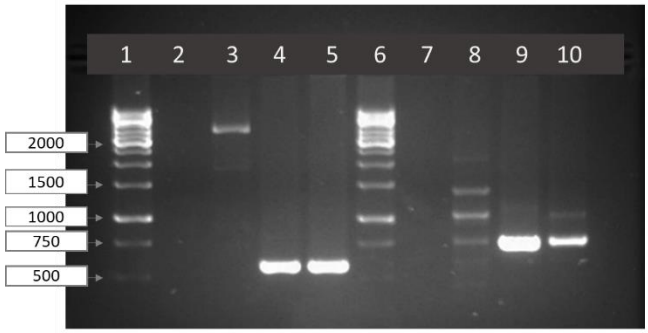

1	GeneRuler 1 kb
2	Primer Set I - Negative control
3	Primer Set I - pTHSN-hCD40L-FL
4	Primer Set I - Ad5Δ24
5	Primer Set I - Ad5Δ24-GMCSF
6	GeneRuler 1 kb
7	Primer Set II - Negative control
8	Primer Set II - pTHSN-hCD40L-FL
9	Primer Set II - Ad5Δ24
10	Primer Set II - Ad5Δ24-GMCSF

Primer Set III and Primer Set IV

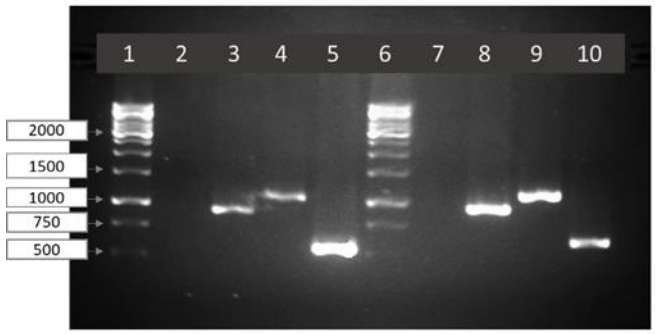

1	GeneRuler 1 kb
2	Primer Set III - Negative control
3	Primer Set III - pTHSN-hCD40L-FL
4	Primer Set III - Ad5Δ24
5	Primer Set III - Ad5Δ24-GMCSF
6	GeneRuler 1 kb
7	Primer Set IV - Negative control
8	Primer Set IV - pTHSN-hCD40L-FL
9	Primer Set IV - Ad5Δ24
10	Primer Set IV - Ad5Δ24-GMCSF

APPENDIX 11: Colony PCR Results for the mCD40L

The results from the first attempt at homologous recombination displaying the mouse CD40L transformed bacterial colonies, ten with mCD40L-FL and ten with mCD40L-S. The same colonies were analyzed with two different primer sets, Primer Set I and II. Those colonies providing a signal with both sets were regarded as potential positives and subsequently underwent plasmid isolation and purification.

Full-length mCD40L

Colony PCR Primer Set I: mCD40L-FL

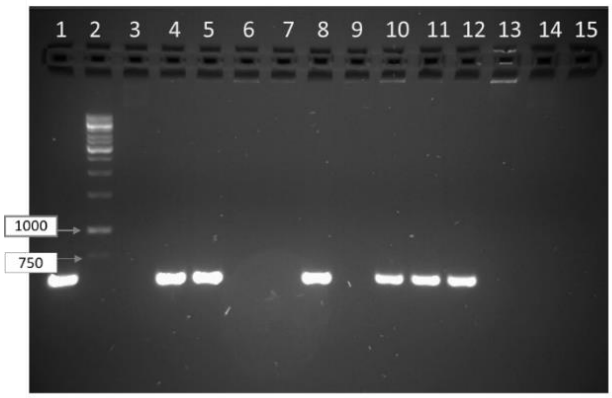

LANE	Sample
1	Control pAd5Δ24 PCR product
2	GeneRuler 1 kb Ladder
3	Control pTHSN-mCD40L-FL PCR product
4-13	Single bacterial colonies
14	Control pTHSN-mCD40L-FL PCR product
15	Negative Control MQ

Colony PCR Primer Set II: mCD40L-FL

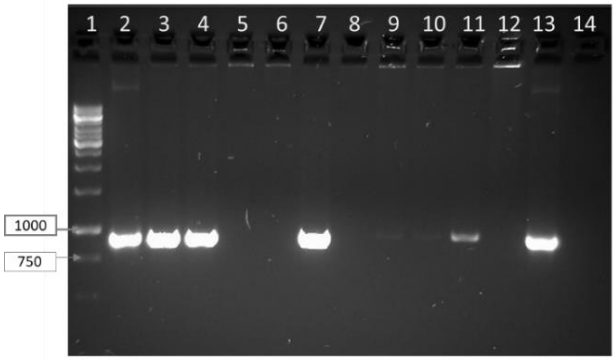

LANE	Sample
1	GeneRuler 1 kb Ladder
2	Control pTHSN-mCD40L-FL PCR product
3-12	Single bacterial colonies
13	Control pTHSN-mCD40L-FL PCR product
14	Negative Control MQ

Soluble mCD40L

Colony PCR Primer Set I: mCD40L-S

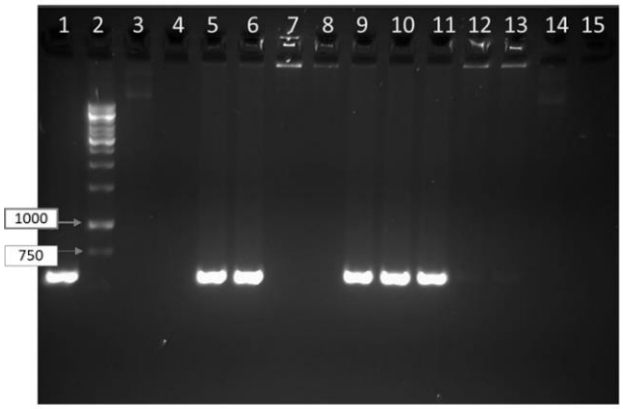

LANE	Sample
1	Control pAd5Δ24 PCR product
2	GeneRuler 1 kb Ladder
3	Control pTHSN-mCD40L-S PCR product
4-13	Single bacterial colonies
14	Control pTHSN-mCD40L-S PCR product
15	Negative Control MQ

Colony PCR Primer Set II: mCD40L-S

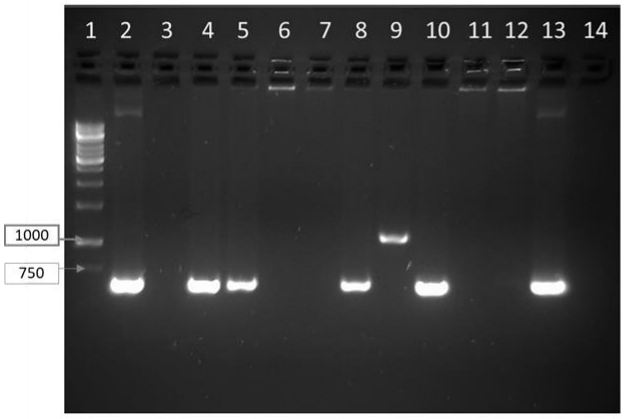

LANE	Sample
1	GeneRuler 1 kb Ladder
2	Control pTHSN-mCD40L-S PCR product
3-12	Single bacterial colonies
13	Control pTHSN-mCD40L-S PCR product
14	Negative Control MQ